1971

Laminar boundary layer development downstream of a suction slot

Cigdem, Sabri

LAMINAR BOUNDARY LAYER DEVELOPMENT DOWNSTREAM OF A SUCTION SLOT

Sabri Çiğdem

NAVAL POSTGRADUATE SCHOOL
Monterey, California

THESIS

LAMINAR BOUNDARY LAYER DEVELOPMENT
DOWNSTREAM OF A SUCTION SLOT

by

Sabri Cigdem

Thesis Advisor: C. J. Garrison

December 1971

Laminar Boundary Layer Development Downstream of a Suction Slot

by

Sabri Çiğdem
Lieutenant (junior grade), Turkish Navy
B.S., Naval Postgraduate School, 1971

Submitted in partial fulfillment of the
requirements for the degree of

MASTER OF SCIENCE IN MECHANICAL ENGINEERING

from the

NAVAL POSTGRADUATE SCHOOL
December 1971

ABSTRACT

Laminar boundary layer development downstream of a suction slot was investigated in a low velocity wind tunnel. In order to observe the effect of suction on the boundary layer, detailed boundary layer profiles were measured at various stations upstream and downstream of a suction slot for different suction flow rates. The investigation was carried out for zero suction, 53.33 SCFH/FT. and 133.33 SCFH/FT. suction, by using 1/16 inch suction slot. The velocity profiles were plotted for 22 stations with different suction flow rates with respect to the no suction flow case. At the far upstream and downstream side of the slot, suction was ineffective and velocity profiles had the Blasius velocity profile shape. Suction had the maximum effectiveness a short distance in front of and downstream of the slot. As the distance from the slot increased both upstream and downstream, the velocity profiles tended to approach Blasius velocity profiles asymptotically.

TABLE OF CONTENTS

LIST OF TABLES

LIST OF FIGURES

NOMENCLATURE

A,B	constants depending on fluid properties
A_n	area
c_p	pressure coefficient
CFM	cubic feet per minute
E_b	bridge voltage
F, f	function
H	shape factor = δ/θ
L	boundary layer length from suction slot with no suction
P_n	pressure
Q_s	suction flow rate
R_e	Reynolds number
R_c	resistance of wire at environmental (cold) temperature
R_h	resistance of wire at operating (hot) conditions
SCFH	standard cubic feet per hour
t_e	temperature of the environment
t_s	surface temperature of the wire
u	velocity in boundary layer
U	linear velocity equation
U_n	velocity
U_o	free stream velocity
x	boundary layer starting length
x_e	effective boundary layer length from suction slot
X	distance at the downstream of suction slot
Y	distance normal to bottom surface
α_c	temperature coefficient of resistance

δ	displacement thickness
θ	momentum thickness
μ	dynamic viscosity
ν	kinematic viscosity
ρ	density of air

NONDIMENSIONAL PARAMETERS

$$C_p = \frac{P_1 \quad P_n}{\frac{1}{2}\rho U_1^2}$$ pressure coefficient

$$H = \delta/\theta$$ shape factor

$$\frac{x_e}{L}$$ effective boundary layer length

$$\frac{Q_s}{U_o L}$$ suction flow rate

$$Re = \frac{U_o L}{\upsilon}$$ Reynolds number

ACKNOWLEDGEMENTS

The author wishes to express his sincere appreciation to his advisor, Dr. C. J. Garrison, for his help and council during the investigation. The special efforts of the members of the Mechanical Engineering Machine Shop in giving their time and talents during the progress of this study are very much appreciated.

I. INTRODUCTION

Since the discovery of the boundary layer phenomenon, many theoretical and experimental studies have been conducted about it and its control. In 1904 Prandtl described several experiments in which the boundary layer was controlled and he was able to formulate the basic differential equation of a fluid motion in the boundary layer. Prandtl proposed the mathematical theory of the boundary layer which was later found to be very fruitful and which received practical application in the calculation of the skin-friction drag which acts on a body as it moves through a fluid, for example, the drag experienced by a flat plate at zero incidence, the drag of a ship, of an airplane wing and turbine blade.

The problem of boundary layer control has become very important in recent times, in particular, in the field of aeronautical engineering; in actual applications it is often necessary to reduce drag and to attain high lift. The attempts to reduce the drag caused by fluid motion along a solid wall have led to experiments aimed at preserving laminar flow in the boundary layer. One of the methods of maintaining laminar flow has been to remove, by suction, a portion of the decelerated fluid in the boundary layer. This has the effect of altering the structure of the boundary layer by creating a more stable velocity profile, thus delaying or eliminating the transition to turbulent flow, and the resulting boundary layer downstream of the suction region is thinner.

A fairly complete history of the research performed on boundary layer control both in the United States and abroad is given by Lachmann in Reference (1).

First boundary later control was performed in Germany by Prandtl in 1904. The flow past a circular cylinder was controlled by suction on one side and indications were that the drag was reduced appreciably on the suction side.

Later, in Germany, boundary layer control found practical utilization with slotted airplane wings being used for increasing lift coefficient. In 1921 Handley Page and Lachmann independently found about 60% increase of lift coefficient with slotted wings compared with the unslotted aerofoils.

The method of influencing the maximum lift by sucking the boundary layer was investigated on the first experimental aircrafts by Schrenk, et.al., in 1940, taking as starting point an aerofoil with a flap. A lift coefficient $c_1 = 4.2$ was obtained compared with $c_1 = 2.3$ without suction applied to the flaps.

Aside from the application of suction to increase lift, it was also applied to reduce drag. As flying speeds were increased, surface friction gained more and more in importance since its percentage share in the total drag increased. For a given Reynolds number, a laminar boundary layer produces less surface friction than a turbulent one. In order to take advantage of this Doetsch designed so-called laminar wing sections, to extend, as far as possible, the regime of laminar flow in the down-stream direction. This causes the drag coefficient to decrease, because laminar drag is substantially smaller than turbulent drag.

Holstein in 1942, by using single slots, experimentally reduced drag, by maintaining the boundary layer thickness by suction below the limit which transition sets in.

Until the end of Second World War, the majority of work on boundary layer control was done in Germany. The development of this subject which has taken place in France since the end of the Second World War, also found applications to the aircraft wings. The first experimental research in France was carried out by O.N.E.R.A. at the Institut of Aerotechnique of St. Cyr in 1946. Systematic study has been done with a wing which was fitted with a flap and the suction applied at the knee of the flap. It was found that the width of the suction slot had little influence on lift increase, and the lift was limited by separation, which is created at the wing nose. In further studies, a pivotable leading edge or nose flat with suction applied at the knee of this flap was used to prevent nose separation, therefore the angle of incidence of maximum lift and maximum lift coefficient was increased in this way.

In 1947-1948 at O.N.E.R.A., special wing sections were designed with a favorable pressure gradient to maintain laminar flow over a large part of the wing chord. Separation which would normally occur at the pressure discontinuity on the chord, was avoided by a suction slot and with very low suction intensity.

Later experiments were performed with combined suction and blowing on the double flap wing and the results were much better than a typical slotted flap wing.

British research on boundary layer control with suction includes the proper aerofoil design for getting maximum lift coefficient. Griffith suggested designing the aerofoil according the the potential flow theory with a stabilising velocity gradient along the whole chord except at one position where a velocity discontinuity occurs. Thus, if sufficient suction is applied at this one point to prevent separation, laminar boundary

layer may be expected right to the trailing edge. In 1943 Richards and Burge reported the results of small-scale tests of a new type of aerofoil that had a thickness-chord ratio of 16% with a symmetrical section.

Later, a 30% thick symmetric aerofoil was tested by Richards, Walker and Taylor, and in 1945, Glauert designed a thick suction wing finding an increasing disadvantage and further support did not come because the boundary layer removal by area suction was shown to be more economic than by slot suction, and the studies were mostly concentrated on it.

In the United States, studies about the boundary layer control have been done by U. S. Air Force, N.A.C.A., and commercial avaition companies. Boundary layer control in the United States was divided into two broad categories of High Lift and Low Drag.

For the High Lift boundary layer control, the first report was published in 1928, by Reid and Bamber by N.A.C.A.. They used a U.S.A.-27 aerofoil for the tests and showed the effectiveness of the boundary layer control by suction for improving maximum lift. Perhaps the most outstanding and active American proponent of boundary layer control prior to 1946 was Stalker. He conducted numerous wind tunnel and aeroplane design studies in the late 1930s and in 1942 was given a contract by the U. S. Army-Air Force to modify an L-1 liaison aeroplane with a suction flap arrangement. The modification consisted essentially of providing for a new plywood wing which contained full span double segment flaps together with full span suction slots and ducts plus the addition of a suction blower in the fuselage. In 1945, Stalker reviewed the L-1 program; he noted that the mechanism for boundary layer control was bulky and complicated although it worked satisfactorily. After this program, no progress of note was made until World War II.

In the late 1940s and early 1950s, the Air Force effort in high lift boundary layer control primarily emphasized the applications to combat aircraft. The first complete airborne operation of the boundary layer control system by suction and blowing was made with a C-123 U.S.A.F. cargo aircraft in 1955, and was reported very successful in regard to maximum lift and stability.

By using standard slotted flaps on the leading edge of an F-86A fighter aircraft was tested by suction, and flight test results were quite encouraging with flap effectiveness reaching nearly theoretical values. Aircraft handling characteristics, particularly lateral control, were noticeably improved and no adverse effects were noted.

For Low Drag boundary layer control, N.A.C.A. in 1941 conducted the first laminar suction experiments ever made. The results of these tests were not impressive regarding either extent of laminar flow or measured drag reduction.

During World War II, it is understood that Lockheed Aircraft Company conducted a limited flight test program on laminar suction using a P-38 fighter with a wing glove containing one suction slot aft of the mid-chord point. It was reported that no drag reduction was found.

After World War II, in the United States, first studies were sponsored by U. S. Air Force and carried out by Northrop Aircraft Company under the direction of Dr. Pfenninger. Before this program was initiated in 1949, the first postwar experiments were made by N.A.C.A. and the tests clearly demonstrated that with suction through finite slots, the boundary layer could be maintained in a laminar state to reasonably high Reynolds numbers.

Under the direction of Dr. Pfenninger, the Air Force-Northrop program started as a modest effort - the design and fabrication of a slotted wing panel for test in N.A.C.A. TDT Wind Tunnel at Langley Field. The tests, run in 1950 and 1951, were very encouraging, laminar flow that was obtained to higher Reynolds numbers than had the earlier N.A.C.A. slotted suction tests. The important finding was that laminar flow could be maintained at high Reynolds numbers through the use of properly designed suction slots and that the design of the suction slot arrangement could be determined in a rational, analytical manner. Northrop applied these test results to the F-94A aircraft wings for the design of a low-drag, long range aircraft. In 1955, final tests were made with the F-94A aircraft utilizing a new glow type suction wing panel on which 69 fine slots were used in lieu of the 12 large slots. These tests were very encouraging, demonstrating complete laminar flow up to a Reynolds number of 36×10^6 (the limit of aircraft) and over a realistic range of wing lift coefficients, with very low measured drag coefficients.

Besides the historical development that was briefly summarized above, there have been recent experiments designed to reduce fluid friction drag by maintaining a stable laminar flow. In 1965, Holt [2] observed boundary layer profiles around the suction slot in a single pass wind tunnel. He performed the experiments with varying slot widths which gives various Reynolds numbers. Slot Reynolds numbers were based on the width of the suction slot and the average suction velocity. He indicated that the slot affects a region from 20 to 30 times its own width. An analysis based on the momentum integral equation was found to be inadequate based on the standard method of assuming a velocity function.

The purpose of this present experiment was the investigation of the behavior of the laminar boundary layer downstream of a discrete suction slot. The effect of suction consists in the removal of decelerated fluid particles near the boundary. For every suction flow rate, the boundary layer effective length changes and the boundary layer thickness decreases across the slot, and starts growing beyond the slot. This boundary layer thickness is maximum for no suction flow situation; it is zero and starts anew at the slot for complete suction flow situation.

The experiments were carried out in a 6.0 feet long wind tunnel test section, which had adjustable suction slot at the center. Necessary suction was maintained with a suction blower which had high pressure rise and low suction flow rate. The flow was maintained in the test section by a blower, that was set at the downstream side of test section.

For prediction of the flow behavior, with and without suction, a region 30 inches in length was surveyed with a hot wire anemometer. Velocity profiles were taken at 6, 4, 2, 1, 1/2, 1/4 inches upstream of the slot, at upstream and downstream edges of suction slot, and 1/4, 1/2, 1, 2, 3, 4, 5, 6, 9, 12, 15, 18, 21, 24 inches downstream of the slot, for the zero suction case, with 53.33 SCFH/FT. and 133.33 SCFH/FT. suction. For every station 60 velocity measurements were taken both without and with suction for comparison. The displacement and momentum thickness obtained by a numerical integration of these velocity profiles. The displacement thickness, momentum thickness, and boundary layer shape factor were plotted as a function of distance downstream of the slot for various values of suction flow rates.

In general, the effect of the suction slot is a local phenomena and far downstream the boundary layer asymptotically approaches the Blasius profile. Thus, far downstream the effect of suction is to simply reduce the boundary layer thickness as compared to what it would have been in the absence of suction. Accordingly, one can define an effective boundary layer length with suction. This length is, of course, just equal to the actual boundary layer length when the suction flow is zero and decreases with suction flow. The difference between the actual boundary layer plate length and the effective length with suction is an important parameter and is presented as a function of the suction flow rate.

II. EXPERIMENTAL EQUIPMENT

The experimental equipment consisted of a wind tunnel with an adjustable suction slot, a suction blower and a hot wire anemometer for measuring the air velocity. Figure (1) represents a schematic drawing of the wind tunnel.

The converging inlet nozzle section of the wind tunnel had a four-by-four feet entrance and a contraction ratio of 7.1 to 1. The test section was eighteen-by-eighteen inches and 6.0 feet long. A semi-cylindrical shaped cardboard cowling was set at the entrance edges of nozzle to provide undisturbed flow at the inner faces of the nozzle. Four cheese-cloth and two wire screens were designed from information contained in Reference [4], as turbulence reducing screens having about 67% open area.

The converging inlet nozzle was designed for smooth variation of the pressure coefficient with respect to the distance from entrance to the exit as shown in Figure (2). Bernoulli equation was used to get pressure coefficients

$$\frac{P_1}{\gamma} + \frac{U_1^2}{2g} = \frac{P_n}{\gamma} + \frac{U_n^2}{2g} \qquad (1)$$

in which, P_1 and U_1 are pressure and velocity at the entrance of the nozzle and P_n and U_n are the pressure and velocity inside the nozzle at various distances from entrance.

Equation (1) can be written as follows,

$$\frac{P_1 - P_n}{\frac{1}{2}\rho U_1^2} = C_p = \left[\left(\frac{U_n}{U_1}\right)^2 - 1\right] \qquad (2)$$

After substituting the one dimensional continuity equation into Equation (2),

$$\frac{P_1 - P_n}{\frac{1}{2}\rho U_1^2} = C_p = \left[\left(\frac{A_1}{An}\right)^2 - 1\right] \qquad (3)$$

where as indicated in Equation (3), the pressure coefficient is a function of the square of the area ratio, A_1 being the nozzle entrance area and A_n the inside cross-sectional area of the nozzle.

The nozzle was built from 40/1000 inch thick aluminum sheet metal. The connection of the nozzle and test section was sealed and the inside connecting surfaces were polished for undisturbed flow.

Three sides of the test section were made of 1/4 inch aluminum plate and the front side was made of 1/4 inch plexiglas. Also, in the back plate a removable window was provided for easy access to the probe and slot area.

The bottom of the test section was constructed of 1/4 inch thick aluminum plates. The plate at the upstream side of the suction slot was 34.75 by 18.0 inches rectangular, and the one on the downstream side of the suction slot was 34.50 by 18.0 inches rectangular, and was connected to the side plates with screws. (A picture of experimental equipment can be seen in Figure (3)). The suction slot was formed by machining a beveled edge on two thick pieces of aluminum as shown in Figures (4) and (5). Four aluminum connecting rods were used between two aluminum pieces to align the pieces and keep a smooth surface inside the test section. The inside surfaces of the bottom plate and the aluminum pieces were carefully smoothened and polished.

A manifold or suction box was constructed of 1/2 inch plexiglas around the suction slot. This box was well sealed and was connected by two flexible tubes to a manifold which fed three flowmeters connected in parallel. The capacity of the flowmeters were 20, 50 and 200 SCFH independently. The outlet of the three meters were then manifolded and connected to a suction blower which had a high pressure rise and low suction flow rate to remove the desired amount of the boundary layer.

The top plate of the test section was also 1/4 inch thick, 18.0 by 72.0 inches aluminum plate, and had a 3/8 inch wide, 32.0 inches long slot on it along the center line, which started 30.0 inches from the inlet of the test section, and ended 10.0 inches from the exit of the test section. This long slot was used to insert the hot wire probe into the test section so that it could be moved from 6.0 inches upstream to 24.0 inches downstream of the suction slot. In order to carry the hot wire probe-holder and micrometer, two parallel rails were installed on the outer surface of the top plate. The rails were placed 3.0 inches apart and parallel to the 32.0 inches long slot, as seen in Figure (6). The rails started from 2.0 inches before and ended after the slot and were 36.0 inches long. They were fastened to the top plate along their wider bottom surfaces with screws, and the top surfaces were polished for smooth slide of the traversing mechanism.

The exit of the test section was connected to a nozzle, and sealed with silicone. The converging exit nozzle, 17.0 inches long at the center line, started with a square cross-section and transitioned to circular shape with a 11.5 to 1.0 contraction ratio. It was constructed of thin brass and a 6.0 inches long by 6.0 inches diameter cylindrical copper pipe was welded to the end of the converging exit nozzle which had a pitot-static tube on it and was connected to the inlet of the blower.

The wind tunnel blower was a centrifugal flow type, with 6.0 inches inlet and 7.0 inches outlet diameter having a 923.5 CFM maximum flow rate. The outlet area of the blower was made adjustable by a slide gate so that the flow rate could be adjusted.

III. HOT WIRE ANEMOMETER

The velocity measurements were taken by a Thermo-System, Inc. constant temperature anemometer as described in Reference [5]. The detecting element of the hot wire anemometer consists of a 1500 ohms/ft. resistivity and 0.00015 inch diameter tungsten wire, which is heated by an electric current. The wire is cooled by the flowing fluid, and the voltage changes in the wire required to maintain it at a constant temperature is directly related to the flow velocity. The main variable was the necessary electrical power which maintained the constant temperature difference. Electric power also balances the dissipated heat by the wire which occurs by the forced heat convection due to the flowing fluid.

The output of the bridge was measured by a digital DC voltmeter furnished with the anemometer for measurements of mean quantities and has a sensitivity of ±1.0 milivolt change in the output. An RMS voltmeter and an oscilloscope were used to detect flow fluctuations in the flow.

Calibration:

For taking the mean velocity measurements a calibration curve must first be obtained. For that purpose, the hot wire was calibrated against a pitot tube before the velocity measurements were taken. Before the calibration operation was started, the hot wire probe was set at the center line of the test section and was perpendicular to the air flow. After taking voltage reading for zero velocity, the blower was operated and by controlling the slide gate of the blower outlet the flow rate could be adjusted. A pitot tube was placed in the 6.0 inches diameter section of the flow and used as a standard for calibration.

The relationship between the electric power to the wire and the velocity past the wire was given according to Kings Law as in Reference [2].

$$E_b^2 = (B + A\sqrt{U})(t_s - t_e)R_H \qquad (4)$$

In the practice of hot wire anemometery the factors A and B are determined experimentally if $(t_s - t_e)$ is constant then R_H is constant since

$$R_H / R_C = 1 + \alpha_C (t_s - t_e) \qquad (5)$$

The ratio R_H/R_C is called the overheat ratio or ratio of hot to cold resistance, and R_H/R_C was about 1.5 at ambient temperature for this device, where R_H is operating (hot) resistance of wire, R_C is the resistance of wire at environmental (cold) temperature, α_C is temperature coefficient of resistance for the wire material referenced at environmental temperature, t_s is wire operating temperature and t_e is environmental (fluid) temperature. Since the right hand side of Equation (5) is a constant, it can be seen from Equation (4), that a linear relationship exists between E_b^2 and $\sqrt{U}$. A plot of E_b^2 vs $\sqrt{U}$ then gave the constants A and B, where A is the slope of the curve, and B is the square of the voltage at zero velocity.

R_C is affected by the environment temperature t_e. If t_e changes the calibration curve changes, because of change in A and B.

A typical calibration curve is shown in Figure (7).

IV. EXPERIMENTAL PROCEDURE

After making the hot wire calibration by using a pitot-static tube in the wind tunnel, velocity profiles were measured at 6, 4, 2, 1, 1/2, 1/4 inch before the suction slot, at the upstream and downstream edges of the suction slot, and at 1/4, 1/2, 1, 2, 3, 4, 5, 6, 9, 12, 15, 18, 21, 24 inches downstream of the suction slot. Before taking data for various suction flow rates, the suction slot width was adjusted to 1/16 inch as seen in Figure (4). The hot wire probe was positioned 0.100 inch above the bottom plate of test section by using the optical comparator and small steel block 0.100 inches high. For every station the initial setting was determined so that correction was made for the waveness of the rail and bottom surfaces. The initial starting position of 0.035 inch was chosen, by changing the hot wire distance from surface to the 0.5 inch and reading the voltage indication on the DC voltmeter. False readings were observed very close to the wall due to radiated heat between the wire and the wall, therefore, no readings were taken closer to the wall than 0.035 inches.

The velocity measurements were taken, as the probe was moved away from the wall in increments of 0.005 inch at the beginning of the velocity profile, then 0.010 and 0.025 inches increments at the distances, beginning 0.035 inch from the surface. For every station 60 velocity measurements were taken over the range of 1.0 inch distance upward from the surface as seen in Table (1).

V. PRESENTATION AND DISCUSSION OF RESULTS

The data were taken for 22 stations with three different flow situations and the velocity profiles were plotted as the distance in the vertical direction versus velocity.

For comparison purposes, the Blasius velocity profiles for the flat plate were plotted with the data obtained from Reference [3], for the length between 2.5 feet and 5.0 feet, for every 0.25 feet along the plate, as seen in Figure (8).

As a first step, data without suction and with 133.33 SCFH/FT. suction were plotted together for every station. Figures (9) to (30) show plotted the velocity profile growth with distance as the abscissa and velocity as the ordinate. Figure (9) and (10) show that the velocity profiles were similar to the Blasius velocity profiles and the suction had no effect on the velocity profile beyond 2.0 inches upstream of suction slot as seen in Figure (11). As the distance decreased toward the slot, the profiles tended to fill out as seen in Figures (12), (13) and (14). The effect of suction was maximum at the upstream edge of suction slot as seen in Figure (15). At the downstream edge of the slots, the suction was less effective and this decreased effectiveness extended up to 0.5 inch downstream of the slot as seen in Figures (16), (17) and (18). Suction effectiveness again increased around 1.0 inch after slot and remained effective up to about 9.0 inches, as seen from Figures (19) to (25). After 12.0 inches downstream of the slot the suction effectiveness began to decrease and the velocity profiles tended to approach, asymptotically, the Blasius velocity profiles as seen in Figures (26) to (30).

A second set of velocity profiles were plotted without suction and 53.33 SCFH/FT. suction for the same stations. The previous discussion is also valid for this case and the results are similar for this suction flow rate. But, because of the reduced suction flow rate, the filling out of the velocity profiles was also less than the previous set of profiles, as seen in Figures (31) to (52). The velocity profiles were similar to the Blasius velocity profiles and suction was not too effective on upstream side of the slot as seen in Figures (31) and (32). Effectiveness of the suction started around 2.0 inches upstream of the slot as seen in Figure (33). Suction had the maximum effectiveness at the upstream edge of suction slot, as seen in Figure (37), and at the downstream edge of suction slot, suction effectiveness was reduced as seen in Figure (38). The suction effectiveness increased downstream of the slot, and varied gradually after 1.0 inch downstream of the slot, as seen in Figures (41) to (47). After 9.0 inches distance, the effectiveness of suction decreased and the velocity profiles tended to approach Blasius velocity profiles asymptotically, as seen in Figures (48) to (52).

The velocity profiles were numerically integrated to give displacement thickness and momentum thickness, where the displacement thickness is defined as the velocity retardation in the boundary layer which results in a deficit in the mass flow rate, and is represented as:

$$\delta = \int_{o}^{\infty} \left(1 - \frac{u}{U_o}\right) dy \qquad (6)$$

Equation (6) stands for the thickness of a layer of fluid having velocity U_o that would have to be brought to a standstill to represent the loss in mass flowrate due to boundary layer retardation.

The momentum thickness can be defined as a momentum loss due to boundary layer retardation, and represented as:

$$\Theta = \int_{o}^{\infty} \frac{u}{U_o}\left(1 - \frac{u}{U_o}\right) dy \qquad (7)$$

Equation (7) stands for the thickness of a layer of fluid having velocity U_o that would have to be brought to a standstill to represent the loss in momentum due to boundary layer retardation.

In order to characterize the velocity profiles, a boundary layer shape factor was introduced as $H = \delta/\theta$ to give an indication of the shapes of the profiles and its stability. After numerical integration of velocity profiles, the displacement thickness, momentum thickness and shape factor were plotted with respect to the distance downstream of slot, for three different suction cases as shown in Figures (53) to (55). For the no suction situation, the displacement thickness increased at the upstream side of the slot for increased distance, as seen in Figure (53). About 1.0 inch before the slot there was a sudden decrease of displacement thickness followed by a sudden increase at the slot caused by the disturbance of the slot. This type of disturbance could be introduced by a slight misalignment of the sections of the suction slot. For increased suction flows, the changes of the displacement thickness around the suction slot were also increased, The maximum displacement thickness difference between upstream and downstream edges of slot was reached by 133.33 SCFH/FT. suction as seen in Figure (55).

As can be seen from the same figures, the momentum thickness was affected to a smaller degree than was displacement thickness. A decrease in momentum thickness is normal for higher suction flows,

because as the decelerated fluid is removed by suction and the higher velocity fluid is brought closer to the wall, the momentum thickness would decrease as is apparent from Equation (7).

The bounday layer shape factor $H = \delta/\theta$ is an indication of the stability of the velocity profiles. Figures (53), (54) and (55) show H plotted against the distance for three different suction flow situations. These curves have the same pattern as displacement and momentum thickness.

The value of shape factor for a flat plate with no suction and zero pressure gradient is given as 2.59, in Reference [3]. Increased suction flow in general has the effect of decreasing the shape factor. It may be noted, however, that for the case of zero suction the shape factor still has a value less than 2.59. This is caused by the favorable pressure gradient existing in the test section which in turn caused by the displacement thickness blockage.

For the determination of pressure distribution along the test section, several velocity measurements were taken for different vertical distances. There was decreasing velocity and increasing pressure gradient before the suction slot, for 1.0 inch distance from the bottom surface as seen in Figure (56). At the suction slot, the velocity had an obvious increase while the pressure gradient decreased. After the suction slot, the velocity increased slowly and there was a favorable pressure gradient with a small increase. About 15.0 inches downstream of slot the velocity again started to decrease and an adverse pressure gradient existed for 6.0 inches. The velocity increased again 21.0 inches after slot and a favorable pressure gradient was created by the blower. There was a continuous increase of the velocity through the test section when the probe was set

2.0 and 3.0 inches above the bottom plate. Velocity decrease and adverse pressure effects occurred only at the end of the test section where the probe was set 8.0 inches above the floor.

The asymptotic effect of the suction on the boundary layer is simply to reduce its effective starting length and decrease the boundary layer thickness, as compared to what it could have been in the absence of suction. The effective boundary layer length with suction can be defined as the actual boundary layer length when the suction flow is zero and decreases with increasing suction flow. The difference between the actual boundary layer plate length and the effective length with suction is an important parameter and was plotted in dimensionless form as a function of the suction flow rate, as seen in Figure (57). For laminar boundary layer development with suction, the variables can simply be defined as the suction flow rate Q_s, the distance between the boundary layer starting point and suction slot with no suction, L, the free stream velocity U_o, fluid density ρ, fluid viscosity μ and the effective starting length with suction x_e. A functional relationship can be established using these variables as,

$$F(x_e, L, Q_s, U_o, \mu, \rho) = 0 \tag{8}$$

After selecting repeating variables, writing the π-parameters in terms of unknown exponents and solving the equations simultaneously for the dimensionless effective boundary layer length parameter the following equation results,

$$\frac{x_e}{L} = f\left(\frac{Q_s}{U_o L}, \frac{U_o L \rho}{\mu}\right) \tag{9}$$

Of the dimensionless parameters, the first is the suction flow rate relative to free stream velocity and actual boundary layer plate length. The second parameter is a Reynolds number and accounts for viscous effects. All the variables were known in Equation (9), except the actual and effective boundary layer starting lengths and these were obtained from the momentum thickness by numerical integration of the velocity profiles at different suction flow rates.

For the flat plate at zero incidence the momentum thickness is given in Reference [3] as,

$$\theta = 0.664 \sqrt{\frac{\nu x}{U_o}} \tag{10}$$

where, for the known momentum thickness, the boundary layer starting length is obtained as follows;

$$x = 2.268 \left(\frac{U_o \theta^2}{\nu} \right) \tag{11}$$

The boundary layer starting lengths were calculated by subtituting the momentum thicknesses, which were obtained by numerical integration of the velocity profiles for different stations and suction flow rates, into Equation (11). The differences between the boundary layer starting lengths and the distances from the suction slot for every station gave the effective boundary layer lengths for different suction flow rates. Downstream from the slot the effective starting lengths become approximately constant

indicating that a Blasius profile had been reached. An average of these nearly constant values was then used as the effective starting length. For the no-suction flow situation the effective boundary layer length was found to be L = 2.42 feet from the suction slot. As the suction flow rates increased the effective boundary layer decreased, and was zero for complete suction of the boundary layer.

Another set of data was obtained for the effective boundary layer starting length by using the approximate solution of momentum thickness as given in Reference [3].

$$\frac{U_o \theta^2}{\nu} = \frac{0.470}{U_o^5} \int_{X=0}^{X} U^5 \, dx \qquad (12)$$

Equation (12) is an approximate expression which accounts for the pressure gradient. A linear relationship between velocity and distance along the test section was used for the integration; its slope was obtained from the velocity plots in Figure (56). From Equation (12), three effective boundary layer lengths were obtained from the three suction flow situations. L = 2.69 feet was found for the no-suction case. These data, corrected for pressure gradient, were also plotted in Figure (54), in dimensionless form with respect to the dimensionless suction flow rate and both of the curves decreased asymptotically for increasing non-dimensional suction flow rate. The third dimensionless parameter was the Reynolds number based on the free stream velocity, the average of the actual boundary layer plate lengths, the fluid density and viscosity. It may be seen from Figure (57) that the pressure gradient correction had a considerable effect.

VI. CONCLUSIONS

1. Boundary layer velocity profile shapes are highly dependent on the suction flow rates immediately downstream of the suction slot.
2. The effect of the suction slot is a local phenomena and far downstream the boundary layer asymptotically approaches the Blasius profile.
3. The momentum and displacement thickness decrease around the suction slot with increased suction flow rates because as the decelerated fluid is removed by suction the higher velocity fluid is brought closer to the wall.
4. The effective boundary layer starting length decreases rapidly with suction flow rate at first followed by a rather gradual decrease.
5. In view of (4) it is concluded that a number of suction slots each having a small suction rate would be more effective than one slot with a large suction flow rate.

TABLE 1

Q_s = 0.0 SCFH/FT.

X = -6 inches		X = -4 inches		X = -2 inches	
Y(in.)	U(ft/sec.)	Y(in.)	U(ft/sec.)	Y(in.)	U(ft/sec.)
0.045	1.52	0.045	1.48	0.045	1.48
0.050	1.64	0.050	1.64	0.050	1.62
0.055	1.79	0.055	1.75	0.055	1.77
0.060	2.01	0.060	1.91	0.060	1.91
0.065	2.16	0.065	2.09	0.065	2.10
0.070	2.36	0.075	2.24	0.070	2.22
0.075	2.41	0.075	2.37	0.075	2.34
0.080	2.50	0.080	2.50	0.080	2.46
0.085	2.72	0.085	2.63	0.085	2.55
0.090	2.87	0.090	2.77	0.090	2.70
0.095	2.98	0.095	2.87	0.095	2.77
0.100	3.08	0.100	2.92	0.100	2.84
0.105	3.23	0.105	3.02	0.105	2.89
0.110	3.33	0.110	3.05	0.110	2.92
0.115	3.49	0.115	3.28	0.115	3.05
0.120	3.63	0.120	3.33	0.120	3.15
0.125	3.76	0.125	3.43	0.125	3.29
0.130	3.88	0.130	3.54	0.130	3.45
0.135	4.01	0.135	3.67	0.135	3.53
0.140	4.10	0.140	3.81	0.140	3.58
0.145	4.16	0.145	3.87	0.145	3.65
0.150	4.28	0.150	3.97	0.150	3.73
0.155	4.32	0.155	4.07	0.155	3.81
0.160	4.49	0.160	4.14	0.160	3.98
0.165	4.58	0.165	4.29	0.165	4.07
0.170	4.71	0.170	4.37	0.170	4.17
0.175	4.76	0.175	4.44	0.175	4.23
0.180	4.84	0.180	4.57	0.180	4.29
0.185	4.88	0.185	4.64	0.185	4.37
0.190	4.97	0.195	4.80	0.195	4.57
0.195	5.05	0.210	5.07	0.210	4.79
0.200	5.12	0.220	5.22	0.220	4.93
0.205	5.23	0.235	5.44	0.235	5.13
0.210	5.32	0.245	5.54	0.245	5.28
0.220	5.47	0.260	5.67	0.260	5.44
0.225	5.53	0.270	5.83	0.270	5.56
0.230	5.61	0.285	6.03	0.285	5.65
0.235	5.65	0.295	6.12	0.295	5.78
0.240	5.69	0.310	6.18	0.310	5.94
0.245	5.74	0.320	6.29	0.320	5.99
0.250	5.79	0.335	6.39	0.335	6.09
0.255	5.87	0.360	6.50	0.360	6.22
0.260	5.88	0.385	6.59	0.385	6.28
0.265	5.90	0.410	6.63	0.410	6.34
0.270	5.94	0.435	6.67	0.435	6.42
0.285	5.98	0.460	6.71	0.460	6.46
0.295	6.05	0.485	6.73	0.485	6.51
0.310	6.18	0.510	6.73	0.510	6.51
0.320	6.24	0.535	6.75	0.535	6.53
0.335	6.31	0.560	6.75	0.560	6.55
0.360	6.43	0.585	6.75	0.585	6.55
0.385	6.52	0.600	6.75	0.610	6.55
0.435	6.62	0.625	6.75	0.625	6.55
0.485	6.66	0.650	6.75	0.650	6.55
0.535	6.70	0.700	6.75	0.675	6.55
0.635	6.72	0.750	6.75	0.700	6.55
0.700	6.72	0.800	6.75	0.750	6.55
0.800	6.72	0.850	6.75	0.800	6.55
0.900	6.72	0.900	6.75	0.900	6.55
1.000	6.72	1.000	6.75	1.000	6.55

Q_s = 0.0 SCFH/FT.

X = -1 inch		X = -1/2 inch		x = -1/4 inch	
Y(in.)	U(ft/sec.)	Y(in.)	U(ft/sec.)	Y(in.)	U(ft/sec.)
0.040	1.36	0.040	1.22	0.035	1.10
0.045	1.50	0.045	1.36	0.040	1.28
0.050	1.62	0.050	1.50	0.045	1.47
0.055	1.75	0.055	1.67	0.050	1.59
0.060	1.94	0.060	1.84	0.055	1.80
0.065	2.12	0.065	1.96	0.060	1.98
0.070	2.19	0.070	2.10	0.065	2.07
0.075	2.29	0.075	2.25	0.070	2.17
0.080	2.45	0.080	2.38	0.075	2.41
0.085	2.56	0.085	2.50	0.080	2.50
0.090	2.63	0.090	2.62	0.085	2.57
0.095	2.70	0.095	2.72	0.090	2.77
0.100	2.77	0.100	2.86	0.100	3.02
0.105	2.79	0.105	2.98	0.105	3.08
0.110	3.01	0.110	3.10	0.110	3.22
0.115	3.10	0.115	3.19	0.115	3.37
0.120	3.17	0.120	3.30	0.120	3.43
0.125	3.23	0.125	3.36	0.125	3.49
0.130	3.41	0.130	3.45	0.130	3.59
0.135	3.49	0.135	3.54	0.135	3.76
0.140	3.59	0.140	3.73	0.140	3.93
0.145	3.72	0.145	3.81	0.145	4.05
0.150	3.84	0.150	3.90	0.150	4.11
0.155	3.93	0.155	4.01	0.155	4.31
0.160	4.01	0.160	4.13	0.160	4.49
0.165	4.10	0.165	4.25	0.165	4.60
0.170	4.16	0.170	4.35	0.170	4.69
0.175	4.22	0.175	4.44	0.175	4.80
0.180	4.28	0.180	4.53	0.185	4.95
0.190	4.44	0.190	4.63	0.200	5.02
0.205	4.58	0.205	5.00	0.210	5.15
0.215	4.87	0.215	5.18	0.225	5.37
0.230	5.03	0.230	5.30	0.235	5.51
0.240	5.25	0.240	5.51	0.250	5.79
0.255	5.37	0.255	5.65	0.260	5.98
0.265	5.58	0.265	5.81	0.275	6.12
0.280	5.67	0.280	5.88	0.285	6.20
0.290	5.83	0.290	6.01	0.300	6.31
0.305	5.94	0.305	6.14	0.310	6.43
0.315	6.09	0.315	6.22	0.325	6.51
0.330	6.14	0.330	6.33	0.350	6.62
0.355	6.22	0.355	6.47	0.375	6.72
0.380	6.31	0.380	6.66	0.400	6.73
0.405	6.36	0.405	6.80	0.425	6.73
0.430	6.46	0.430	6.81	0.450	6.83
0.455	6.50	0.455	6.81	0.475	6.83
0.480	6.51	0.480	6.83	0.500	6.85
0.505	6.53	0.505	6.83	0.525	6.85
0.530	6.59	0.530	6.85	0.550	6.85
0.555	6.59	0.555	6.85	0.575	6.87
0.580	6.59	0.580	6.85	0.600	6.87
0.605	6.59	0.605	6.85	0.625	6.87
0.650	6.59	0.650	6.85	0.650	6.87
0.675	6.59	0.700	6.85	0.700	6.87
0.700	6.59	0.750	6.85	0.750	6.87
0.750	6.59	0.800	6.85	0.800	6.87
0.800	6.59	0.850	6.85	0.850	6.87
0.850	6.59	0.900	6.85	0.900	6.87
0.900	6.59	0.950	6.85	0.950	6.87
1.000	6.59	1.000	6.85	1.000	6.87

Q_s = 0.0 SCFH/FT.

X = 0.0 Upst. Edge of Suction Slot		X = 1/4 inch		X = 1/2 inch	
Y(in.)	U(ft/sec.)	Y(in.)	U(ft/sec.)	Y(in.)	U(ft/sec.)
0.035	1.21	0.035	1.15	0.035	1.05
0.040	1.29	0.040	1.30	0.040	1.18
0.045	1.47	0.045	1.43	0.045	1.36
0.050	1.62	0.050	1.64	0.050	1.50
0.055	1.77	0.055	1.85	0.055	1.77
0.060	1.97	0.060	2.01	0.060	1.95
0.065	2.07	0.065	2.13	0.065	2.13
0.070	2.21	0.070	2.25	0.070	2.30
0.075	2.36	0.075	2.41	0.075	2.46
0.080	2.49	0.080	2.57	0.080	2.59
0.085	2.55	0.085	2.67	0.085	2.64
0.090	2.60	0.090	2.77	0.090	2.71
0.095	2.63	0.095	2.84	0.095	2.76
0.100	2.67	0.100	2.97	0.100	2.79
0.105	2.85	0.105	3.10	0.105	2.91
0.110	2.97	0.110	3.20	0.110	2.96
0.115	3.03	0.115	3.34	0.115	3.04
0.120	3.15	0.120	3.54	0.120	3.19
0.125	3.28	0.125	3.62	0.125	3.30
0.130	3.38	0.130	3.78	0.130	3.49
0.135	3.41	0.135	3.93	0.135	3.63
0.140	3.61	0.140	4.00	0.140	3.73
0.145	3.74	0.145	4.07	0.145	3.85
0.150	3.81	0.150	4.16	0.150	3.93
0.155	3.88	0.155	4.34	0.155	3.98
0.160	3.98	0.160	4.47	0.160	4.04
0.165	4.10	0.165	4.64	0.165	4.22
0.170	4.19	0.170	4.77	0.170	4.34
0.175	4.32	0.175	4.88	0.175	4.52
0.180	4.37	0.185	4.93	0.185	4.77
0.185	4.44	0.200	5.13	0.200	4.95
0.190	4.57	0.210	5.27	0.210	5.13
0.195	4.64	0.225	5.60	0.225	5.27
0.200	4.71	0.235	5.74	0.235	5.46
0.205	4.76	0.250	5.94	0.250	5.60
0.210	4.87	0.260	6.07	0.260	5.76
0.215	4.90	0.275	6.24	0.275	5.92
0.220	4.95	0.285	6.33	0.285	6.01
0.225	5.02	0.300	6.43	0.300	6.14
0.230	5.05	0.310	6.50	0.310	6.27
0.235	5.13	0.325	6.53	0.325	6.33
0.240	5.22	0.350	6.55	0.350	6.41
0.245	5.28	0.375	6.64	0.375	6.49
0.250	5.37	0.400	6.76	0.400	6.58
0.260	5.42	0.425	6.81	0.425	6.61
0.275	5.60	0.450	6.83	0.450	6.64
0.285	5.63	0.475	6.86	0.475	6.67
0.300	5.76	0.500	6.86	0.500	6.69
0.310	5.90	0.525	6.87	0.525	6.71
0.325	5.99	0.550	6.87	0.550	6.72
0.335	6.09	0.575	6.87	0.575	6.72
0.350	6.14	0.600	6.87	0.600	6.74
0.360	6.18	0.625	6.87	0.625	6.75
0.375	6.24	0.650	6.87	0.650	6.75
0.385	6.31	0.675	6.87	0.675	6.75
0.450	6.39	0.700	6.87	0.700	6.75
0.500	6.43	0.750	6.87	0.750	6.75
0.600	6.48	0.800	6.87	0.800	6.75
0.800	6.48	0.900	6.87	0.900	6.75
1.000	6.48	1.000	6.87	1.000	6.75

Q_s = 0.0 SCFH/FT.

X = 1 inch

Y(in.)	U(ft/sec.)
0.035	1.22
0.040	1.40
0.045	1.60
0.050	1.76
0.055	1.93
0.060	2.05
0.065	2.30
0.070	2.41
0.075	2.55
0.080	2.70
0.085	2.84
0.090	3.15
0.095	3.34
0.100	3.47
0.105	3.61
0.110	3.76
0.115	3.90
0.120	3.95
0.125	4.03
0.130	4.10
0.135	4.17
0.140	4.28
0.145	4.37
0.150	4.47
0.155	4.63
0.160	4.79
0.165	4.95
0.170	5.07
0.175	5.12
0.180	5.17
0.190	5.23
0.200	5.42
0.210	5.69
0.220	5.83
0.230	5.99
0.240	6.14
0.250	6.29
0.275	6.62
0.300	6.80
0.325	6.98
0.350	7.17
0.375	7.33
0.400	7.44
0.425	7.52
0.450	7.59
0.475	7.59
0.500	7.59
0.525	7.59
0.550	7.59
0.575	7.59
0.600	7.59
0.625	7.59
0.650	7.59
0.675	7.59
0.700	7.59
0.750	7.59
0.800	7.59
0.850	7.59
0.900	7.59
1.000	7.59

X = 2 inches

Y(in.)	U(ft/sec.)
0.035	1.33
0.040	1.52
0.045	1.64
0.050	1.81
0.055	1.94
0.060	2.16
0.065	2.30
0.070	2.41
0.075	2.47
0.080	2.52
0.085	2.63
0.090	2.74
0.095	2.82
0.100	2.91
0.105	2.97
0.110	3.03
0.115	3.17
0.120	3.23
0.125	3.34
0.130	3.45
0.135	3.55
0.140	3.67
0.145	3.78
0.150	3.87
0.155	3.98
0.160	4.07
0.165	4.17
0.170	4.28
0.175	4.40
0.185	4.60
0.200	4.79
0.210	4.93
0.225	5.15
0.235	5.28
0.250	5.46
0.260	5.60
0.275	5.74
0.285	5.92
0.300	6.03
0.310	6.11
0.325	6.20
0.350	6.35
0.375	6.49
0.400	6.57
0.425	6.61
0.450	6.65
0.475	6.69
0.500	6.73
0.525	6.75
0.550	6.75
0.575	6.75
0.600	6.77
0.625	6.79
0.650	6.79
0.675	6.79
0.700	6.79
0.750	6.79
0.800	6.79
0.900	6.79
1.000	6.79

X = 3 inches

Y(in.)	U(ft/sec.)
0.045	1.36
0.050	1.52
0.055	1.67
0.060	1.82
0.065	2.01
0.070	2.13
0.075	2.26
0.080	2.44
0.085	2.57
0.090	2.74
0.095	2.84
0.100	2.91
0.105	2.97
0.110	3.03
0.115	3.10
0.120	3.19
0.125	3.25
0.130	3.36
0.135	3.43
0.140	3.57
0.145	3.69
0.150	3.78
0.155	3.88
0.160	3.94
0.165	4.05
0.170	4.14
0.175	4.25
0.180	4.37
0.185	4.43
0.195	4.63
0.210	4.85
0.220	5.00
0.235	5.18
0.245	5.34
0.260	5.51
0.270	5.58
0.285	5.70
0.295	5.83
0.310	5.99
0.320	6.09
0.335	6.16
0.360	6.31
0.385	6.39
0.410	6.51
0.435	6.55
0.460	6.65
0.485	6.67
0.510	6.71
0.535	6.73
0.560	6.75
0.585	6.75
0.610	6.75
0.650	6.75
0.700	6.75
0.750	6.75
0.800	6.75
0.850	6.75
0.900	6.75
0.950	6.75
1.000	6.75

Q_s = 0.0 SCFH/FT.

X = 4 inches		X = 5 inches		X = 6 inches	
Y(in.)	U(ft/sec.)	Y(in.)	U(ft/sec.)	Y(in.)	U(ft/sec.)
0.040	1.22	0.045	1.18	0.045	1.15
0.045	1.32	0.050	1.33	0.050	1.26
0.050	1.49	0.055	1.46	0.055	1.38
0.055	1.62	0.060	1.56	0.060	1.50
0.060	1.79	0.065	1.76	0.065	1.62
0.065	1.94	0.070	1.89	0.070	1.76
0.070	2.01	0.075	2.00	0.075	1.87
0.075	2.13	0.080	2.11	0.080	2.05
0.080	2.25	0.085	2.23	0.085	2.21
0.085	2.41	0.090	2.34	0.090	2.32
0.090	2.56	0.095	2.43	0.095	2.37
0.095	2.66	0.100	2.52	0.100	2.50
0.100	2.72	0.105	2.64	0.105	2.68
0.105	2.79	0.110	2.77	0.110	2.82
0.110	2.91	0.115	2.83	0.115	2.96
0.115	3.03	0.120	2.97	0.120	3.12
0.120	3.10	0.125	3.08	0.125	3.22
0.125	3.18	0.130	3.24	0.130	3.28
0.130	3.25	0.135	3.38	0.135	3.37
0.135	3.45	0.140	3.43	0.140	3.43
0.140	3.55	0.145	3.54	0.145	3.61
0.145	3.65	0.150	3.67	0.150	3.69
0.150	3.73	0.155	3.78	0.155	3.78
0.155	3.87	0.160	3.83	0.160	3.85
0.160	4.03	0.165	3.93	0.165	3.98
0.165	4.14	0.170	4.04	0.170	4.11
0.170	4.19	0.175	4.14	0.175	4.17
0.175	4.29	0.180	4.25	0.180	4.25
0.180	4.40	0.185	4.34	0.185	4.31
0.190	4.53	0.195	4.47	0.195	4.43
0.205	4.68	0.210	4.72	0.210	4.72
0.215	4.85	0.220	4.87	0.220	4.92
0.230	5.08	0.235	5.15	0.235	5.08
0.240	5.22	0.245	5.27	0.245	5.27
0.255	5.42	0.260	5.44	0.260	5.40
0.265	5.61	0.270	5.53	0.270	5.56
0.280	5.69	0.285	5.65	0.285	5.76
0.290	5.72	0.295	5.81	0.295	5.83
0.305	5.83	0.310	5.92	0.310	5.92
0.315	5.94	0.320	6.12	0.320	6.11
0.330	6.05	0.335	6.18	0.335	6.22
0.355	6.16	0.360	6.29	0.360	6.29
0.380	6.35	0.385	6.35	0.385	6.37
0.405	6.51	0.410	6.45	0.410	6.51
0.430	6.54	0.435	6.51	0.435	6.53
0.455	6.56	0.460	6.57	0.460	6.57
0.480	6.57	0.485	6.63	0.485	6.61
0.505	6.59	0.510	6.63	0.510	6.65
0.530	6.61	0.535	6.65	0.535	6.69
0.555	6.63	0.560	6.67	0.570	6.69
0.580	6.63	0.585	6.67	0.610	6.69
0.605	6.63	0.610	6.67	0.635	6.71
0.630	6.63	0.635	6.69	0.660	6.71
0.655	6.63	0.660	6.71	0.690	6.73
0.680	6.63	0.700	6.71	0.735	6.74
0.700	6.63	0.750	6.71	0.760	6.75
0.750	6.63	0.800	6.71	0.810	6.75
0.800	6.63	0.850	6.71	0.850	6.75
0.900	6.63	0.900	6.71	0.900	6.75
1.000	6.63	1.000	6.71	1.000	6.75

Q_s = 0.0 SCFH/FT.

X = 9 inches

Y(in.)	U(ft/sec.)
0.045	1.07
0.047	1.18
0.050	1.22
0.052	1.28
0.054	1.33
0.055	1.36
0.056	1.39
0.058	1.43
0.059	1.45
0.060	1.47
0.065	1.60
0.070	1.77
0.075	1.86
0.080	1.98
0.085	2.13
0.090	2.24
0.095	2.36
0.100	2.48
0.105	2.59
0.110	2.71
0.115	2.87
0.120	2.98
0.125	3.09
0.130	3.20
0.135	3.33
0.145	3.43
0.150	3.58
0.155	3.70
0.160	3.76
0.165	3.88
0.170	4.00
0.180	4.13
0.185	4.22
0.190	4.31
0.195	4.43
0.200	4.55
0.205	4.64
0.210	4.74
0.215	4.84
0.225	4.97
0.235	5.05
0.245	5.18
0.255	5.28
0.275	5.51
0.300	5.74
0.310	5.99
0.325	6.12
0.350	6.26
0.375	6.37
0.400	6.49
0.425	6.54
0.450	6.64
0.500	6.70
0.550	6.82
0.600	6.83
0.700	6.83
0.750	6.85
0.800	6.85
0.900	6.85
1.000	6.85

X = 12 inches

Y(in.)	U(ft/sec.)
0.045	1.15
0.050	1.36
0.055	1.44
0.060	1.64
0.065	1.69
0.070	1.82
0.075	2.00
0.080	2.10
0.085	2.30
0.090	2.46
0.095	2.68
0.100	2.79
0.105	2.91
0.110	3.05
0.115	3.15
0.120	3.27
0.125	3.41
0.130	3.53
0.135	3.59
0.140	3.67
0.145	3.81
0.150	3.95
0.160	4.10
0.165	4.20
0.170	4.40
0.180	4.55
0.190	4.63
0.200	4.74
0.205	4.80
0.210	4.93
0.220	5.03
0.225	5.12
0.235	5.20
0.240	5.30
0.245	5.37
0.250	5.46
0.260	5.53
0.270	5.67
0.280	5.83
0.290	5.92
0.300	6.01
0.310	6.14
0.320	6.35
0.330	6.39
0.350	6.51
0.375	6.64
0.425	6.80
0.450	6.86
0.500	6.96
0.525	7.04
0.550	7.04
0.600	7.05
0.625	7.07
0.650	7.07
0.675	7.07
0.700	7.07
0.725	7.07
0.800	7.09
0.850	7.11
1.000	7.11

X = 15 inches

Y(in.)	U(ft/sec.)
0.045	1.22
0.050	1.40
0.055	1.48
0.060	1.60
0.065	1.77
0.070	1.86
0.075	1.96
0.080	2.06
0.085	2.17
0.090	2.26
0.095	2.47
0.100	2.60
0.105	2.62
0.110	2.75
0.115	2.89
0.120	3.03
0.125	3.10
0.130	3.24
0.135	3.32
0.140	3.38
0.145	3.47
0.150	3.54
0.155	3.61
0.160	3.70
0.165	3.81
0.170	3.87
0.175	3.94
0.180	4.01
0.185	4.16
0.190	4.26
0.195	4.35
0.200	4.44
0.205	4.55
0.210	4.60
0.220	4.74
0.230	4.85
0.240	4.98
0.250	5.12
0.260	5.30
0.270	5.40
0.280	5.49
0.290	5.58
0.300	5.70
0.310	5.79
0.320	5.85
0.330	5.96
0.340	6.07
0.350	6.11
0.375	6.18
0.400	6.29
0.425	6.39
0.450	6.51
0.475	6.56
0.500	6.62
0.550	6.67
0.575	6.69
0.650	6.69
0.750	6.71
0.800	6.71
1.000	6.71

Q_s = 0.0 SCFH/FT.

X = 18 inches		X = 21 inches		X = 24 inches	
Y(in.)	U(ft/sec.)	Y(in.)	U(ft/sec.)	Y(in.)	U(ft/sec.)
0.045	1.29	0.045	1.44	0.045	1.56
0.050	1.38	0.050	1.57	0.050	1.67
0.055	1.47	0.055	1.73	0.055	1.77
0.060	1.56	0.060	1.81	0.060	1.90
0.065	1.78	0.065	1.94	0.065	2.07
0.070	1.98	0.070	2.01	0.070	2.16
0.076	2.06	0.075	2.18	0.075	2.31
0.080	2.15	0.080	2.29	0.080	2.45
0.085	2.27	0.085	2.37	0.085	2.50
0.090	2.44	0.090	2.45	0.090	2.63
0.095	2.55	0.095	2.56	0.095	2.72
0.100	2.63	0.100	2.66	0.100	2.80
0.105	2.69	0.105	2.74	0.105	2.86
0.110	2.84	0.110	2.82	0.110	2.92
0.115	2.97	0.115	3.08	0.115	3.04
0.120	3.12	0.120	3.29	0.120	3.18
0.125	3.20	0.125	3.49	0.125	3.32
0.130	3.29	0.130	3.51	0.130	3.43
0.135	3.45	0.135	3.62	0.135	3.57
0.140	3.51	0.140	3.74	0.140	3.67
0.145	3.70	0.145	3.81	0.150	3.80
0.150	3.73	0.150	3.85	0.155	3.93
0.155	3.81	0.155	3.94	0.160	4.04
0.160	3.90	0.160	4.00	0.165	4.17
0.165	4.00	0.165	4.07	0.170	4.25
0.170	4.07	0.170	4.19	0.175	4.34
0.175	4.16	0.175	4.23	0.185	4.50
0.180	4.26	0.180	4.29	0.190	4.63
0.185	4.40	0.185	4.41	0.195	4.71
0.190	4.52	0.190	4.53	0.215	4.80
0.195	4.60	0.195	4.61	0.220	4.85
0.200	4.74	0.200	4.74	0.225	4.97
0.205	4.85	0.205	4.77	0.230	5.10
0.210	4.92	0.210	4.80	0.235	5.25
0.215	5.00	0.220	4.88	0.240	5.34
0.220	5.08	0.230	5.07	0.245	5.35
0.225	5.13	0.240	5.22	0.250	5.40
0.230	5.22	0.250	5.40	0.270	5.54
0.240	5.34	0.260	5.58	0.280	5.65
0.250	5.47	0.270	5.81	0.290	5.76
0.260	5.65	0.280	5.88	0.300	5.90
0.270	5.81	0.300	5.99	0.310	6.01
0.280	5.90	0.320	6.14	0.320	6.07
0.290	5.98	0.330	6.22	0.330	6.12
0.300	6.11	0.340	6.29	0.340	6.16
0.320	6.27	0.350	6.41	0.350	6.20
0.340	6.35	0.375	6.60	0.370	6.27
0.350	6.39	0.400	6.68	0.380	6.39
0.375	6.49	0.425	6.80	0.390	6.49
0.400	6.58	0.450	6.81	0.410	6.54
0.425	6.68	0.475	6.85	0.420	6.56
0.475	6.75	0.500	6.89	0.440	6.62
0.500	6.87	0.525	6.91	0.450	6.66
0.550	6.95	0.550	6.93	0.475	6.72
0.600	6.99	0.575	7.01	0.500	6.74
0.650	7.01	0.625	7.03	0.550	6.78
0.700	7.01	0.700	7.03	0.650	6.80
0.800	7.03	0.800	7.05	0.800	6.82
0.900	7.03	0.900	7.05	0.900	6.82
1.000	7.03	1.000	7.05	1.000	6.82

TABLE 2

Q_s = 53.33 SCFH/FT.

X = -6 inches		X = -4 inches		X = -2 inches	
Y(in.)	U(ft/sec.)	Y(in.)	U(ft/sec.)	Y(in.)	U(ft/sec.)
0.045	1.19	0.045	1.38	0.045	1.58
0.050	1.32	0.050	1.48	0.050	1.69
0.055	1.46	0.055	1.62	0.055	1.80
0.060	1.61	0.060	1.74	0.060	1.98
0.065	1.81	0.065	1.91	0.065	2.13
0.070	1.95	0.070	2.05	0.070	2.33
0.075	2.08	0.075	2.17	0.075	2.66
0.080	2.19	0.080	2.35	0.080	2.83
0.085	2.34	0.085	2.42	0.085	2.97
0.090	2.49	0.090	2.58	0.090	3.03
0.095	2.58	0.095	2.72	0.095	3.13
0.100	2.71	0.100	2.81	0.100	3.24
0.105	2.89	0.105	2.97	0.105	3.37
0.110	2.97	0.110	3.09	0.110	3.49
0.115	3.08	0.115	3.18	0.115	3.61
0.120	3.20	0.120	3.32	0.120	3.76
0.125	3.33	0.125	3.46	0.125	3.85
0.130	3.45	0.130	3.53	0.130	3.95
0.135	3.57	0.135	3.61	0.135	4.02
0.140	3.68	0.140	3.69	0.140	4.17
0.145	3.73	0.145	3.82	0.145	4.26
0.150	3.79	0.150	3.89	0.150	4.32
0.155	3.86	0.155	3.99	0.155	4.42
0.160	3.95	0.160	4.06	0.160	4.58
0.165	4.05	0.165	4.14	0.165	4.64
0.170	4.17	0.170	4.26	0.170	4.69
0.175	4.26	0.175	4.36	0.175	4.77
0.180	4.33	0.180	4.47	0.180	4.87
0.185	4.39	0.185	4.53	0.185	5.02
0.190	4.45	0.190	4.63	0.190	5.17
0.195	4.60	0.195	4.69	0.195	5.31
0.200	4.72	0.200	4.79	0.200	5.38
0.210	4.92	0.210	4.92	0.210	5.46
0.220	5.03	0.220	5.05	0.220	5.64
0.230	5.22	0.230	5.22	0.230	5.79
0.240	5.36	0.240	5.36	0.240	5.90
0.250	5.43	0.250	5.52	0.250	6.03
0.260	5.50	0.260	5.61	0.260	6.16
0.270	5.62	0.270	5.66	0.270	6.21
0.280	5.75	0.280	5.77	0.280	6.27
0.290	5.82	0.290	5.82	0.290	6.35
0.300	5.90	0.300	5.88	0.300	6.43
0.325	6.06	0.310	6.01	0.325	6.54
0.350	6.18	0.320	6.12	0.350	6.66
0.375	6.27	0.330	6.13	0.375	6.82
0.400	6.33	0.340	6.16	0.400	6.86
0.425	6.35	0.350	6.20	0.425	6.92
0.450	6.37	0.375	6.23	0.450	6.94
0.475	6.39	0.400	6.33	0.475	6.94
0.500	6.41	0.425	6.38	0.500	6.96
0.525	6.41	0.450	6.42	0.525	6.96
0.550	6.43	0.475	6.44	0.550	6.96
0.575	6.43	0.500	6.46	0.575	6.96
0.600	6.43	0.525	6.47	0.600	6.98
0.625	6.46	0.550	6.47	0.625	6.98
0.650	6.46	0.600	6.47	0.650	6.98
0.700	6.46	0.700	6.47	0.700	6.98
0.800	6.46	0.800	6.47	0.800	6.98
0.900	6.46	0.900	6.47	0.900	6.98
1.000	6.46	1.000	6.47	1.000	6.98

Q_s = 53.33 SCFH/FT.

X = -1 inch		X = -1/2 inch		X = -1/4 inch	
Y(in.)	U(ft/sec.)	Y(in.)	U(ft/sec.)	Y(in.)	U(ft/sec.)
0.040	1.71	0.040	1.80	0.035	1.96
0.045	1.83	0.045	1.96	0.040	2.18
0.050	1.98	0.050	2.09	0.045	2.28
0.055	2.13	0.055	2.24	0.050	2.42
0.060	2.28	0.060	2.36	0.055	2.62
0.065	2.45	0.065	2.49	0.060	2.83
0.070	2.62	0.070	2.66	0.065	3.04
0.075	2.79	0.075	2.87	0.070	3.18
0.080	2.95	0.080	3.05	0.075	3.32
0.085	3.14	0.085	3.20	0.080	3.47
0.090	3.25	0.090	3.38	0.085	3.60
0.095	3.46	0.095	3.61	0.090	3.71
0.100	3.60	0.100	3.68	0.095	3.79
0.105	3.71	0.105	3.73	0.100	3.89
0.110	3.79	0.110	3.83	0.105	4.06
0.115	3.90	0.115	3.93	0.110	4.17
0.120	3.99	0.120	4.11	0.115	4.27
0.125	4.12	0.125	4.24	0.120	4.38
0.130	4.24	0.130	4.33	0.125	4.52
0.135	4.33	0.135	4.44	0.130	4.64
0.140	4.47	0.140	4.49	0.135	4.79
0.145	4.60	0.145	4.56	0.140	4.85
0.150	4.71	0.150	4.68	0.145	4.90
0.155	4.79	0.155	4.89	0.150	4.95
0.160	4.87	0.160	5.02	0.155	5.05
0.165	4.95	0.165	5.20	0.160	5.17
0.170	5.00	0.170	5.34	0.165	5.27
0.175	5.10	0.175	5.45	0.170	5.39
0.180	5.22	0.180	5.53	0.175	5.50
0.185	5.31	0.185	5.66	0.180	5.64
0.190	5.36	0.190	5.73	0.185	5.70
0.195	5.41	0.195	5.79	0.190	5.77
0.200	5.48	0.200	5.86	0.195	5.84
0.210	5.68	0.210	6.04	0.200	5.90
0.220	5.79	0.220	6.08	0.210	6.01
0.230	5.90	0.230	6.16	0.220	6.16
0.240	6.01	0.240	6.20	0.230	6.27
0.250	6.12	0.250	6.31	0.240	6.39
0.260	6.21	0.260	6.37	0.250	6.52
0.270	6.25	0.270	6.43	0.260	6.60
0.280	6.33	0.280	6.46	0.270	6.64
0.290	6.46	0.290	6.54	0.280	6.68
0.300	6.58	0.300	6.60	0.290	6.74
0.325	6.72	0.325	6.70	0.300	6.78
0.350	6.76	0.350	6.80	0.325	6.80
0.375	6.84	0.375	6.90	0.350	6.82
0.400	6.86	0.400	6.92	0.375	6.86
0.425	6.96	0.425	6.98	0.400	6.90
0.450	6.96	0.450	6.98	0.425	6.92
0.475	6.98	0.475	7.01	0.450	6.94
0.500	6.98	0.500	7.01	0.475	6.94
0.525	6.98	0.525	7.03	0.500	6.98
0.550	6.98	0.550	7.04	0.525	6.98
0.575	6.98	0.575	7.05	0.550	6.98
0.600	7.01	0.600	7.05	0.575	6.98
0.650	7.01	0.650	7.05	0.600	6.98
0.700	7.01	0.700	7.05	0.700	6.98
0.800	7.01	0.800	7.05	0.800	6.98
0.900	7.03	0.900	7.05	0.900	6.98
1.000	7.03	1.000	7.05	1.000	6.98

Q_s = 53.33 SCFH/FT.

X = 0.0 Upst. Edge of Suction Slot		X = 1/4 inch		X = 1/2 inch	
Y(in.)	U(ft/sec.)	Y(in.)	U(ft/sec.)	Y(in.)	U(ft/sec.)
0.035	2.49	0.035	1.80	0.035	1.71
0.040	2.60	0.040	1.89	0.040	1.89
0.045	2.72	0.045	2.13	0.045	2.13
0.050	2.88	0.050	2.24	0.050	2.38
0.055	3.21	0.055	2.44	0.055	2.59
0.060	3.32	0.060	2.60	0.060	2.86
0.065	3.47	0.065	2.85	0.065	2.99
0.070	3.54	0.070	3.01	0.070	3.18
0.075	3.62	0.075	3.20	0.075	3.32
0.080	3.68	0.080	3.34	0.080	3.45
0.085	3.73	0.085	3.44	0.085	3.54
0.090	3.82	0.090	3.52	0.090	3.64
0.095	3.95	0.095	3.64	0.095	3.72
0.100	4.05	0.100	3.73	0.100	3.80
0.105	4.17	0.105	3.80	0.105	3.87
0.110	4.33	0.110	3.90	0.110	3.98
0.115	4.44	0.115	3.98	0.115	4.09
0.120	4.58	0.120	4.08	0.120	4.20
0.125	4.72	0.125	4.20	0.125	4.26
0.130	4.82	0.130	4.24	0.130	4.33
0.135	4.95	0.135	4.29	0.135	4.39
0.140	4.98	0.140	4.38	0.140	4.47
0.145	5.02	0.145	4.45	0.145	4.53
0.150	5.05	0.150	4.53	0.150	4.60
0.155	5.12	0.155	4.63	0.155	4.64
0.160	5.17	0.160	4.71	0.160	4.69
0.165	5.26	0.165	4.77	0.165	4.77
0.170	5.34	0.170	4.80	0.170	4.85
0.175	5.41	0.175	4.87	0.175	4.92
0.180	5.50	0.180	4.94	0.180	4.97
0.185	5.57	0.185	5.00	0.185	5.05
0.190	5.68	0.190	5.05	0.190	5.14
0.195	5.77	0.195	5.12	0.195	5.19
0.200	5.84	0.200	5.19	0.200	5.24
0.210	5.90	0.210	5.27	0.210	5.29
0.220	6.06	0.220	5.36	0.220	5.39
0.230	6.16	0.230	5.45	0.230	5.46
0.240	6.21	0.240	5.53	0.240	5.53
0.250	6.23	0.250	5.64	0.250	5.61
0.260	6.37	0.260	5.79	0.260	5.68
0.270	6.43	0.270	5.82	0.270	5.75
0.280	6.48	0.280	5.84	0.280	5.82
0.290	6.54	0.290	5.90	0.290	5.86
0.300	6.56	0.300	5.95	0.300	5.90
0.325	6.70	0.325	6.01	0.325	5.99
0.350	6.80	0.350	6.10	0.350	6.08
0.375	6.86	0.375	6.16	0.375	6.12
0.400	6.86	0.400	6.21	0.400	6.16
0.425	6.90	0.425	6.23	0.425	6.21
0.450	6.92	0.450	6.25	0.450	6.23
0.475	6.94	0.475	6.27	0.475	6.23
0.500	6.94	0.500	6.29	0.500	6.25
0.525	6.94	0.525	6.31	0.525	6.26
0.550	6.94	0.550	6.31	0.550	6.27
0.575	6.95	0.575	6.33	0.575	6.27
0.600	6.96	0.600	6.33	0.600	6.29
0.700	6.97	0.700	6.35	0.700	6.30
0.800	6.97	0.800	6.35	0.800	6.31
0.900	6.98	0.900	6.35	0.900	6.33
1.000	6.98	1.000	6.35	1.000	6.33

Q_s = 53.33 SCFH/FT.

X = 1 inch		X = 2 inches		X = 3 inches	
Y(in.)	U(ft/sec.)	Y(in.)	U(ft/sec.)	Y(in.)	U(ft/sec.)
0.035	1.66	0.035	1.80	0.040	2.03
0.040	1.87	0.040	2.06	0.045	2.26
0.045	2.13	0.045	2.28	0.050	2.60
0.050	2.44	0.050	2.49	0.055	2.75
0.055	2.58	0.055	2.71	0.060	2.91
0.060	2.82	0.060	2.89	0.065	3.08
0.065	2.95	0.065	3.05	0.070	3.20
0.070	3.14	0.070	3.19	0.075	3.34
0.080	3.40	0.075	3.40	0.080	3.50
0.085	3.54	0.080	3.52	0.085	3.68
0.090	3.65	0.085	3.64	0.090	3.85
0.095	3.75	0.090	3.79	0.095	4.17
0.100	3.82	0.095	3.87	0.100	4.27
0.105	3.89	0.100	3.96	0.105	4.35
0.110	3.99	0.105	4.09	0.110	4.39
0.115	4.06	0.110	4.18	0.115	4.49
0.120	4.23	0.115	4.26	0.120	4.56
0.125	4.36	0.120	4.38	0.125	4.66
0.130	4.50	0.125	4.47	0.130	4.76
0.135	4.58	0.130	4.52	0.135	4.82
0.140	4.64	0.135	4.56	0.140	4.92
0.145	4.68	0.140	4.68	0.145	5.00
0.150	4.71	0.145	4.76	0.150	5.09
0.155	4.80	0.150	4.82	0.155	5.12
0.160	4.89	0.155	4.85	0.160	5.26
0.165	4.94	0.160	4.89	0.165	5.38
0.170	5.02	0.165	5.00	0.170	5.46
0.175	5.03	0.170	5.09	0.175	5.52
0.180	5.09	0.175	5.15	0.180	5.57
0.185	5.15	0.180	5.24	0.185	5.62
0.190	5.19	0.185	5.27	0.190	5.70
0.195	5.24	0.190	5.36	0.195	5.73
0.200	5.29	0.195	5.39	0.200	5.77
0.210	5.36	0.200	5.45	0.210	5.86
0.220	5.46	0.210	5.57	0.220	5.97
0.230	5.57	0.220	5.64	0.230	6.03
0.240	5.62	0.230	5.71	0.240	6.12
0.250	5.68	0.240	5.80	0.250	6.16
0.260	5.77	0.250	5.86	0.260	6.23
0.270	5.82	0.260	5.95	0.270	6.29
0.280	5.88	0.270	6.03	0.280	6.33
0.290	5.93	0.280	6.06	0.290	6.43
0.300	5.99	0.290	6.08	0.300	6.46
0.325	6.04	0.300	6.10	0.325	6.56
0.350	6.10	0.325	6.14	0.350	6.60
0.375	6.16	0.350	6.16	0.375	6.62
0.400	6.18	0.375	6.20	0.400	6.66
0.425	6.20	0.400	6.21	0.425	6.68
0.450	6.21	0.425	6.23	0.450	6.76
0.475	6.22	0.450	6.25	0.475	6.80
0.500	6.24	0.475	6.27	0.500	6.80
0.525	6.24	0.500	6.29	0.525	6.80
0.550	6.25	0.525	6.31	0.550	6.80
0.575	6.25	0.550	6.32	0.575	6.80
0.600	6.25	0.575	6.32	0.600	6.80
0.650	6.26	0.600	6.32	0.650	6.80
0.700	6.27	0.700	6.32	0.700	6.80
0.800	6.28	0.800	6.33	0.800	6.80
0.900	6.29	0.900	6.33	0.900	6.80
1.000	6.29	1.000	6.33	1.000	6.80

Q_s = 53.33 SCFH/FT.

X = 4 inches		X = 5 inches		X = 6 inches	
Y(in.)	U(ft/sec.)	Y(in.)	U(ft/sec.)	Y(in.)	U(ft/sec.)
0.040	1.89	0.045	1.54	0.045	1.62
0.045	2.03	0.050	1.73	0.050	1.73
0.050	2.16	0.055	1.84	0.055	1.91
0.055	2.38	0.060	2.08	0.060	2.13
0.060	2.60	0.065	2.40	0.065	2.34
0.065	2.83	0.070	2.55	0.070	2.50
0.070	3.01	0.075	2.72	0.075	2.72
0.075	3.23	0.080	2.93	0.080	2.89
0.080	3.44	0.085	3.14	0.085	2.98
0.085	3.52	0.090	3.33	0.090	3.13
0.090	3.68	0.095	3.52	0.095	3.27
0.095	3.85	0.100	3.66	0.100	3.38
0.100	3.96	0.105	3.82	0.105	3.46
0.105	4.15	0.110	3.93	0.110	3.57
0.110	4.27	0.115	4.02	0.115	3.68
0.115	4.32	0.120	4.24	0.120	3.78
0.120	4.42	0.125	4.35	0.125	3.90
0.125	4.52	0.130	4.41	0.130	3.98
0.130	4.77	0.135	4.49	0.135	4.05
0.135	4.87	0.140	4.56	0.140	4.17
0.140	4.94	0.145	4.69	0.145	4.36
0.145	5.03	0.150	4.84	0.150	4.47
0.150	5.12	0.155	4.90	0.155	4.53
0.155	5.20	0.160	4.95	0.160	4.60
0.160	5.32	0.165	5.03	0.165	4.63
0.165	5.39	0.170	5.17	0.170	4.68
0.170	5.50	0.175	5.26	0.175	4.74
0.175	5.57	0.190	5.53	0.180	4.84
0.180	5.61	0.180	5.39	0.185	4.92
0.185	5.66	0.185	5.48	0.190	4.98
0.190	5.75	0.200	5.70	0.195	5.10
0.195	5.84	0.195	5.66	0.200	5.17
0.200	5.90	0.210	5.77	0.210	5.24
0.210	5.97	0.220	5.91	0.220	5.36
0.220	6.04	0.230	6.03	0.230	5.45
0.230	6.12	0.240	6.06	0.240	5.53
0.240	6.20	0.250	6.16	0.250	5.64
0.250	6.25	0.260	6.21	0.260	5.71
0.260	6.29	0.270	6.31	0.270	5.84
0.270	6.35	0.280	6.43	0.280	5.86
0.280	6.37	0.290	6.46	0.290	5.93
0.290	6.43	0.300	6.48	0.300	6.01
0.300	6.46	0.325	6.54	0.325	6.12
0.325	6.54	0.350	6.60	0.350	6.16
0.350	6.64	0.375	6.72	0.375	6.18
0.375	6.72	0.400	6.82	0.400	6.25
0.400	6.74	0.425	6.86	0.425	6.29
0.425	6.78	0.450	6.86	0.450	6.33
0.450	6.78	0.475	6.88	0.475	6.33
0.475	6.82	0.500	6.88	0.500	6.35
0.500	6.82	0.525	6.90	0.525	6.35
0.525	6.84	0.550	6.90	0.550	6.37
0.550	6.84	0.575	6.90	0.575	6.37
0.575	6.84	0.600	6.90	0.600	6.37
0.600	6.84	0.650	6.92	0.625	6.37
0.650	6.86	0.700	6.92	0.650	6.39
0.700	6.86	0.800	6.92	0.700	6.39
0.800	6.88	0.850	6.92	0.800	6.39
0.900	6.88	0.900	6.92	0.800	6.39
1.000	6.88	1.000	6.92	1.000	6.39

Q_s = 53.33 SCFH/FT.

X = 9 inches		X = 12 inches		X = 15 inches	
Y(in.)	U(ft/sec.)	Y(in.)	U(ft/sec.)	Y(in.)	U(ft/sec.)
0.045	1.23	0.045	1.30	0.045	1.23
0.050	1.42	0.050	1.46	0.050	1.34
0.055	1.62	0.055	1.62	0.055	1.54
0.060	1.80	0.060	1.84	0.060	1.71
0.065	2.00	0.065	2.04	0.065	1.81
0.070	2.17	0.070	2.13	0.070	1.96
0.075	2.32	0.075	2.23	0.075	2.12
0.080	2.45	0.080	2.34	0.080	2.28
0.085	2.58	0.085	2.52	0.085	2.43
0.090	2.72	0.090	2.66	0.090	2.60
0.095	2.83	0.095	2.81	0.095	2.74
0.100	2.98	0.100	2.95	0.100	2.83
0.105	3.13	0.105	3.09	0.105	2.93
0.110	3.21	0.110	3.20	0.110	3.03
0.115	3.30	0.115	3.30	0.115	3.13
0.120	3.41	0.120	3.38	0.120	3.25
0.125	3.50	0.125	3.54	0.125	3.38
0.130	3.60	0.130	3.71	0.130	3.50
0.135	3.78	0.135	3.89	0.135	3.62
0.140	3.96	0.140	4.03	0.140	3.73
0.145	4.03	0.145	4.11	0.145	3.85
0.150	4.09	0.150	4.26	0.150	3.95
0.155	4.18	0.155	4.38	0.155	4.05
0.160	4.26	0.160	4.47	0.160	4.17
0.165	4.38	0.165	4.55	0.165	4.29
0.170	4.45	0.170	4.64	0.170	4.38
0.175	4.52	0.175	4.72	0.175	4.50
0.180	4.68	0.180	4.82	0.180	4.63
0.185	4.72	0.185	4.90	0.185	4.74
0.190	4.80	0.190	4.97	0.190	4.80
0.195	4.87	0.195	5.02	0.195	4.84
0.200	4.90	0.200	5.09	0.200	4.89
0.210	5.05	0.210	5.22	0.210	4.98
0.220	5.12	0.220	5.29	0.220	5.12
0.230	5.22	0.230	5.43	0.230	5.29
0.240	5.41	0.240	5.53	0.240	5.45
0.250	5.55	0.250	5.64	0.250	5.50
0.260	5.66	0.260	5.79	0.260	5.64
0.270	5.73	0.270	5.93	0.270	5.79
0.280	5.79	0.280	6.01	0.280	5.88
0.290	5.82	0.290	6.04	0.290	5.99
0.300	5.88	0.300	6.10	0.300	6.03
0.325	5.97	0.325	6.21	0.325	6.16
0.350	6.04	0.350	6.29	0.350	6.31
0.375	6.12	0.375	6.39	0.375	6.41
0.400	6.20	0.400	6.48	0.400	6.48
0.425	6.27	0.425	6.48	0.425	6.54
0.450	6.29	0.450	6.52	0.450	6.60
0.475	6.31	0.475	6.60	0.475	6.64
0.500	6.33	0.500	6.60	0.500	6.64
0.525	6.39	0.525	6.60	0.525	6.64
0.550	6.39	0.550	6.60	0.550	6.66
0.575	6.39	0.575	6.60	0.575	6.66
0.600	6.39	0.600	6.60	0.600	6.68
0.650	6.39	0.650	6.60	0.650	6.70
0.700	6.39	0.700	6.60	0.700	6.70
0.750	6.39	0.750	6.60	0.750	6.70
0.800	6.39	0.800	6.60	0.800	6.70
0.900	6.39	0.900	6.60	0.900	6.70
1.000	6.39	1.000	6.60	1.000	6.70

Q_s = 53.33 SCFH/FT.

X = 18 inches		X = 21 inches		X = 24 inches	
Y(in.)	U(ft/sec.)	Y(in.)	U(ft/sec.)	Y(in.)	U(ft/sec.)
0.045	1.46	0.045	1.38	0.045	1.46
0.050	1.66	0.050	1.58	0.050	1.68
0.055	1.89	0.055	1.75	0.055	1.85
0.060	1.98	0.060	1.89	0.060	2.00
0.065	2.11	0.065	2.13	0.065	2.14
0.070	2.24	0.070	2.23	0.070	2.28
0.075	2.35	0.075	2.33	0.075	2.41
0.080	2.40	0.080	2.45	0.080	2.49
0.085	2.54	0.085	2.54	0.085	2.60
0.090	2.66	0.090	2.60	0.090	2.69
0.095	2.75	0.095	2.69	0.095	2.80
0.100	2.89	0.100	2.81	0.100	2.89
0.105	2.98	0.105	2.91	0.105	3.00
0.110	3.05	0.110	3.01	0.110	3.11
0.115	3.13	0.115	3.13	0.115	3.21
0.120	3.28	0.120	3.24	0.120	3.33
0.125	3.42	0.125	3.37	0.125	3.47
0.130	3.58	0.130	3.49	0.130	3.60
0.135	3.65	0.135	3.62	0.135	3.71
0.140	3.82	0.140	3.73	0.140	3.82
0.145	3.92	0.145	3.85	0.145	3.95
0.150	4.08	0.150	3.93	0.150	4.08
0.155	4.24	0.155	4.02	0.155	4.20
0.160	4.38	0.160	4.17	0.160	4.26
0.165	4.47	0.165	4.24	0.165	4.36
0.170	4.56	0.170	4.32	0.170	4.49
0.175	4.63	0.175	4.41	0.175	4.58
0.180	4.64	0.180	4.49	0.180	4.69
0.185	4.66	0.185	4.53	0.185	4.76
0.190	4.68	0.190	4.61	0.190	4.80
0.195	4.71	0.195	4.69	0.195	4.97
0.200	4.79	0.200	4.79	0.200	5.03
0.210	4.92	0.210	4.95	0.210	5.12
0.220	5.12	0.220	5.09	0.220	5.31
0.230	5.26	0.230	5.19	0.230	5.46
0.240	5.41	0.240	5.31	0.240	5.61
0.250	5.61	0.250	5.41	0.250	5.68
0.260	5.75	0.260	5.50	0.260	5.79
0.270	5.82	0.270	5.61	0.270	5.86
0.280	5.97	0.280	5.70	0.280	5.93
0.290	6.01	0.290	5.79	0.290	6.03
0.300	6.08	0.300	5.88	0.300	6.16
0.325	6.16	0.325	6.08	0.325	6.31
0.350	6.21	0.350	6.21	0.350	6.45
0.375	6.25	0.375	6.39	0.375	6.60
0.400	6.31	0.400	6.50	0.400	6.68
0.425	6.37	0.425	6.50	0.425	6.78
0.450	6.48	0.450	6.56	0.450	6.88
0.475	6.58	0.475	6.64	0.475	6.88
0.500	6.60	0.500	6.64	0.500	6.90
0.525	6.60	0.525	6.66	0.525	6.98
0.550	6.60	0.550	6.70	0.550	6.98
0.575	6.62	0.575	6.70	0.575	6.98
0.600	6.62	0.600	6.72	0.600	6.98
0.650	6.64	0.625	6.72	0.650	7.01
0.700	6.66	0.650	6.72	0.700	7.01
0.750	6.66	0.700	6.74	0.750	7.01
0.800	6.66	0.800	6.76	0.800	7.01
0.900	6.66	0.900	6.76	0.900	7.01
1.000	6.66	1.000	6.76	1.000	7.01

TABLE 3

Q_s = 133.33 SCFH/FT.

X = -6 inches		X = -4 inches		X = -2 inches	
Y(in.)	U(ft/sec.)	Y(in.)	U(ft/sec.)	Y(in.)	U(ft/sec.)
0.045	1.60	0.045	1.67	0.045	1.91
0.050	1.77	0.050	1.82	0.050	2.01
0.055	1.92	0.055	1.98	0.055	2.23
0.060	2.11	0.060	2.13	0.060	2.45
0.065	2.28	0.065	2.30	0.065	2.57
0.070	2.38	0.070	2.44	0.070	2.69
0.075	2.55	0.075	2.59	0.075	2.84
0.080	2.68	0.080	2.68	0.080	2.96
0.085	2.79	0.085	2.87	0.085	3.10
0.090	2.98	0.090	3.02	0.090	3.22
0.095	3.10	0.095	3.13	0.095	3.33
0.100	3.18	0.100	3.19	0.100	3.42
0.105	3.23	0.105	3.25	0.105	3.50
0.110	3.28	0.110	3.30	0.110	3.55
0.115	3.38	0.115	3.51	0.115	3.65
0.120	3.53	0.120	3.62	0.120	3.76
0.125	3.57	0.125	3.67	0.125	3.87
0.130	3.70	0.130	3.73	0.130	3.90
0.135	3.81	0.135	3.84	0.135	4.04
0.140	3.91	0.140	3.95	0.140	4.11
0.145	3.98	0.145	4.08	0.145	4.19
0.150	4.14	0.150	4.25	0.150	4.28
0.155	4.25	0.155	4.37	0.155	4.34
0.160	4.40	0.160	4.41	0.160	4.52
0.165	4.46	0.165	4.52	0.165	4.58
0.170	4.53	0.170	4.60	0.170	4.71
0.175	4.69	0.175	4.68	0.175	4.74
0.180	4.80	0.180	4.74	0.180	4.84
0.185	4.84	0.185	4.93	0.185	4.92
0.195	5.03	0.195	5.12	0.195	5.07
0.210	5.20	0.210	5.42	0.210	5.17
0.220	5.35	0.220	5.54	0.220	5.35
0.235	5.49	0.235	5.67	0.235	5.58
0.245	5.67	0.245	5.83	0.245	5.69
0.260	5.87	0.260	5.96	0.260	5.83
0.270	5.99	0.270	6.09	0.270	6.01
0.285	6.12	0.285	6.18	0.285	6.12
0.295	6.22	0.295	6.22	0.295	6.20
0.310	6.27	0.310	6.35	0.310	6.26
0.320	6.35	0.320	6.37	0.320	6.29
0.335	6.45	0.335	6.47	0.335	6.35
0.360	6.51	0.360	6.55	0.360	6.49
0.385	6.58	0.385	6.65	0.385	6.55
0.410	6.59	0.410	6.75	0.410	6.59
0.435	6.66	0.435	6.77	0.435	6.63
0.460	6.71	0.460	6.83	0.460	6.63
0.485	6.75	0.485	6.83	0.485	6.67
0.510	6.75	0.510	6.83	0.510	6.70
0.535	6.76	0.535	6.83	0.535	6.71
0.560	6.76	0.550	6.83	0.560	6.71
0.610	6.76	0.575	6.83	0.610	6.71
0.625	6.76	0.600	6.83	0.650	6.71
0.650	6.76	0.625	6.83	0.675	6.71
0.675	6.76	0.650	6.83	0.700	6.71
0.700	6.76	0.700	6.83	0.725	6.71
0.750	6.76	0.750	6.83	0.750	6.71
0.800	6.76	0.800	6.83	0.800	6.71
0.850	6.76	0.850	6.83	0.900	6.71
0.900	6.76	0.900	6.83	0.950	6.71
1.000	6.76	1.000	6.83	1.000	6.71

Q_s = 133.33 SCFH/FT.

X = -1 inch		X = -1/2 inch		X = -1/4 inch	
Y(in.)	U(ft/sec.)	Y(in.)	U(ft/sec.)	Y(in.)	U(ft/sec.)
0.040	2.17	0.040	2.42	0.035	3.01
0.045	2.33	0.045	2.64	0.040	3.17
0.050	2.51	0.050	2.80	0.045	3.33
0.055	2.67	0.055	2.98	0.050	3.53
0.060	2.78	0.060	3.17	0.055	3.70
0.065	3.01	0.065	3.29	0.060	3.83
0.070	3.13	0.070	3.45	0.065	3.95
0.075	3.25	0.075	3.57	0.070	4.07
0.080	3.37	0.080	3.67	0.075	4.20
0.085	3.49	0.085	3.80	0.080	4.37
0.090	3.57	0.090	3.94	0.085	4.46
0.095	3.62	0.095	4.03	0.090	4.64
0.100	3.67	0.100	4.14	0.095	4.71
0.105	3.73	0.105	4.23	0.100	4.84
0.110	3.93	0.110	4.40	0.105	4.93
0.115	3.98	0.115	4.47	0.110	5.03
0.120	4.04	0.120	4.55	0.115	5.17
0.125	4.10	0.125	4.64	0.120	5.27
0.130	4.19	0.130	4.72	0.125	5.51
0.135	4.31	0.135	4.85	0.130	5.58
0.140	4.41	0.140	4.98	0.135	5.67
0.145	4.52	0.145	5.10	0.140	5.74
0.150	4.58	0.150	5.18	0.145	5.81
0.155	4.64	0.155	5.27	0.150	5.87
0.160	4.72	0.160	5.34	0.155	5.90
0.165	4.77	0.165	5.37	0.160	5.94
0.170	4.90	0.170	5.51	0.165	5.98
0.175	5.00	0.175	5.56	0.170	6.11
0.180	5.13	0.180	5.67	0.175	6.18
0.190	5.27	0.190	5.79	0.185	6.33
0.205	5.49	0.205	5.94	0.200	6.47
0.215	5.67	0.215	6.11	0.210	6.58
0.230	5.81	0.230	6.18	0.225	6.62
0.240	5.87	0.240	6.29	0.235	6.70
0.255	6.05	0.255	6.39	0.250	6.78
0.265	6.14	0.265	6.62	0.260	6.80
0.280	6.22	0.280	6.84	0.275	6.82
0.290	6.27	0.290	6.94	0.285	6.90
0.305	6.33	0.305	6.97	0.300	6.92
0.315	6.37	0.315	6.97	0.310	7.04
0.330	6.45	0.330	6.97	0.325	7.08
0.355	6.55	0.355	6.97	0.350	7.10
0.380	6.58	0.380	6.98	0.375	7.10
0.405	6.67	0.405	6.99	0.400	7.10
0.430	6.67	0.430	6.99	0.425	7.10
0.455	6.69	0.455	7.03	0.450	7.10
0.480	6.73	0.480	7.03	0.500	7.10
0.505	6.73	0.505	7.03	0.550	7.10
0.530	6.73	0.530	7.04	0.600	7.10
0.555	6.73	0.555	7.04	0.625	7.10
0.575	6.73	0.580	7.04	0.650	7.10
0.600	6.73	0.605	7.04	0.675	7.11
0.625	6.73	0.625	7.04	0.700	7.11
0.650	6.73	0.650	7.04	0.725	7.11
0.675	6.73	0.700	7.04	0.750	7.11
0.700	6.73	0.750	7.04	0.800	7.11
0.750	6.73	0.800	7.04	0.850	7.11
0.800	6.73	0.850	7.04	0.900	7.11
0.900	6.73	0.900	7.04	0.950	7.11
1.000	6.73	1.000	7.04	1.000	7.11

Q_s = 133.33 SCFH/FT.

X = 0.0 Upst. Edge of Suction Slot		X = 1/4 inch		X = 1/2 inch	
Y(in.)	U(ft/sec.)	Y(in.)	U(ft/sec.)	Y(in.)	U(ft/sec.)
0.035	4.92	0.035	3.61	0.035	3.65
0.040	4.95	0.040	3.74	0.040	3.87
0.045	4.98	0.045	3.84	0.045	4.01
0.050	5.00	0.050	3.98	0.050	4.19
0.055	5.02	0.055	4.10	0.055	4.37
0.060	5.03	0.060	4.17	0.060	4.60
0.065	5.05	0.065	4.29	0.065	4.68
0.070	5.07	0.070	4.37	0.070	4.71
0.075	5.08	0.075	4.46	0.075	4.74
0.080	5.12	0.080	4.52	0.080	4.76
0.085	5.17	0.085	4.53	0.085	4.77
0.090	5.23	0.090	4.58	0.090	4.82
0.095	5.25	0.095	4.61	0.095	4.87
0.100	5.30	0.100	4.68	0.100	4.97
0.105	5.37	0.105	4.77	0.105	5.13
0.110	5.40	0.110	4.87	0.110	5.20
0.115	5.44	0.115	5.03	0.115	5.25
0.120	5.53	0.120	5.17	0.120	5.30
0.125	5.60	0.125	5.25	0.125	5.35
0.130	5.65	0.130	5.34	0.130	5.40
0.135	5.67	0.135	5.39	0.135	5.47
0.140	5.78	0.140	5.42	0.140	5.56
0.145	5.87	0.145	5.49	0.145	5.63
0.150	5.90	0.150	5.56	0.150	5.67
0.155	5.94	0.155	5.60	0.155	5.70
0.160	5.99	0.160	5.63	0.160	5.74
0.165	6.05	0.165	5.69	0.165	5.76
0.170	6.09	0.170	5.74	0.170	5.78
0.175	6.12	0.175	5.79	0.175	5.79
0.180	6.20	0.185	5.90	0.185	5.85
0.190	6.22	0.200	5.96	0.200	5.92
0.200	6.29	0.210	5.99	0.210	6.01
0.210	6.37	0.225	6.09	0.225	6.12
0.220	6.43	0.235	6.14	0.235	6.22
0.230	6.47	0.250	6.20	0.250	6.27
0.240	6.49	0.260	6.24	0.260	6.29
0.250	6.58	0.275	6.27	0.275	6.33
0.260	6.62	0.285	6.33	0.285	6.37
0.270	6.68	0.300	6.41	0.300	6.39
0.280	6.72	0.310	6.47	0.310	6.41
0.290	6.74	0.325	6.48	0.325	6.45
0.300	6.76	0.350	6.50	0.350	6.47
0.325	6.78	0.375	6.51	0.375	6.49
0.350	6.84	0.400	6.55	0.400	6.49
0.375	6.88	0.425	6.59	0.425	6.49
0.400	6.90	0.450	6.61	0.450	6.50
0.425	6.92	0.475	6.63	0.475	6.51
0.450	6.92	0.500	6.64	0.500	6.51
0.475	6.92	0.525	6.64	0.525	6.51
0.500	6.92	0.550	6.67	0.550	6.51
0.525	6.92	0.575	6.69	0.575	6.52
0.550	6.92	0.600	6.69	0.600	6.52
0.600	6.92	0.625	6.71	0.625	6.52
0.650	6.92	0.650	6.71	0.650	6.54
0.700	6.92	0.675	6.71	0.675	6.54
0.750	6.92	0.700	6.71	0.700	6.54
0.800	6.92	0.750	6.71	0.750	6.56
0.850	6.92	0.800	6.71	0.800	6.56
0.900	6.92	0.900	6.71	0.900	6.56
1.000	6.92	1.000	6.71	1.000	6.56

Q_s = 133.33 SCFH/FT.

X = 1 inch		X = 2 inches		X = 3 inches	
Y(in.)	U(ft/sec.)	Y(in.)	U(ft/sec.)	Y(in.)	U(ft/sec.)
0.035	3.54	0.035	3.20	0.045	3.15
0.040	4.10	0.040	3.37	0.050	3.34
0.045	4.49	0.045	3.59	0.055	3.55
0.050	4.61	0.050	4.07	0.060	3.78
0.055	4.77	0.055	4.17	0.065	4.03
0.060	4.95	0.060	4.28	0.070	4.19
0.065	5.12	0.065	4.40	0.075	4.37
0.070	5.27	0.070	4.53	0.080	4.49
0.075	5.49	0.075	4.64	0.085	4.63
0.080	5.63	0.080	4.72	0.090	4.76
0.085	5.70	0.085	4.87	0.095	4.88
0.090	5.76	0.090	5.02	0.100	5.03
0.095	5.79	0.095	5.17	0.105	5.17
0.100	5.90	0.100	5.30	0.110	5.30
0.105	5.94	0.105	5.35	0.115	5.34
0.110	5.99	0.110	5.40	0.120	5.37
0.115	6.05	0.115	5.44	0.125	5.44
0.120	6.12	0.120	5.49	0.130	5.51
0.125	6.20	0.125	5.56	0.135	5.60
0.130	6.27	0.130	5.63	0.140	5.69
0.135	6.31	0.135	5.67	0.145	5.74
0.140	6.35	0.140	5.72	0.150	5.76
0.145	6.37	0.145	5.78	0.155	5.81
0.150	6.41	0.150	5.81	0.160	5.87
0.160	6.47	0.155	5.85	0.165	5.92
0.170	6.52	0.160	5.88	0.170	5.94
0.180	6.58	0.165	5.90	0.175	5.98
0.190	6.62	0.170	6.01	0.180	6.01
0.200	6.78	0.175	6.05	0.185	6.07
0.210	6.90	0.185	6.09	0.195	6.16
0.220	6.98	0.200	6.16	0.210	6.20
0.230	7.02	0.210	6.26	0.220	6.27
0.240	7.04	0.225	6.27	0.235	6.37
0.250	7.08	0.235	6.29	0.245	6.41
0.275	7.12	0.250	6.33	0.260	6.43
0.300	7.17	0.260	6.43	0.270	6.45
0.325	7.19	0.275	6.45	0.285	6.51
0.350	7.19	0.285	6.47	0.295	6.51
0.375	7.21	0.300	6.49	0.310	6.55
0.400	7.21	0.310	6.51	0.320	6.56
0.425	7.23	0.325	6.55	0.335	6.56
0.450	7.25	0.350	6.57	0.360	6.63
0.475	7.25	0.375	6.58	0.385	6.63
0.500	7.25	0.400	6.59	0.410	6.66
0.525	7.25	0.425	6.60	0.435	6.67
0.550	7.27	0.450	6.61	0.460	6.67
0.600	7.27	0.475	6.61	0.485	6.69
0.650	7.27	0.500	6.61	0.510	6.69
0.675	7.33	0.525	6.61	0.535	6.69
0.700	7.35	0.550	6.61	0.560	6.71
0.725	7.35	0.575	6.61	0.585	6.71
0.750	7.37	0.600	6.61	0.610	6.71
0.775	7.37	0.625	6.61	0.650	6.71
0.800	7.40	0.650	6.61	0.700	6.71
0.825	7.40	0.675	6.61	0.750	6.71
0.850	7.42	0.700	6.61	0.800	6.71
0.875	7.42	0.750	6.61	0.850	6.71
0.900	7.42	0.800	6.61	0.900	6.71
0.950	7.42	0.900	6.61	0.950	6.71
1.000	7.42	1.000	6.61	1.000	6.71

Q_s = 133.33 SCFH/FT.

X = 4 inches		X = 5 inches		X = 6 inches	
Y(in.)	U(ft/sec.)	Y(in.)	U(ft/sec.)	Y(in.)	U(ft/sec.)
0.040	2.79	0.045	2.41	0.045	2.57
0.045	2.97	0.050	2.52	0.050	2.69
0.050	3.19	0.055	2.71	0.055	2.83
0.055	3.41	0.060	2.97	0.060	2.98
0.060	3.70	0.065	3.19	0.065	3.13
0.065	3.87	0.070	3.43	0.070	3.28
0.070	4.00	0.075	3.65	0.075	3.46
0.075	4.17	0.080	3.84	0.080	3.65
0.080	4.35	0.085	4.01	0.085	3.83
0.085	4.52	0.090	4.14	0.090	3.98
0.090	4.61	0.095	4.31	0.095	4.11
0.095	4.76	0.100	4.41	0.100	4.22
0.100	4.85	0.105	4.53	0.105	4.34
0.105	4.93	0.110	4.64	0.110	4.47
0.110	5.00	0.115	4.74	0.115	4.64
0.115	5.07	0.120	4.97	0.120	4.76
0.120	5.15	0.125	5.07	0.125	4.85
0.125	5.25	0.130	5.13	0.130	4.92
0.130	5.32	0.135	5.32	0.135	5.05
0.135	5.37	0.140	5.40	0.140	5.18
0.140	5.42	0.145	5.44	0.145	5.23
0.145	5.47	0.150	5.47	0.150	5.37
0.150	5.56	0.155	5.54	0.155	5.53
0.155	5.65	0.160	5.60	0.160	5.58
0.160	5.70	0.165	5.67	0.165	5.61
0.165	5.78	0.170	5.76	0.170	5.65
0.170	5.81	0.175	5.78	0.175	5.78
0.175	5.87	0.180	5.83	0.180	5.83
0.180	5.90	0.185	5.94	0.185	5.88
0.190	5.99	0.195	6.01	0.195	5.90
0.205	6.12	0.210	6.09	0.210	5.98
0.215	6.16	0.220	6.15	0.220	6.11
0.230	6.24	0.235	6.21	0.235	6.20
0.240	6.31	0.245	6.27	0.245	6.22
0.255	6.41	0.260	6.36	0.260	6.31
0.280	6.43	0.270	6.42	0.270	6.39
0.290	6.47	0.285	6.44	0.285	6.43
0.305	6.49	0.295	6.48	0.295	6.45
0.315	6.50	0.310	6.50	0.310	6.47
0.330	6.51	0.320	6.55	0.320	6.49
0.355	6.55	0.335	6.55	0.335	6.51
0.380	6.57	0.360	6.55	0.360	6.58
0.405	6.58	0.385	6.58	0.385	6.61
0.430	6.61	0.410	6.61	0.410	6.61
0.455	6.61	0.435	6.63	0.435	6.63
0.480	6.61	0.460	6.64	0.460	6.63
0.505	6.61	0.485	6.64	0.485	6.63
0.530	6.61	0.510	6.66	0.535	6.65
0.555	6.61	0.535	6.66	0.540	6.65
0.580	6.61	0.560	6.66	0.560	6.65
0.600	6.61	0.575	6.66	0.585	6.65
0.630	6.62	0.600	6.66	0.610	6.65
0.655	6.63	0.625	6.66	0.635	6.67
0.680	6.63	0.650	6.66	0.660	6.67
0.700	6.63	0.700	6.66	0.700	6.67
0.750	6.63	0.750	6.66	0.750	6.67
0.800	6.63	0.800	6.66	0.800	6.67
0.850	6.63	0.850	6.66	0.850	6.67
0.900	6.63	0.900	6.66	0.900	6.67
1.000	6.63	1.000	6.66	1.000	6.67

Q_s = 133.33 SCFH/FT.

X - 9 inches		X = 12 inches		X = 15 inches	
Y(in.)	U(ft/sec.)	Y(in.)	U(ft/sec.)	Y(in.)	U(ft/sec.)
0.045	1.77	0.045	1.77	0.045	1.69
0.050	1.94	0.050	1.91	0.050	1.94
0.055	2.15	0.055	2.10	0.055	2.09
0.060	2.46	0.060	2.25	0.060	2.17
0.065	2.56	0.065	2.42	0.065	2.44
0.070	2.74	0.070	2.57	0.070	2.61
0.075	2.93	0.075	2.76	0.075	2.67
0.080	3.07	0.080	2.93	0.080	2.90
0.085	3.23	0.085	3.10	0.085	3.08
0.090	3.45	0.090	3.28	0.090	3.22
0.095	3.67	0.095	3.45	0.095	3.37
0.100	3.76	0.100	3.62	0.100	3.53
0.105	3.95	0.105	3.80	0.105	3.59
0.110	4.16	0.110	3.88	0.110	3.77
0.115	4.25	0.115	3.98	0.115	3.90
0.120	4.41	0.120	4.19	0.120	3.98
0.125	4.55	0.125	4.43	0.125	4.07
0.130	4.60	0.130	4.68	0.130	4.19
0.135	4.72	0.135	4.76	0.135	4.31
0.140	4.80	0.140	4.80	0.140	4.50
0.145	4.95	0.145	4.85	0.145	4.58
0.150	5.17	0.150	4.95	0.150	4.64
0.155	5.27	0.155	5.07	0.155	4.72
0.160	5.39	0.160	5.22	0.160	4.84
0.165	5.47	0.165	5.32	0.165	4.90
0.170	5.54	0.170	5.46	0.170	4.93
0.175	5.65	0.175	5.58	0.175	4.97
0.180	5.69	0.180	5.65	0.180	5.03
0.185	5.72	0.185	5.72	0.185	5.10
0.200	5.88	0.190	5.81	0.190	5.23
0.210	5.98	0.195	5.94	0.195	5.37
0.220	6.11	0.200	6.01	0.200	5.51
0.230	6.16	0.210	6.11	0.205	5.54
0.240	6.26	0.220	6.14	0.210	5.58
0.250	6.33	0.230	6.22	0.220	5.72
0.260	6.39	0.240	6.33	0.230	5.76
0.270	6.47	0.250	6.49	0.240	5.87
0.280	6.51	0.260	6.56	0.250	5.94
0.290	6.56	0.270	6.60	0.260	6.05
0.300	6.62	0.280	6.66	0.270	6.12
0.310	6.65	0.290	6.72	0.280	6.18
0.320	6.66	0.300	6.78	0.290	6.31
0.330	6.70	0.310	6.82	0.300	6.39
0.340	6.74	0.320	6.86	0.310	6.43
0.350	6.74	0.330	6.87	0.320	6.45
0.375	6.77	0.340	6.89	0.330	6.49
0.400	6.83	0.350	6.93	0.340	6.52
0.425	6.84	0.375	6.95	0.350	6.56
0.450	6.85	0.400	6.99	0.375	6.64
0.475	6.85	0.425	7.01	0.400	6.70
0.500	6.85	0.450	7.03	0.425	6.72
0.525	6.85	0.500	7.07	0.450	6.73
0.550	6.87	0.525	7.09	0.500	6.73
0.575	6.87	0.550	7.11	0.525	6.75
0.600	6.87	0.600	7.11	0.600	6.75
0.650	6.87	0.650	7.11	0.675	6.75
0.700	6.87	0.700	7.11	0.700	6.77
0.800	6.87	0.800	7.11	0.800	6.79
0.900	6.87	0.900	7.11	0.900	6.79
1.000	6.87	1.000	7.11	1.000	6.79

Q_s = 133.33 SCFH/FT.

X = 18 inches		X = 21 inches		X = 24 inches	
Y(in.)	U(ft/sec.)	Y(in.)	U(ft/sec.)	Y(in.)	U(ft/sec.)
0.045	1.73	0.045	1.86	0.045	1.96
0.050	1.91	0.050	2.04	0.050	2.06
0.055	2.15	0.055	2.20	0.055	2.17
0.060	2.28	0.060	2.42	0.060	2.28
0.065	2.39	0.065	2.48	0.065	2.42
0.070	2.48	0.070	2.57	0.070	2.66
0.075	2.62	0.075	2.74	0.075	2.77
0.080	2.77	0.080	2.86	0.080	2.84
0.085	2.85	0.085	3.13	0.085	2.95
0.090	2.98	0.090	3.32	0.090	3.10
0.095	3.22	0.100	3.39	0.095	3.25
0.100	3.41	0.105	3.47	0.100	3.41
0.105	3.54	0.110	3.57	0.105	3.50
0.110	3.67	0.115	3.69	0.110	3.62
0.115	3.85	0.120	3.81	0.115	3.73
0.120	4.01	0.125	3.98	0.120	3.91
0.125	4.19	0.130	4.19	0.125	3.98
0.130	4.31	0.135	4.29	0.130	4.04
0.135	4.47	0.140	4.46	0.135	4.14
0.140	4.61	0.145	4.55	0.140	4.28
0.145	4.80	0.150	4.58	0.145	4.50
0.150	4.88	0.155	4.63	0.150	4.58
0.155	4.97	0.160	4.71	0.155	4.61
0.160	5.05	0.165	4.88	0.160	4.66
0.165	5.08	0.170	4.95	0.165	4.77
0.170	5.17	0.175	5.05	0.170	4.79
0.175	5.23	0.180	5.12	0.175	4.90
0.180	5.28	0.185	5.18	0.180	4.97
0.190	5.46	0.190	5.35	0.190	5.13
0.200	5.56	0.195	5.47	0.200	5.27
0.210	5.69	0.210	5.54	0.210	5.42
0.220	5.83	0.220	5.65	0.220	5.58
0.230	5.96	0.230	5.76	0.230	5.74
0.240	6.09	0.240	6.01	0.240	5.83
0.250	6.29	0.250	6.12	0.250	5.88
0.275	6.47	0.260	6.24	0.260	5.96
0.300	6.60	0.270	6.29	0.270	6.03
0.325	6.62	0.280	6.35	0.280	6.12
0.350	6.66	0.290	6.45	0.300	6.20
0.375	6.72	0.310	6.54	0.310	6.33
0.400	6.79	0.320	6.60	0.320	6.37
0.425	6.89	0.340	6.70	0.330	6.47
0.450	6.93	0.360	6.73	0.350	6.52
0.475	6.93	0.370	6.77	0.370	6.58
0.500	6.93	0.380	6.81	0.380	6.66
0.525	6.93	0.400	6.81	0.400	6.69
0.550	6.97	0.425	6.85	0.410	6.69
0.575	6.97	0.450	6.85	0.430	6.69
0.600	6.97	0.475	6.89	0.450	6.69
0.625	6.97	0.500	6.89	0.475	6.73
0.650	6.97	0.550	6.90	0.500	6.76
0.700	7.01	0.575	6.91	0.550	6.77
0.750	7.01	0.600	6.91	0.575	6.78
0.775	7.01	0.650	6.92	0.600	6.78
0.800	7.01	0.700	6.93	0.625	6.78
0.825	7.01	0.750	6.93	0.650	6.78
0.850	7.01	0.800	6.93	0.700	6.78
0.900	7.01	0.850	6.93	0.800	6.79
0.950	7.02	0.900	6.93	0.900	6.79
1.000	7.03	1.000	6.93	1.000	6.79

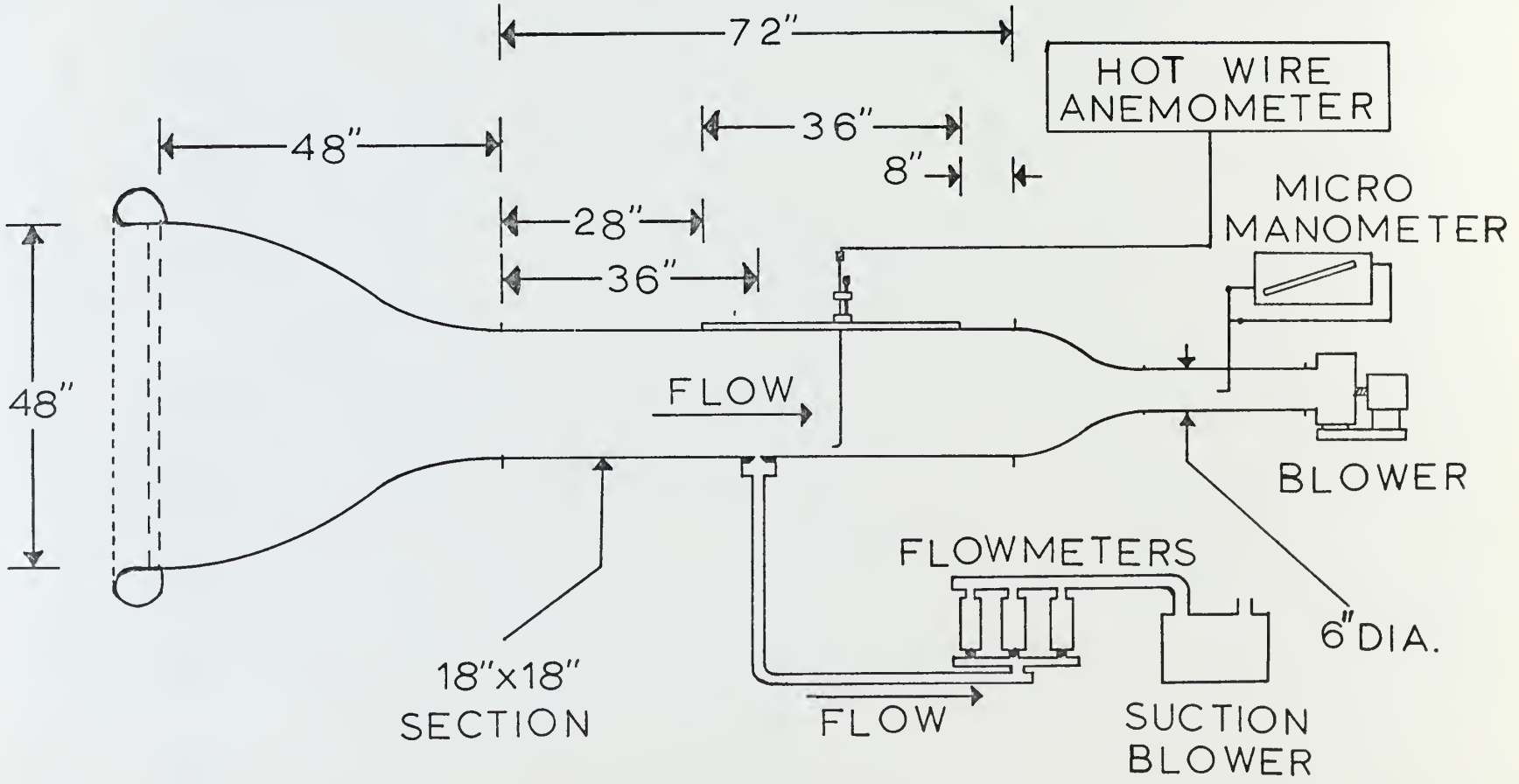

FIGURE 1
EXPERIMENTAL EQUIPMENT

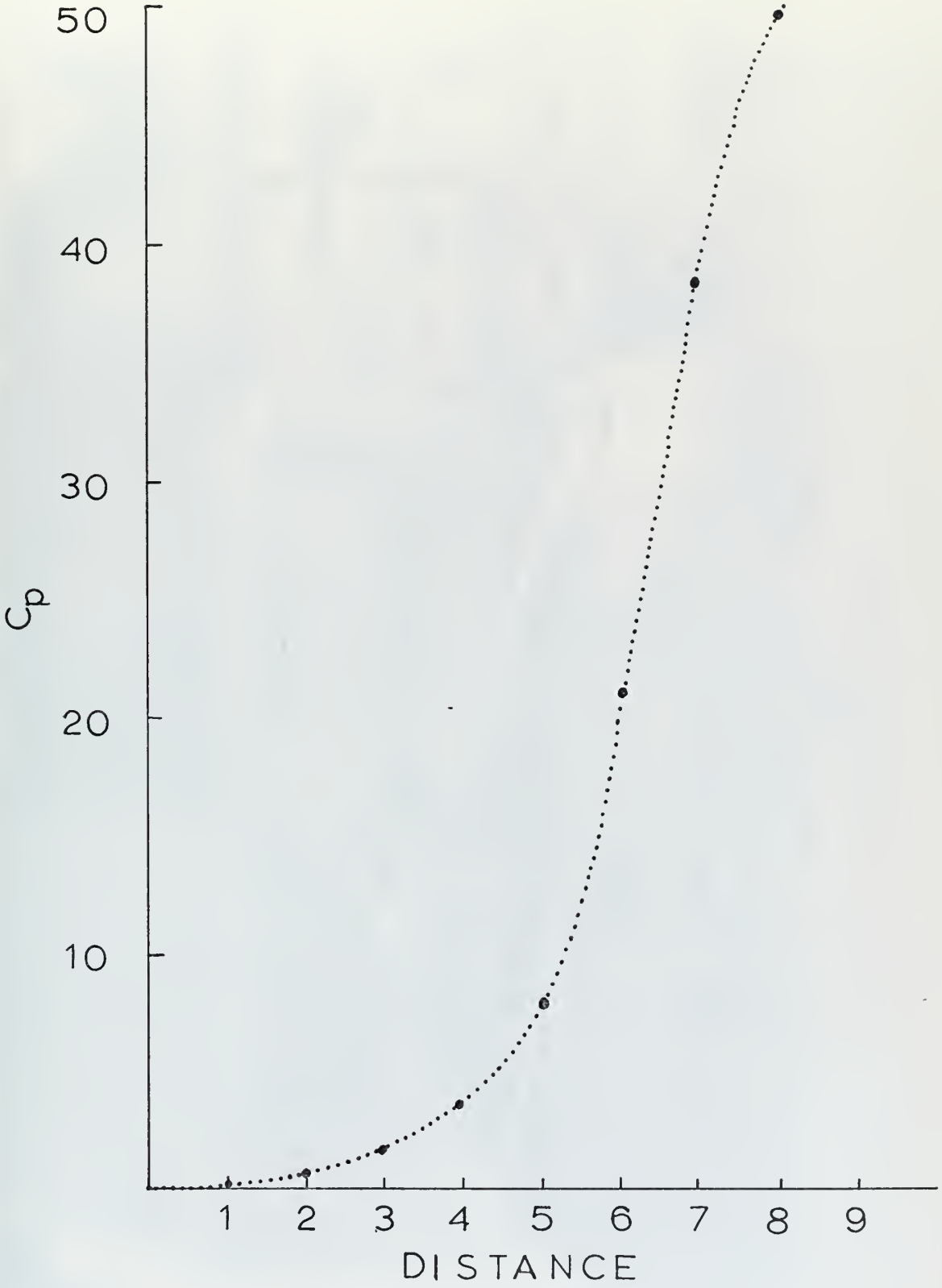

FIGURE 2
INLET NOZZLE PRESSURE DISTRIBUTION

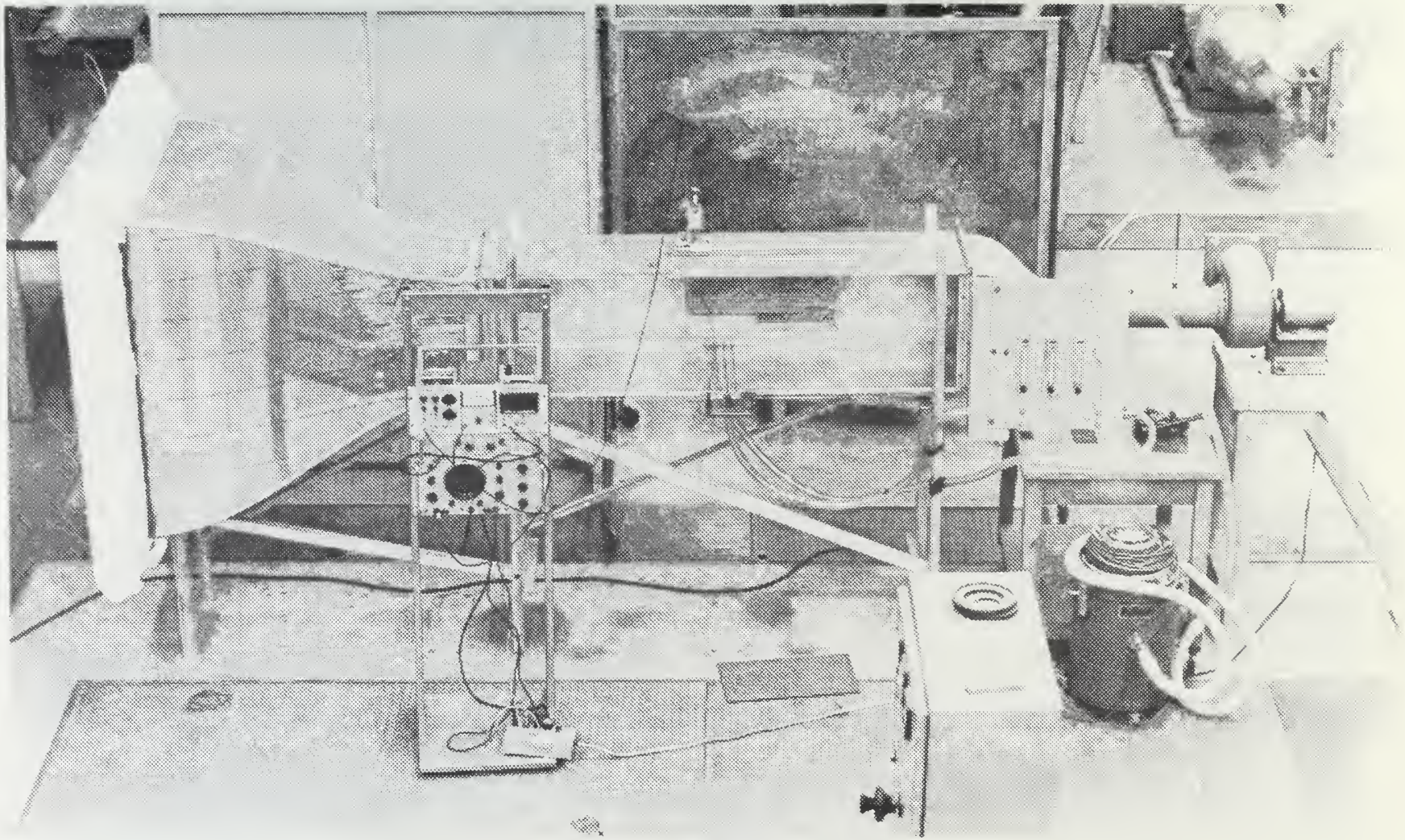

FIGURE 3
EXPERIMENTAL APPARATUS

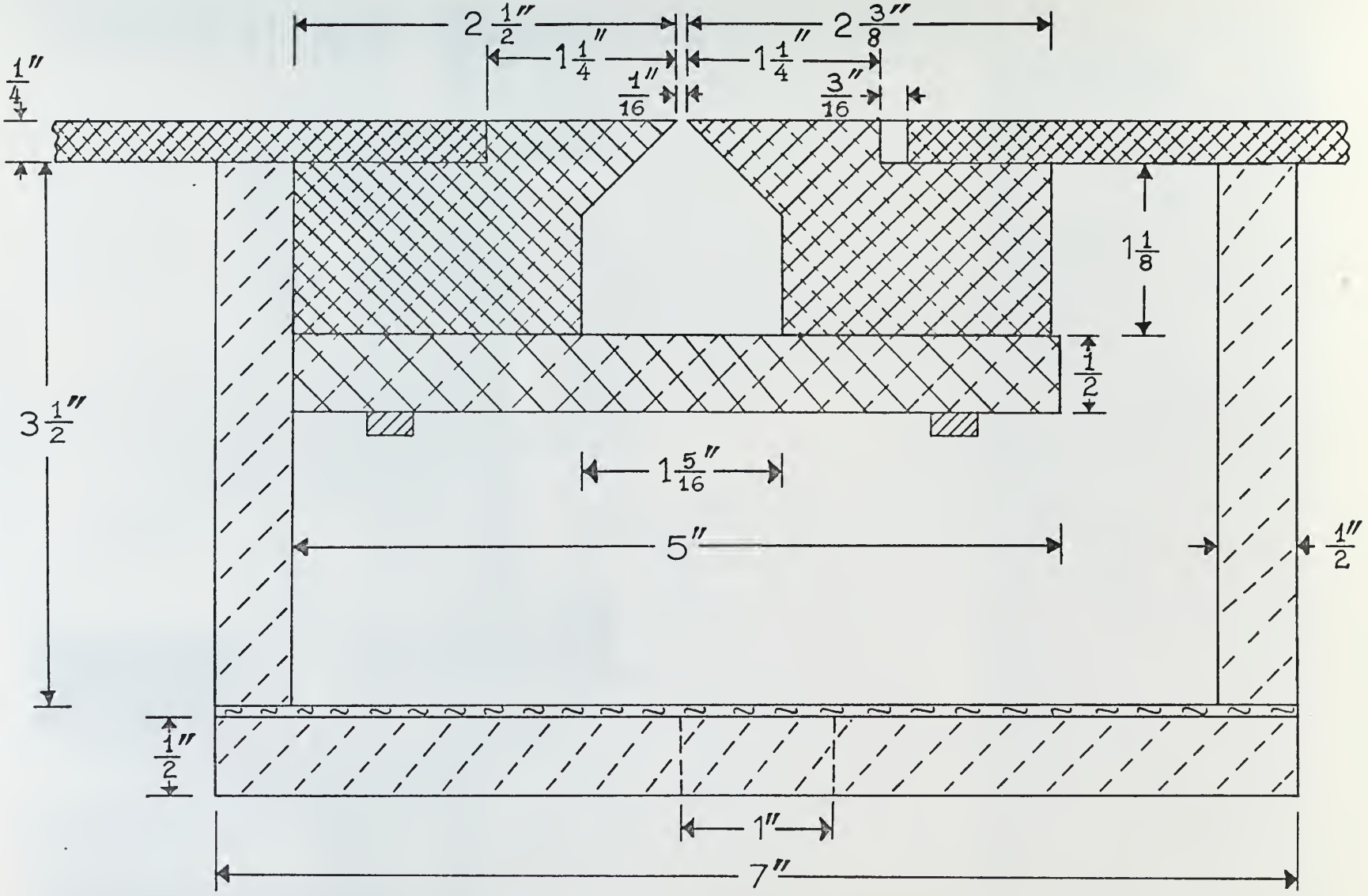

FIGURE 4
SUCTION SLOT AND MANIFOLD

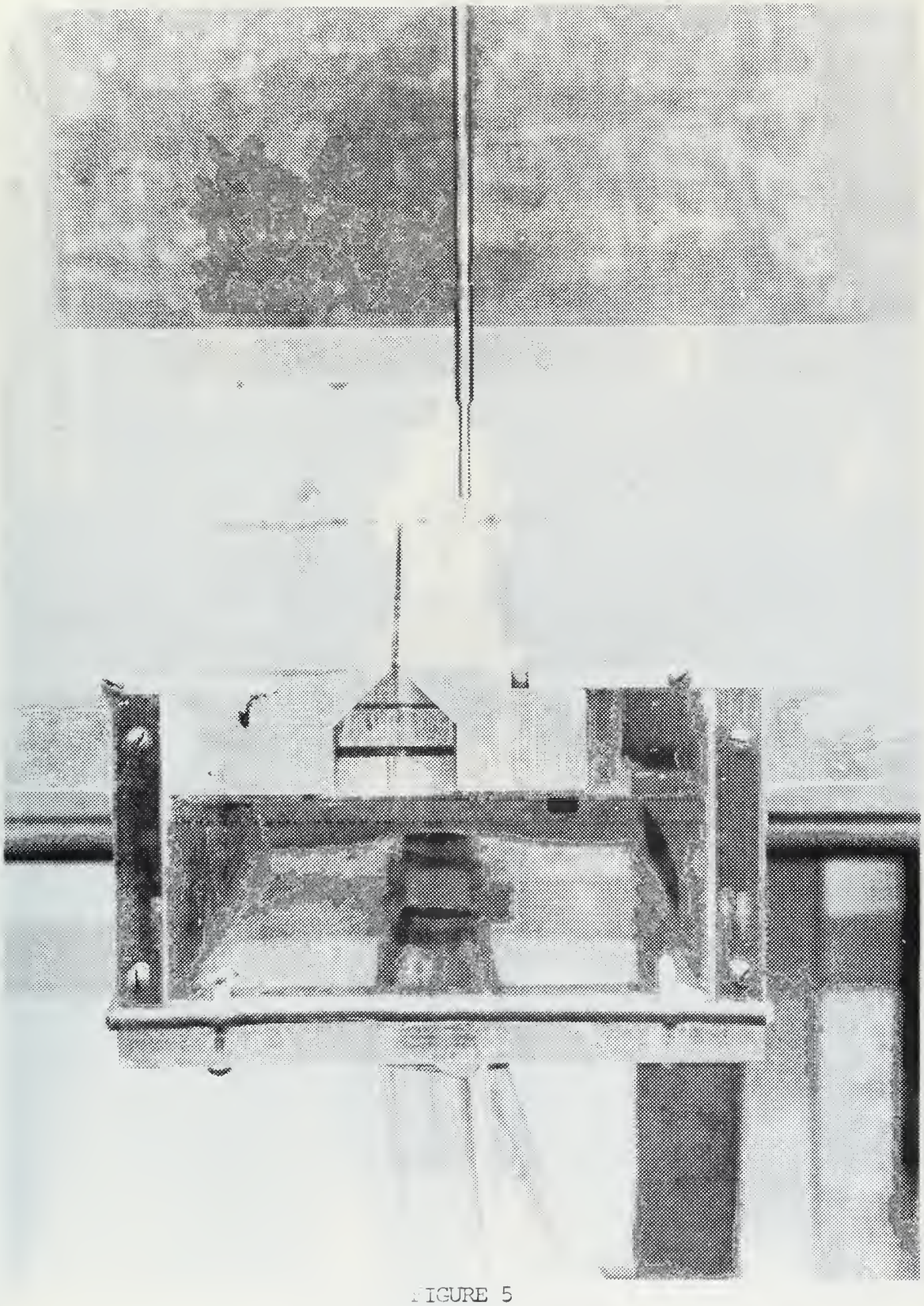

FIGURE 5
SUCTION SLOT AND MANIFOLD

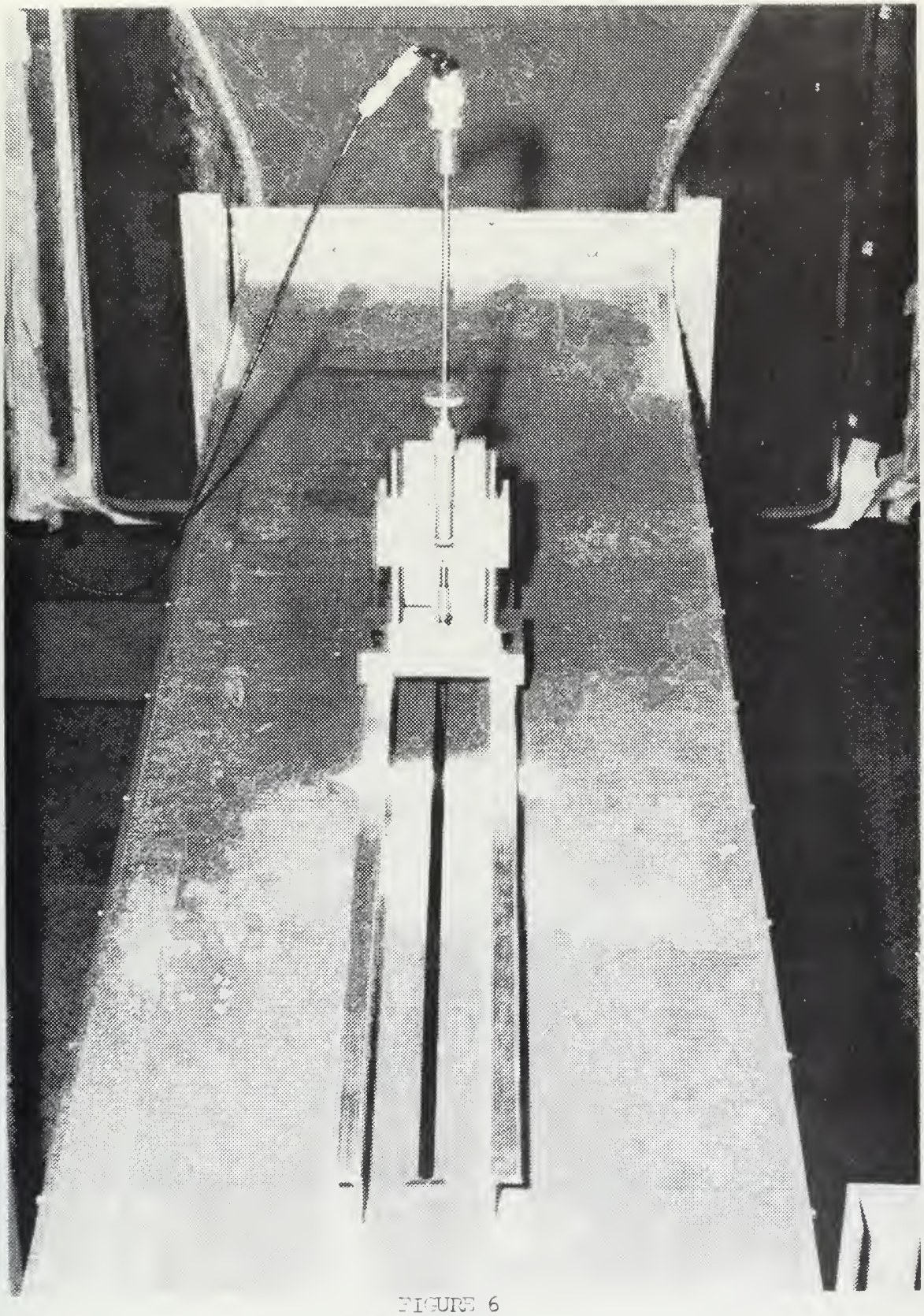

FIGURE 6
MICROMETER

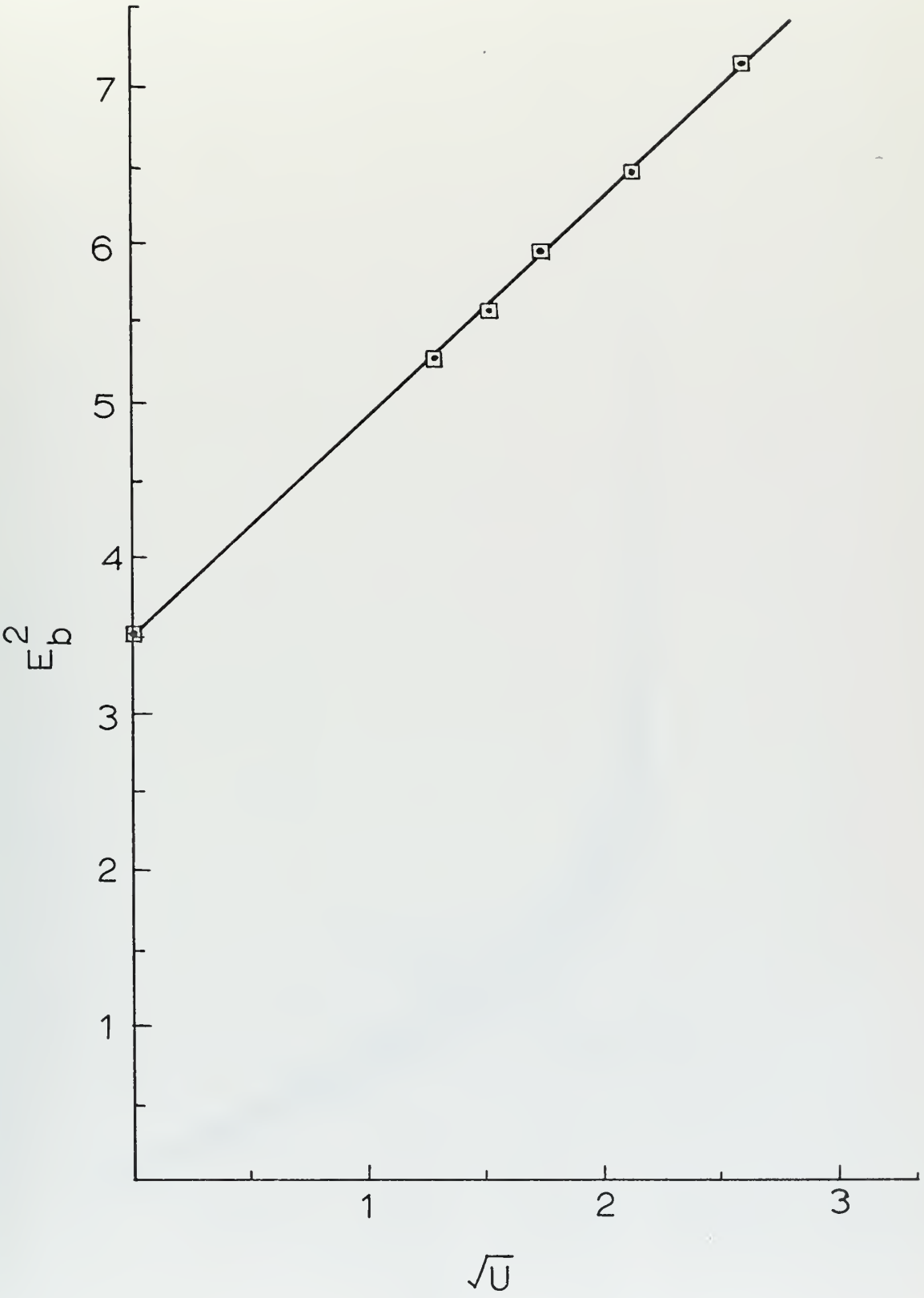

FIGURE 7
HOT WIRE ANEMOMETER CALIBRATION CURVE

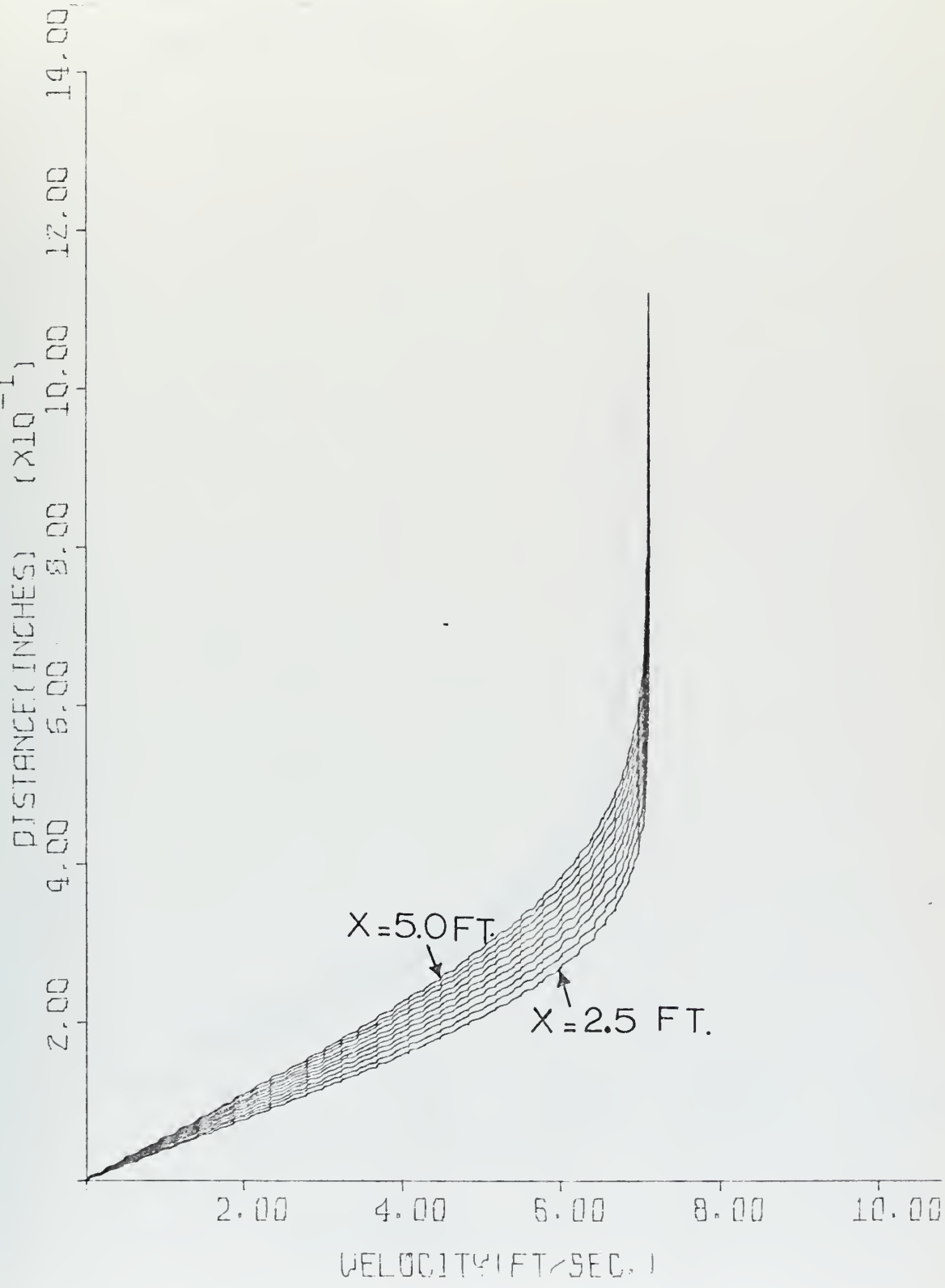

FIGURE 8
BLASIUS PROFILES

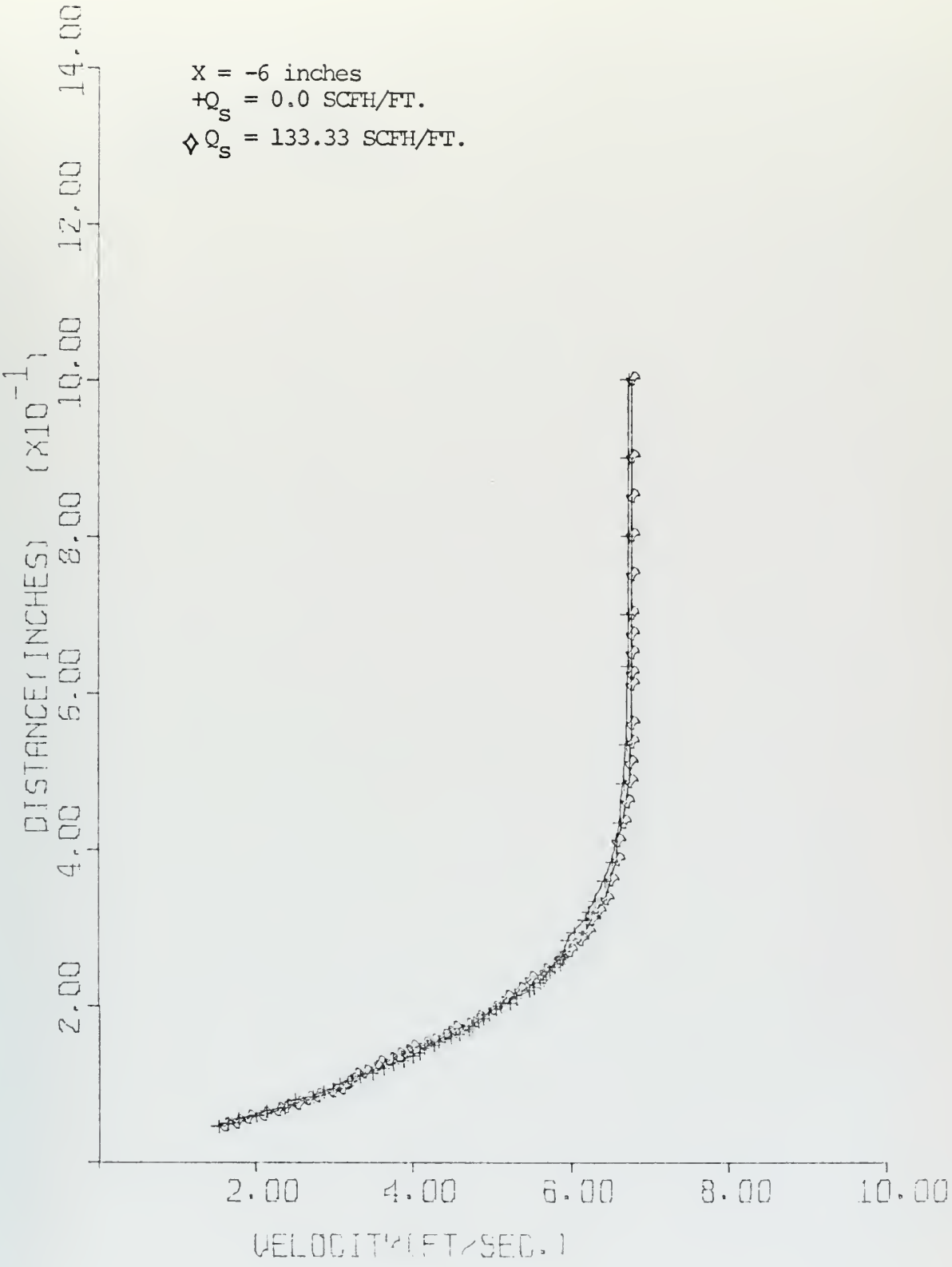

FIGURE 9
VELOCITY PROFILE

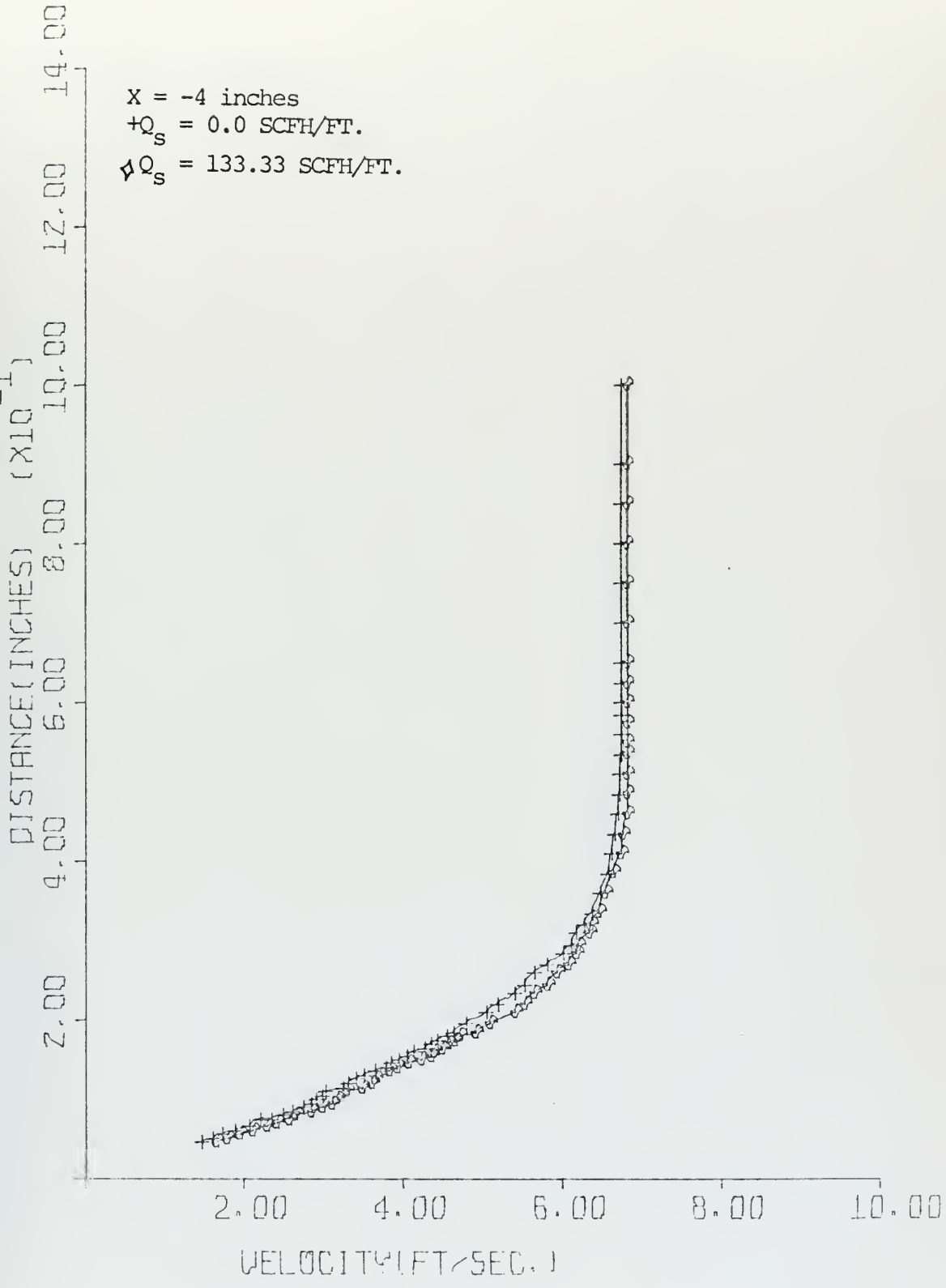

FIGURE 10
VELOCITY PROFILE

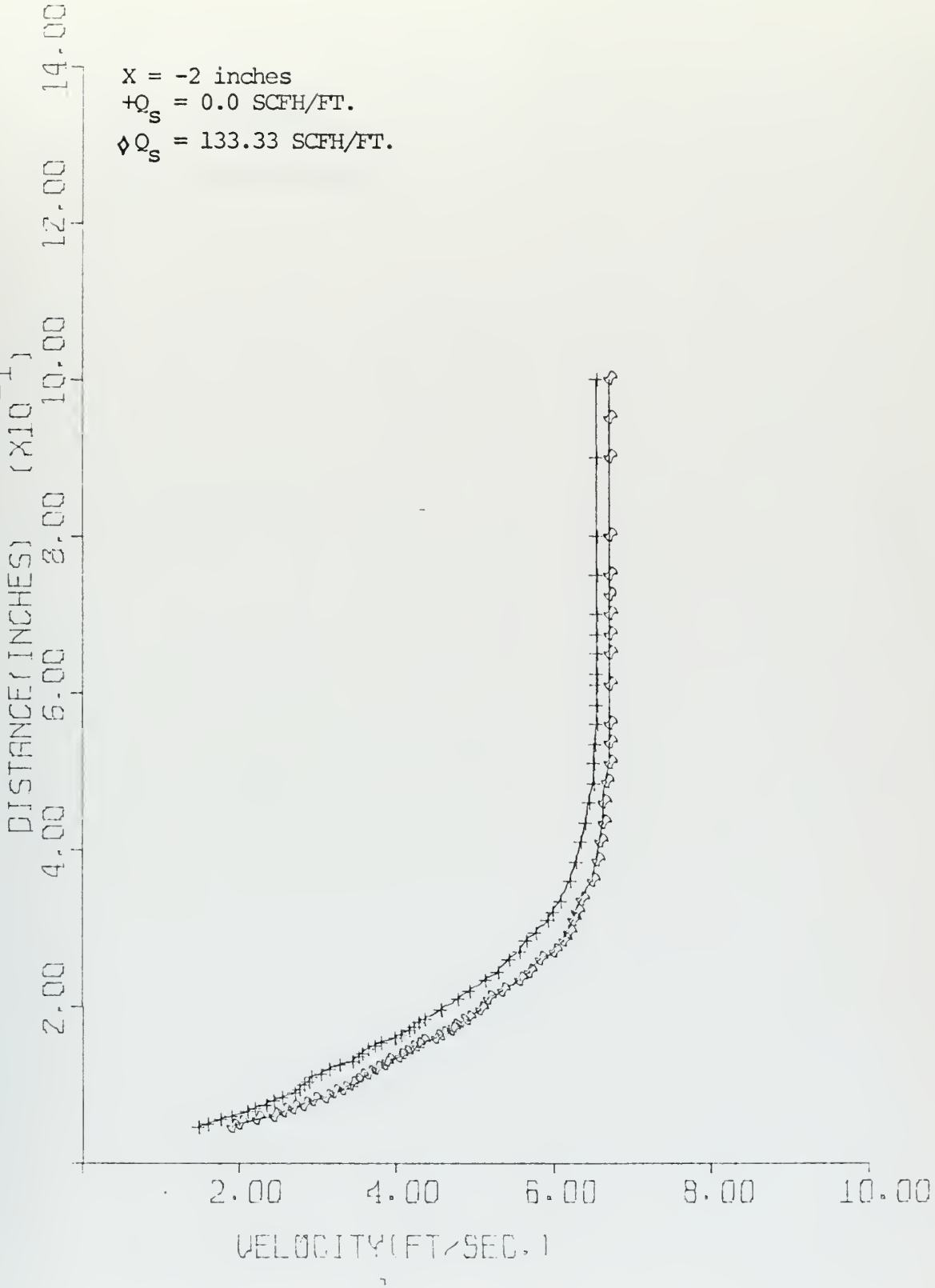

FIGURE 11
VELOCITY PROFILE

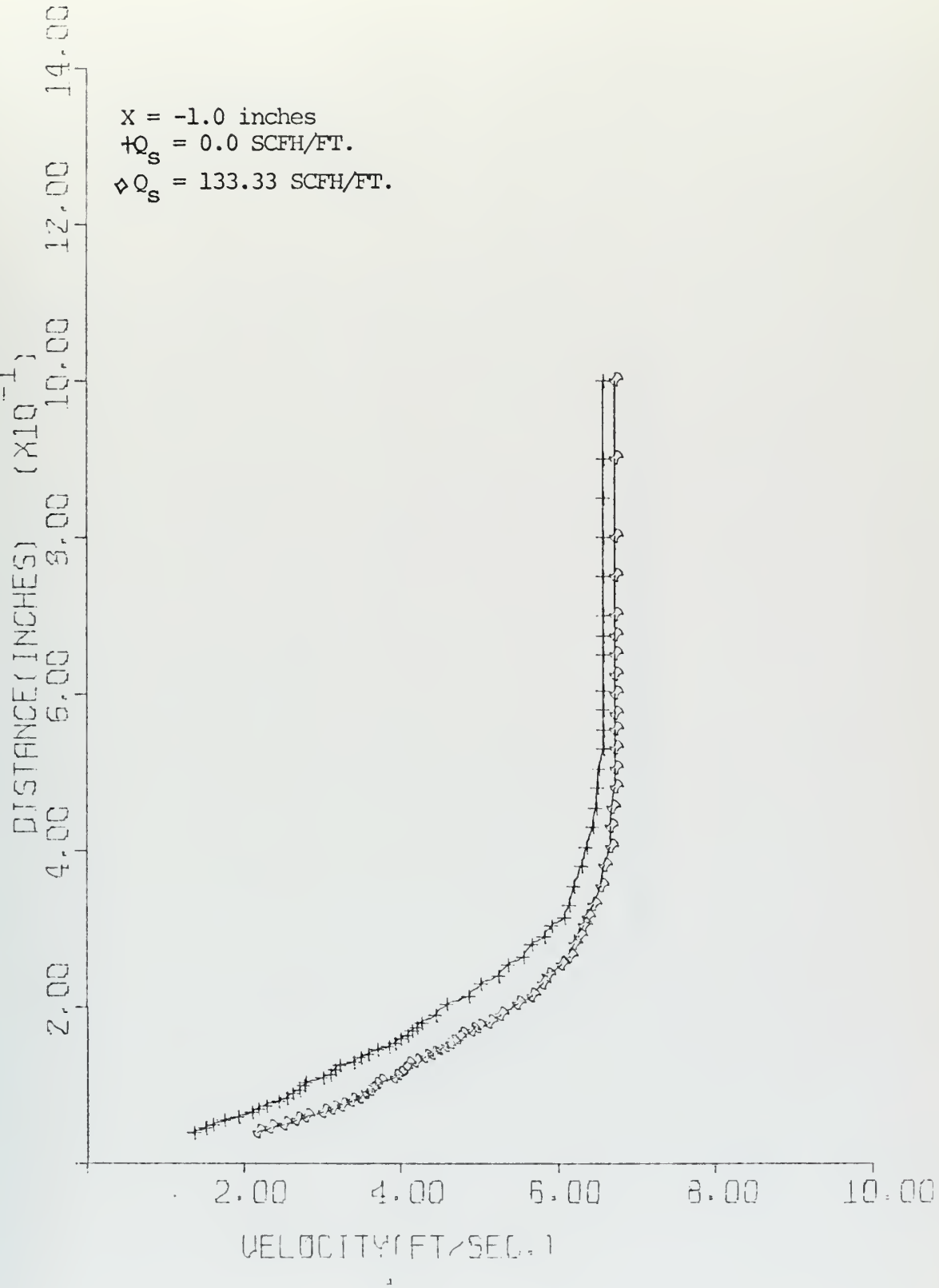

FIGURE 12
VELOCITY PROFILE

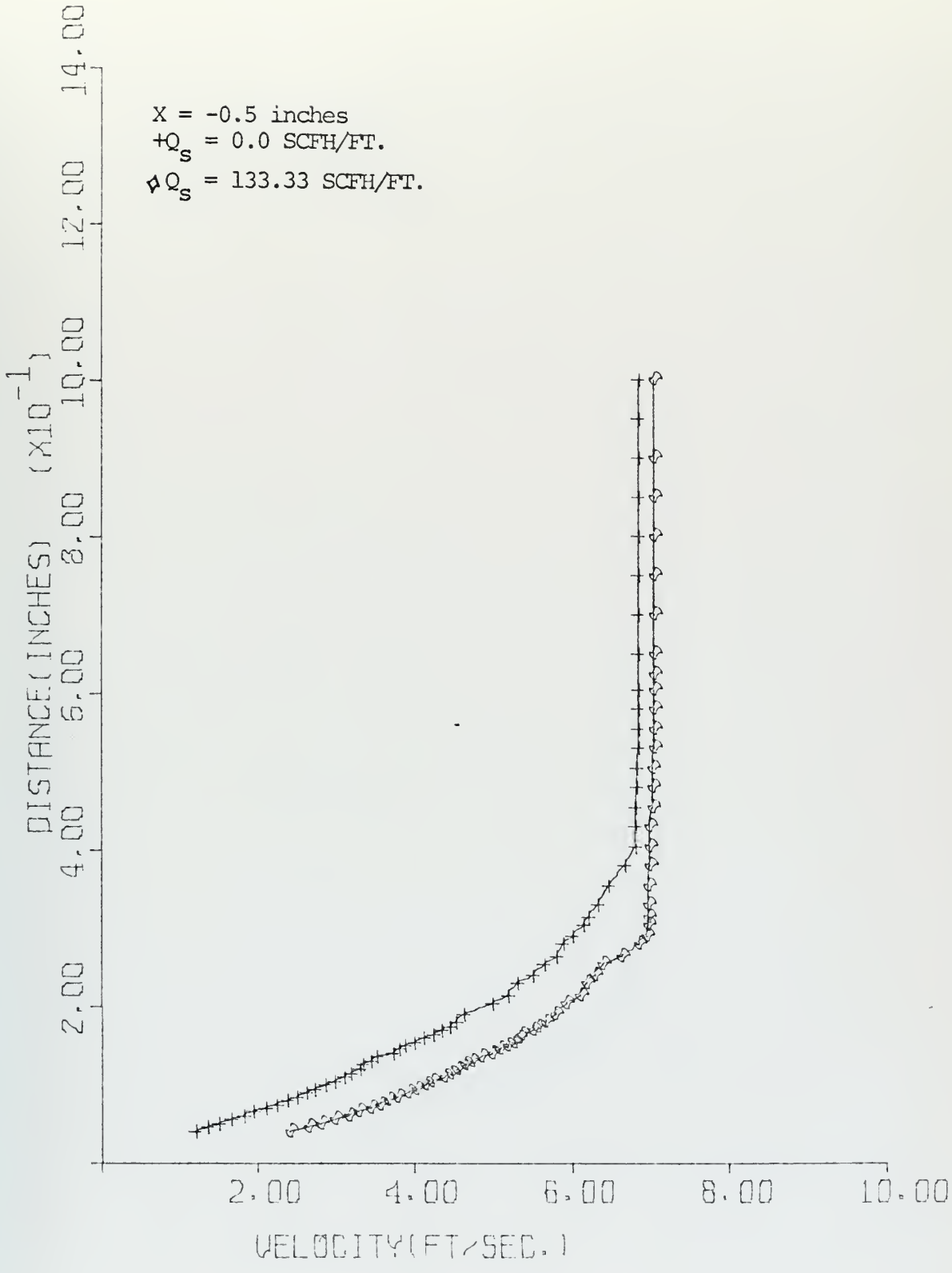

FIGURE 13
VELOCITY PROFILE

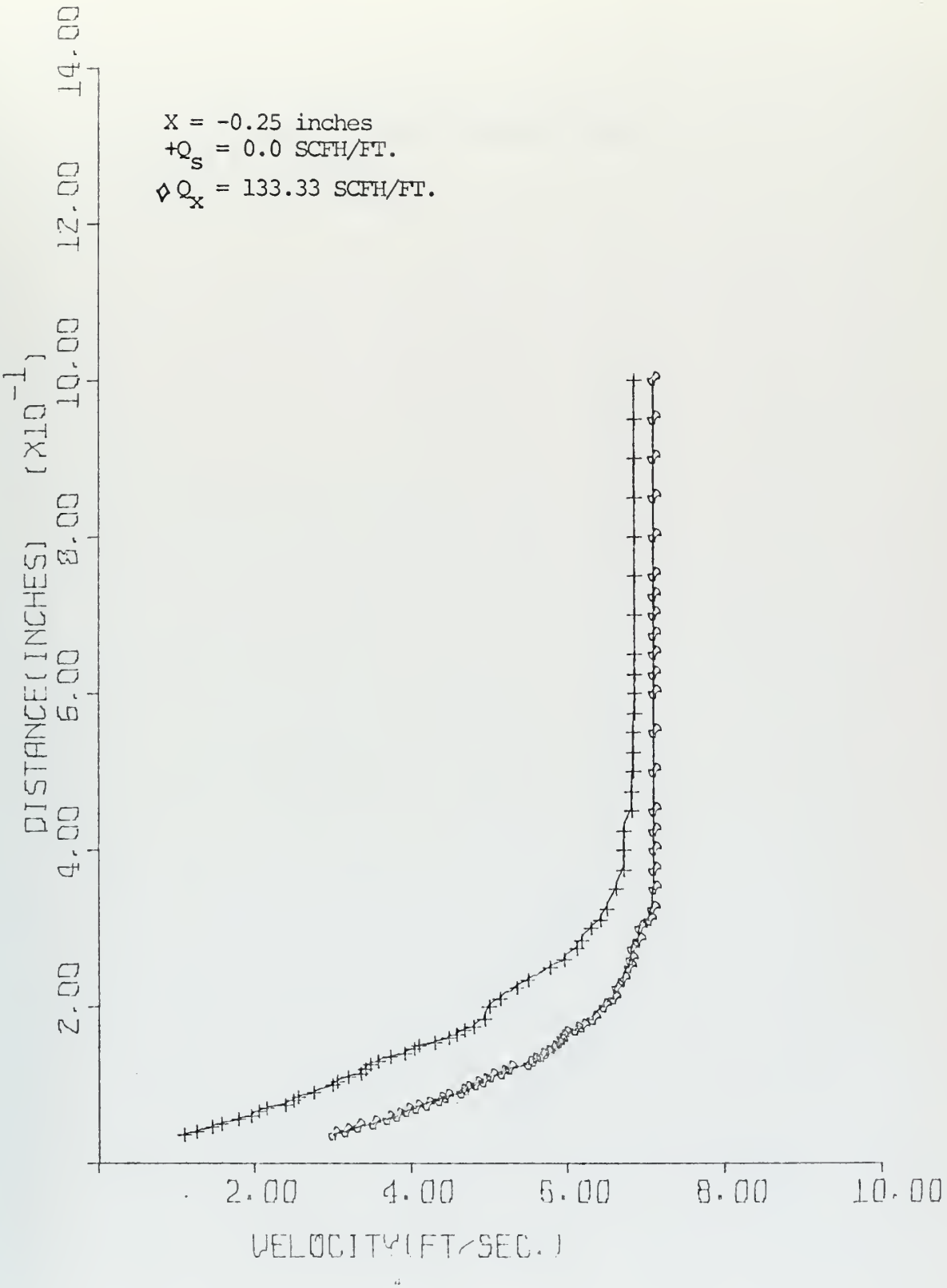

FIGURE 14
VELOCITY PROFILE

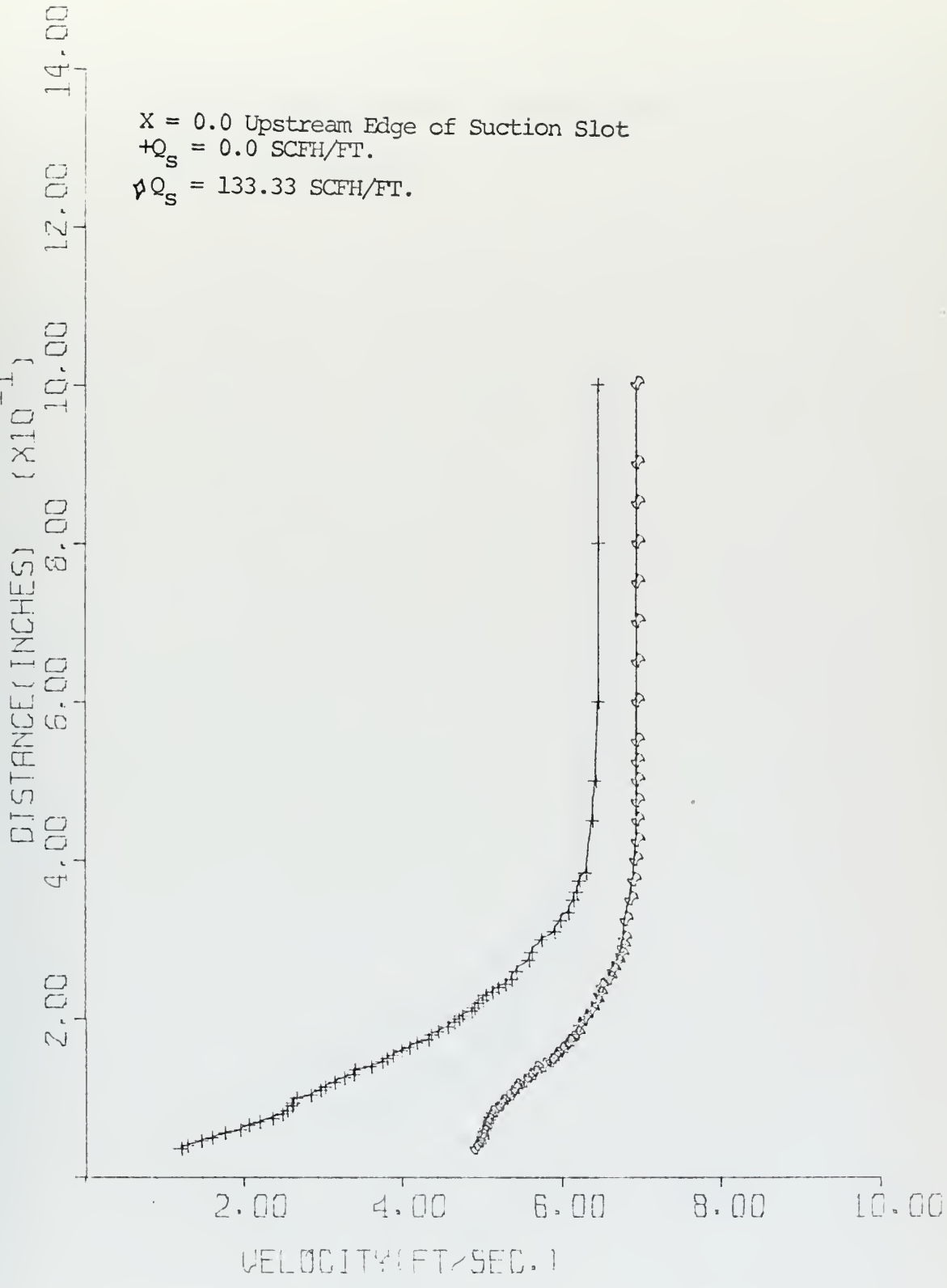

FIGURE 15
VELOCITY PROFILE

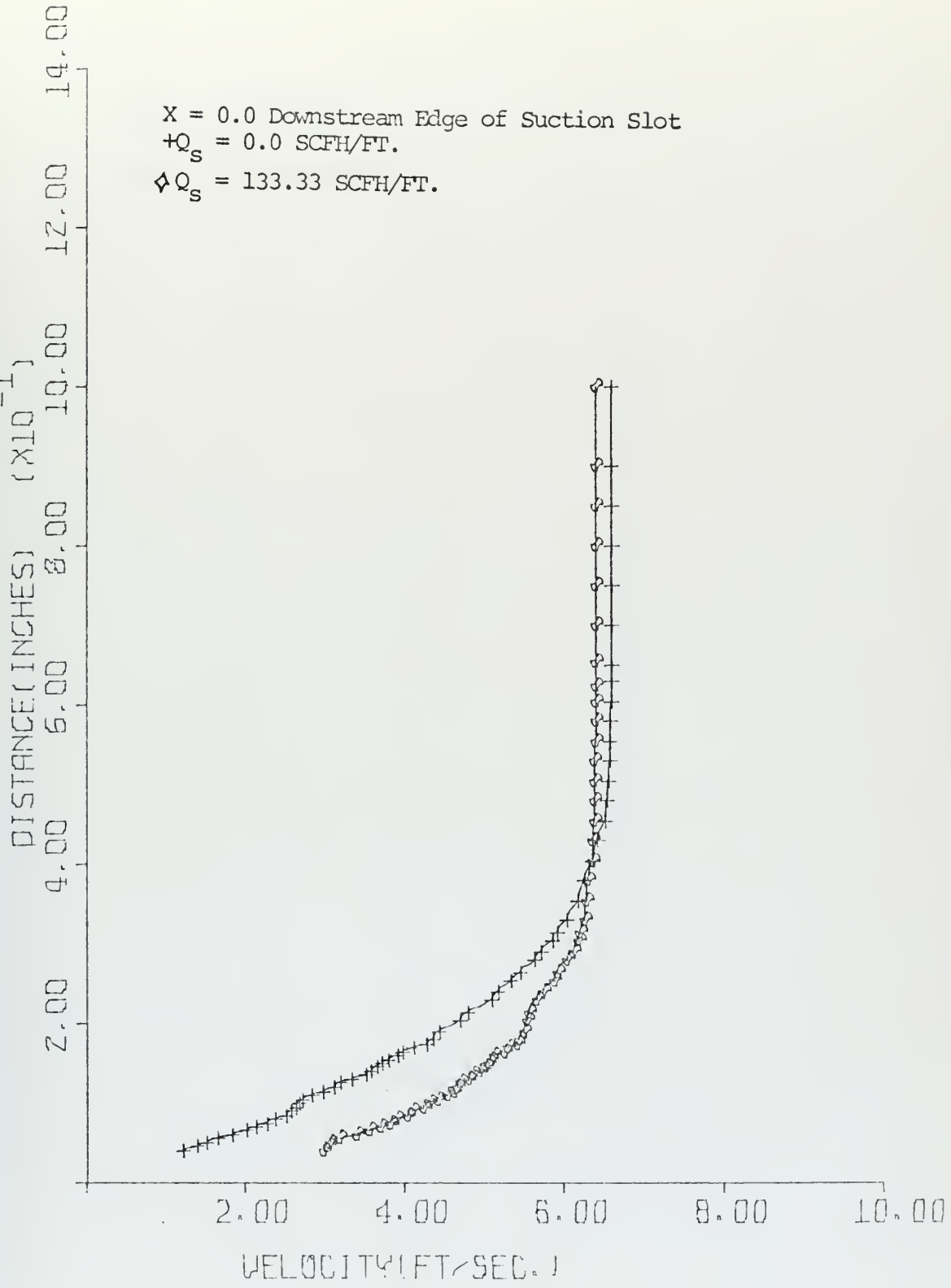

FIGURE 16
VELOCITY PROFILE

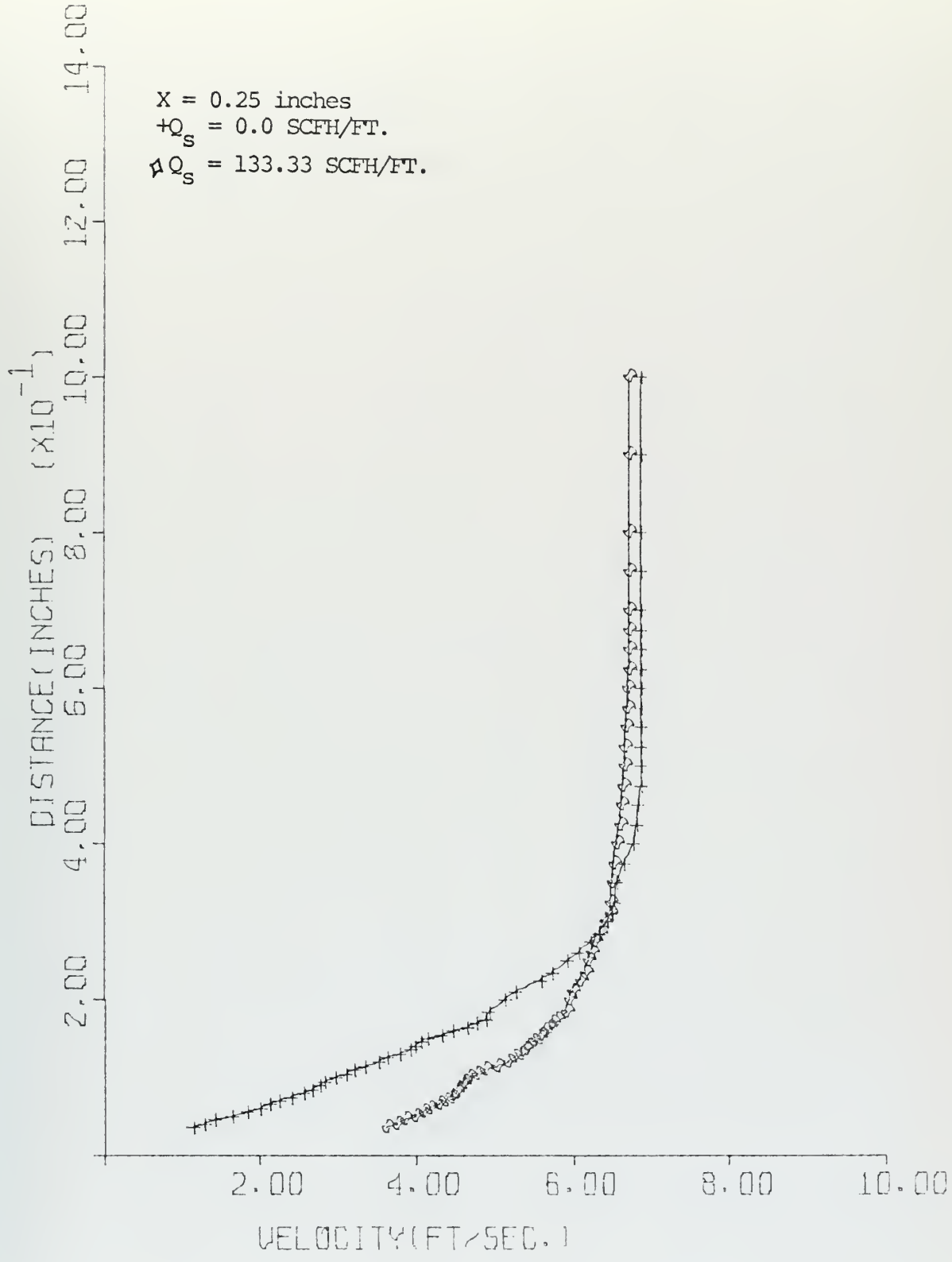

FIGURE 17
VELOCITY PROFILE

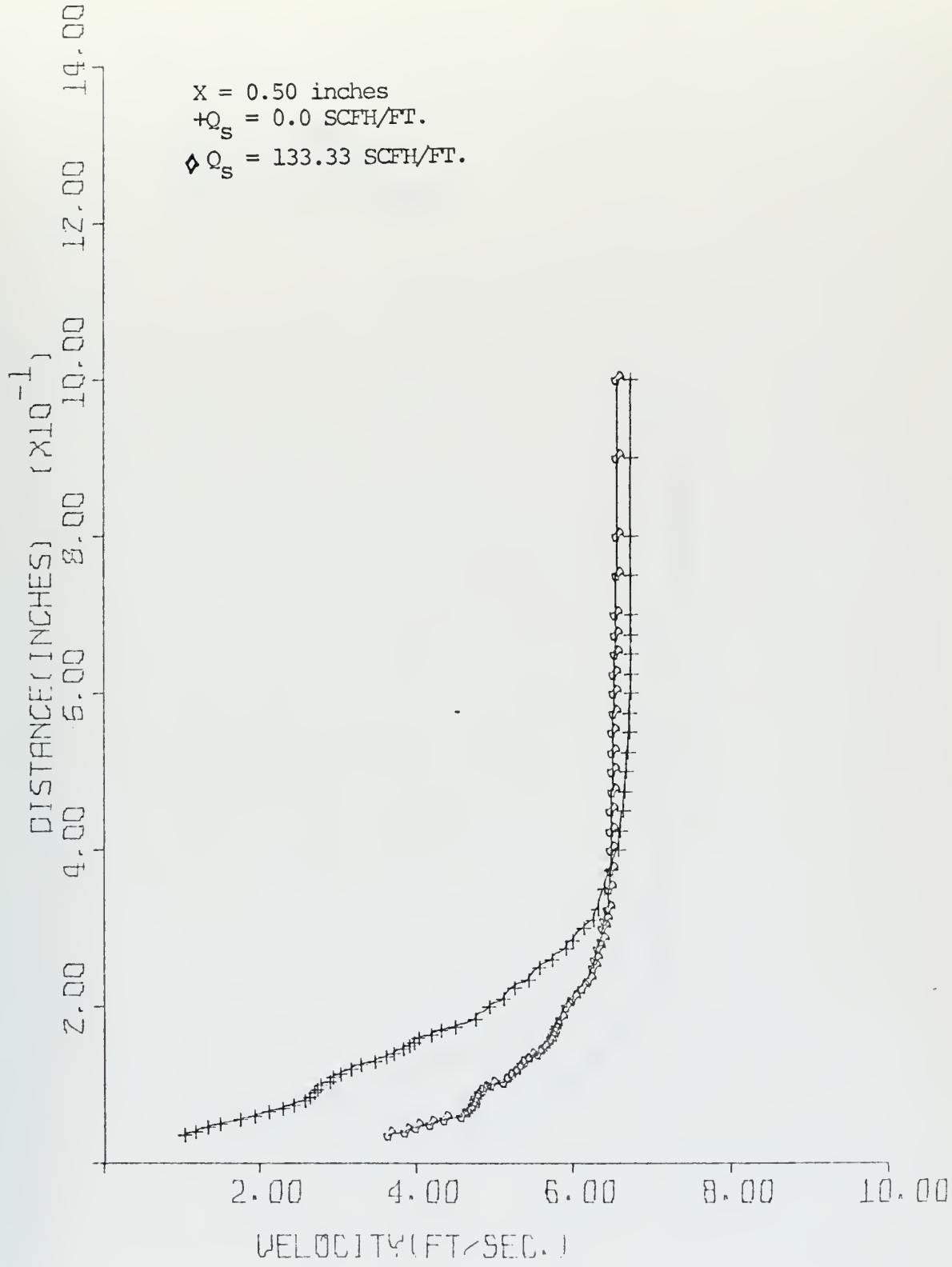

FIGURE 18

VELOCITY PROFILE

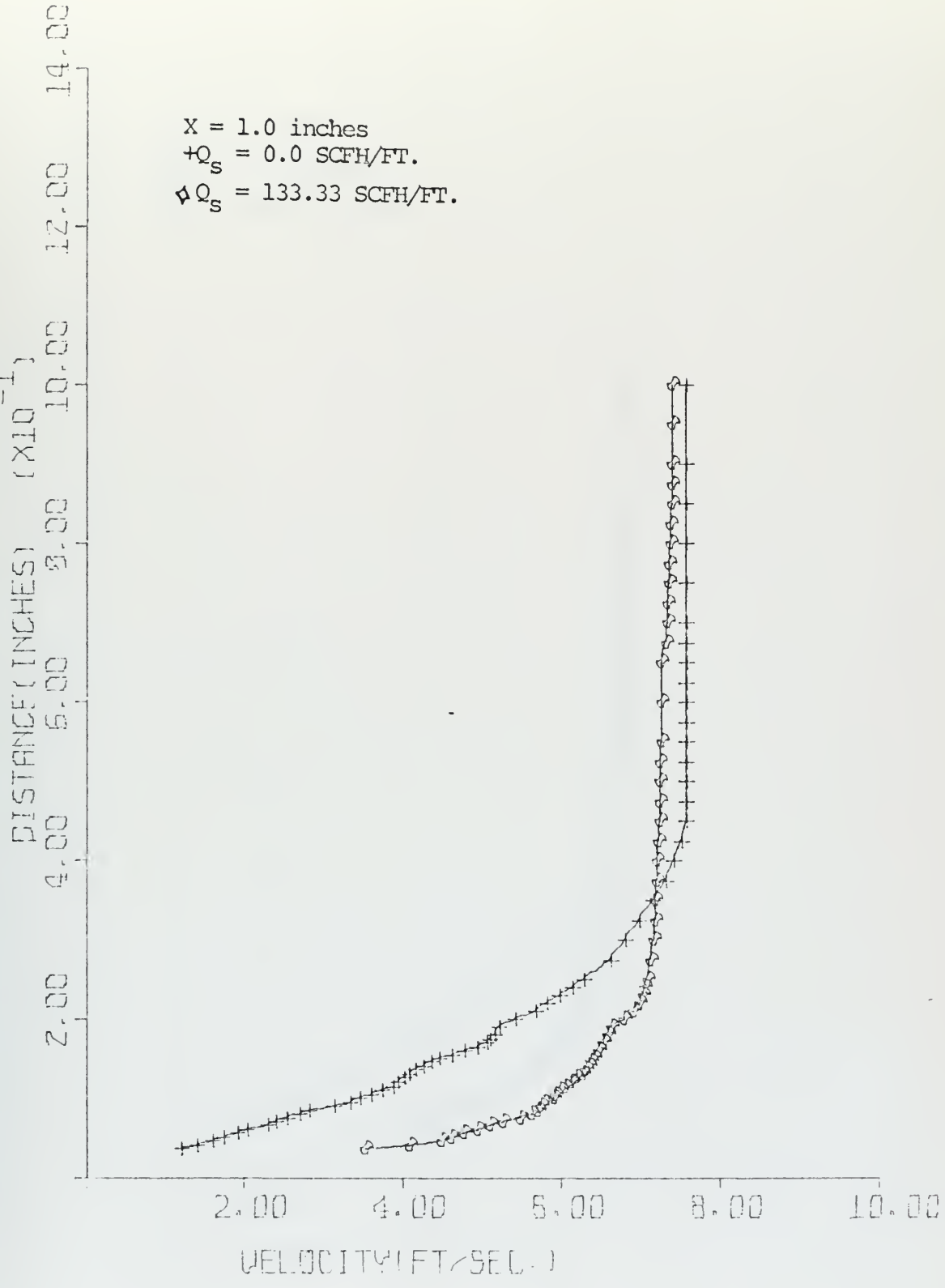

FIGURE 19
VELOCITY PROFILE

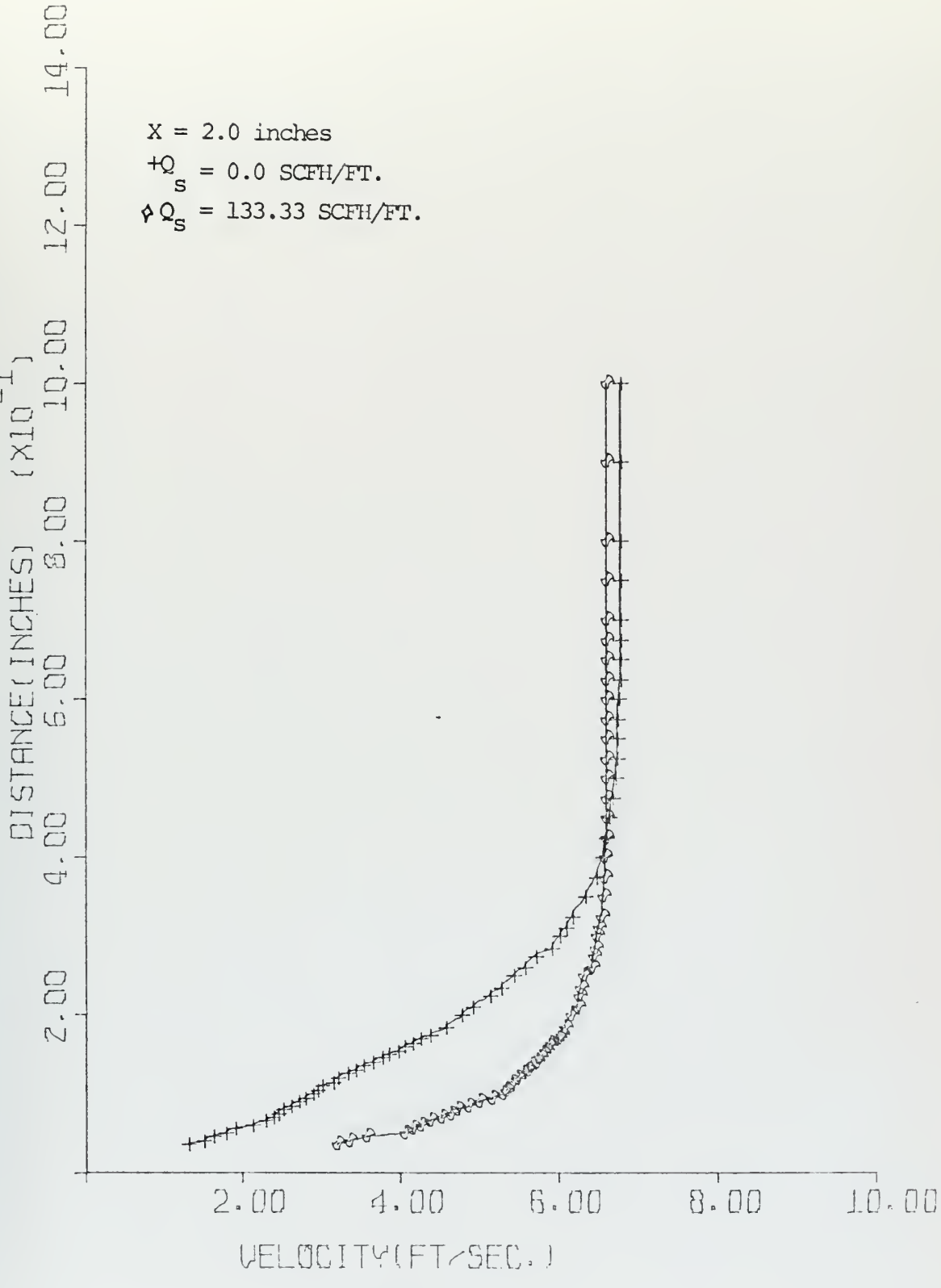

FIGURE 20
VELOCITY PROFILE

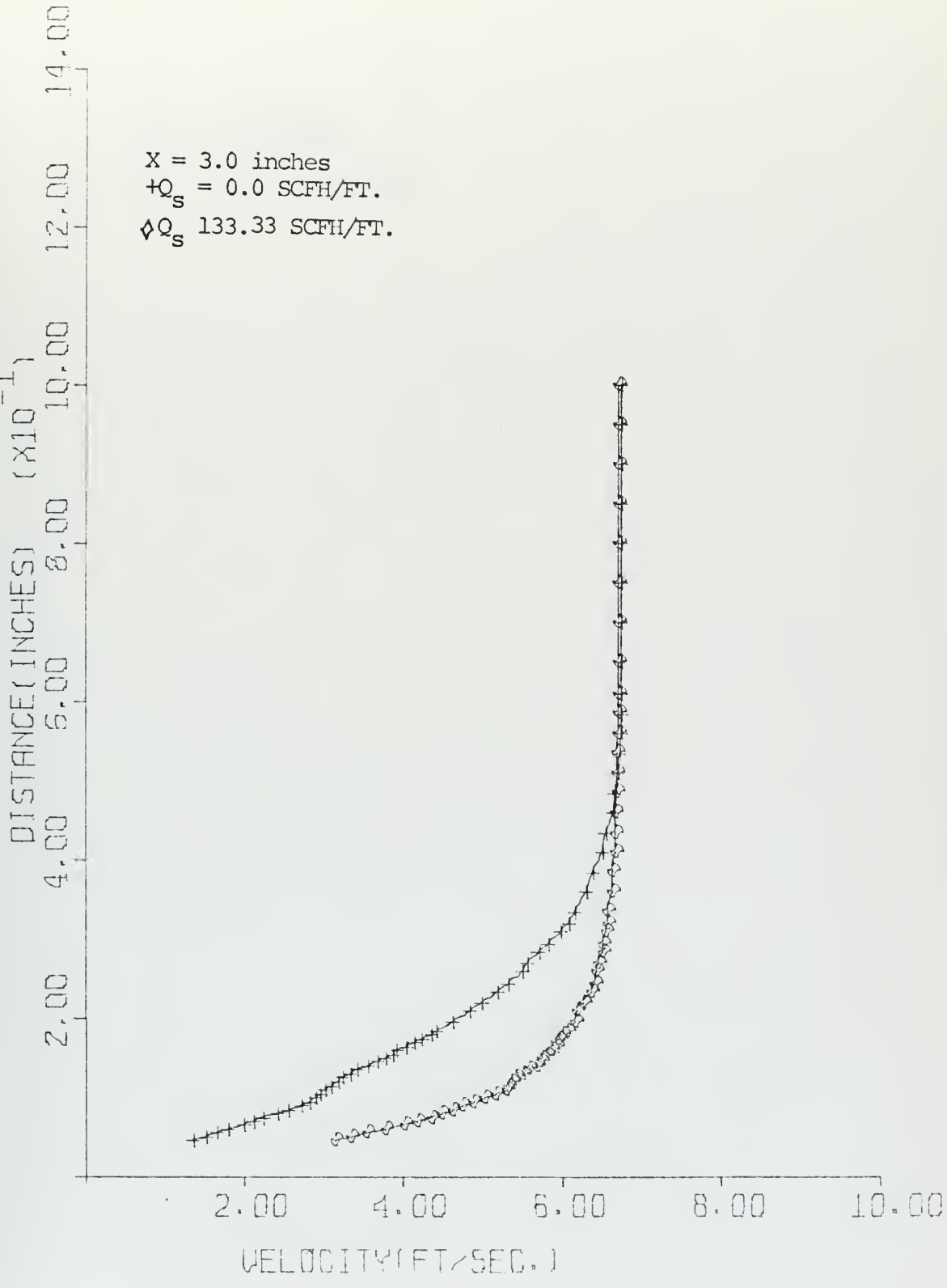

FIGURE 21
VELOCITY PROFILE

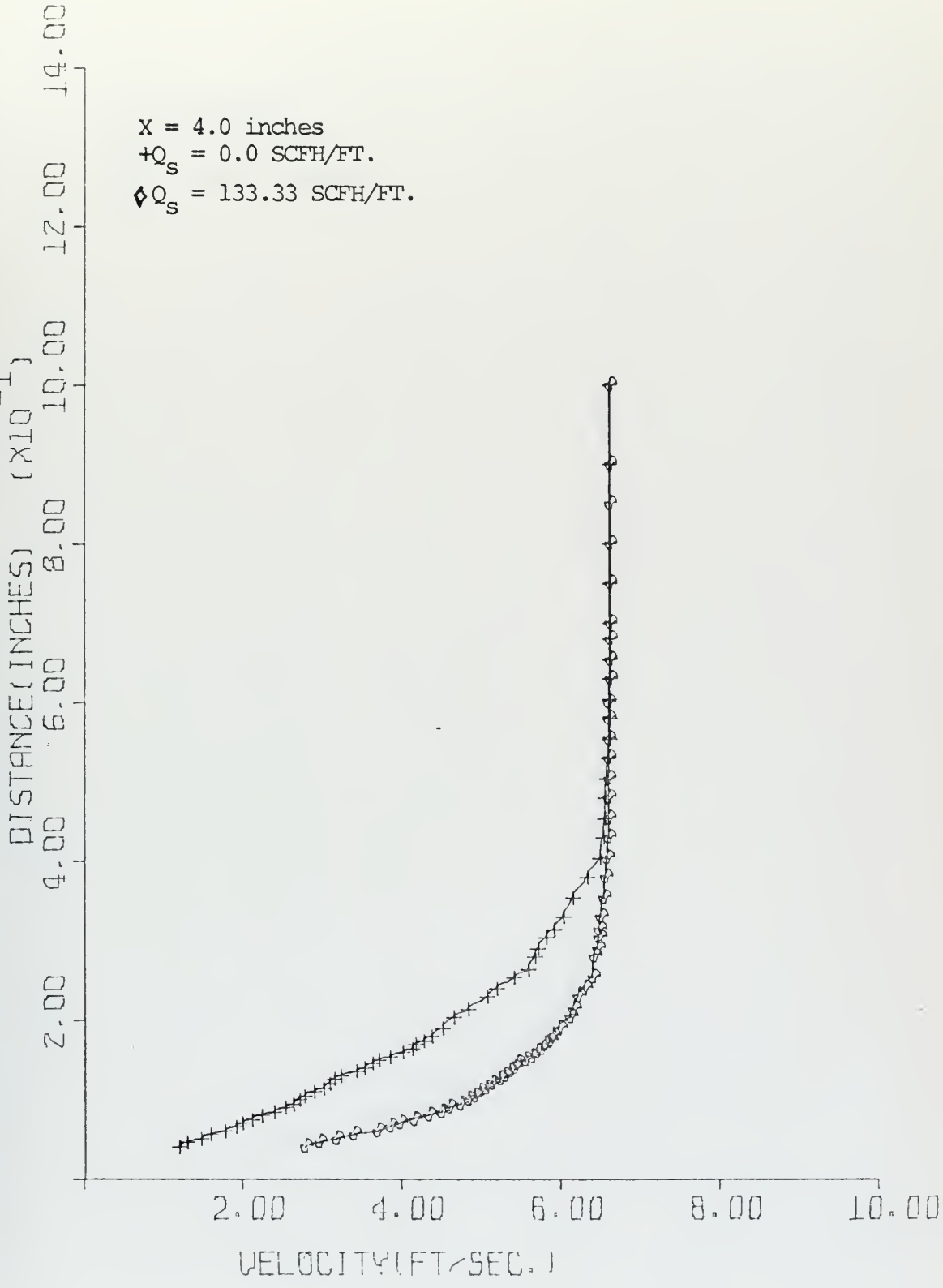

FIGURE 22
VELOCITY PROFILE

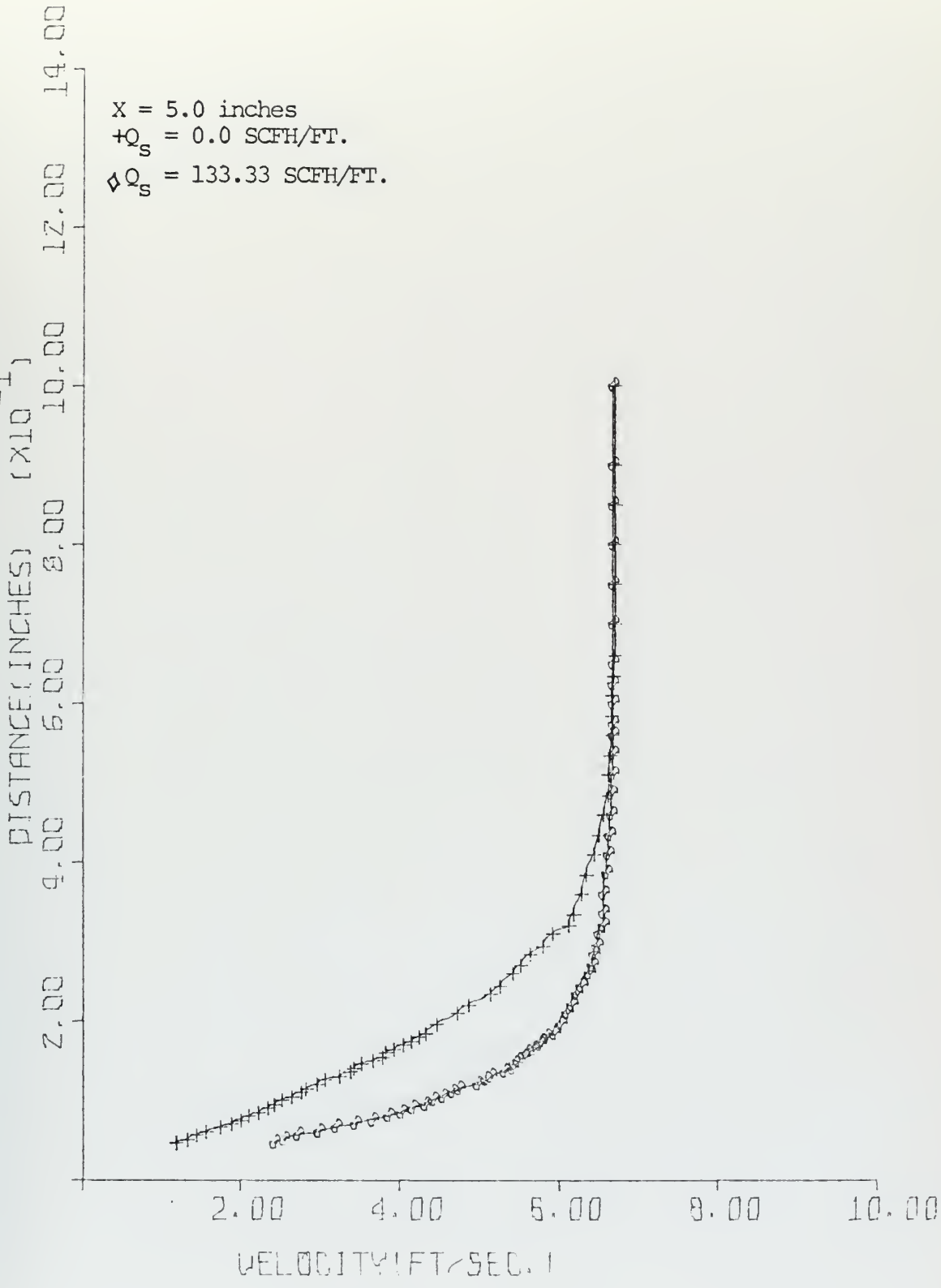

FIGURE 23
VELOCITY PROFILE

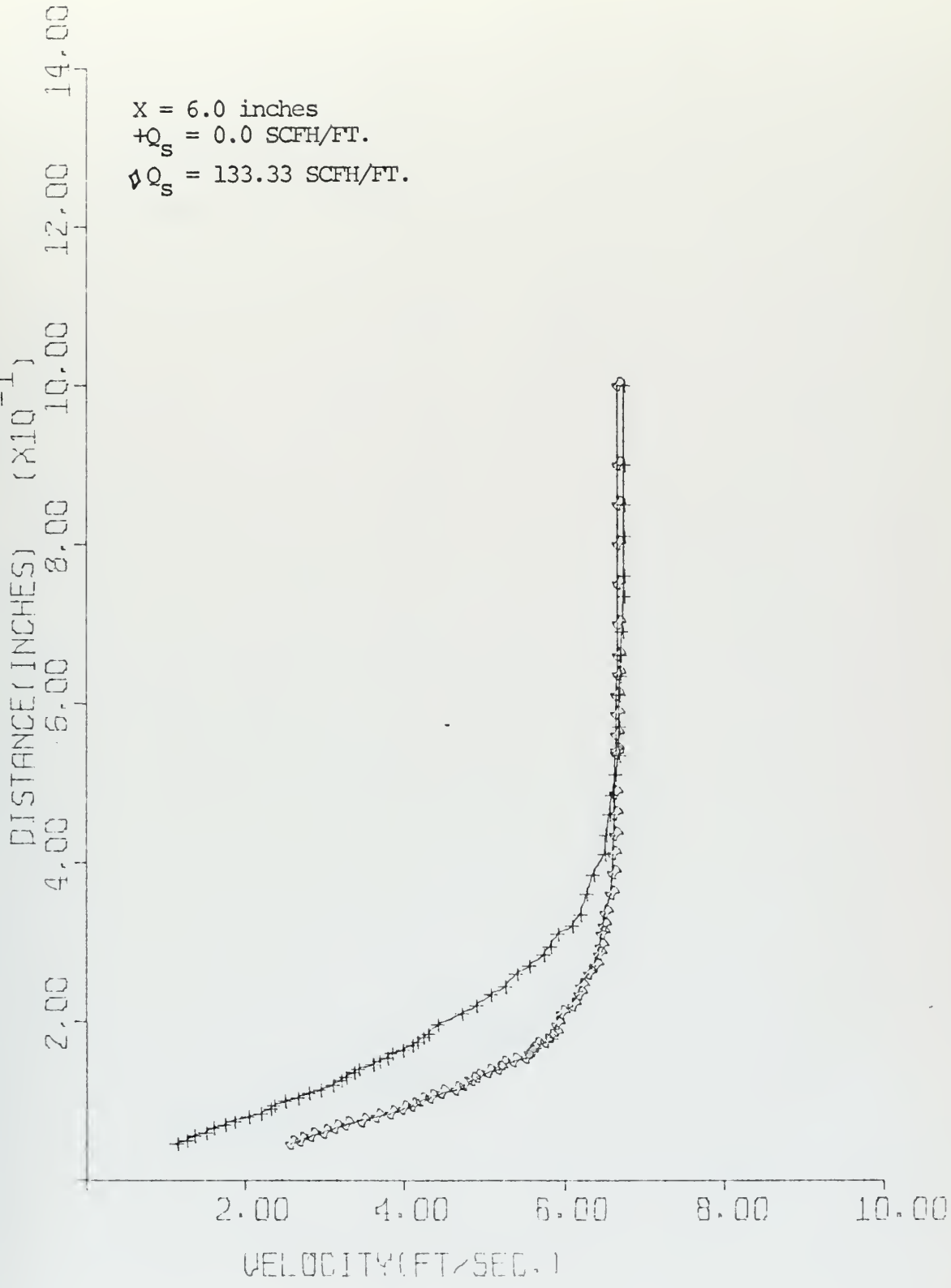

FIGURE 24
VELOCITY PROFILE

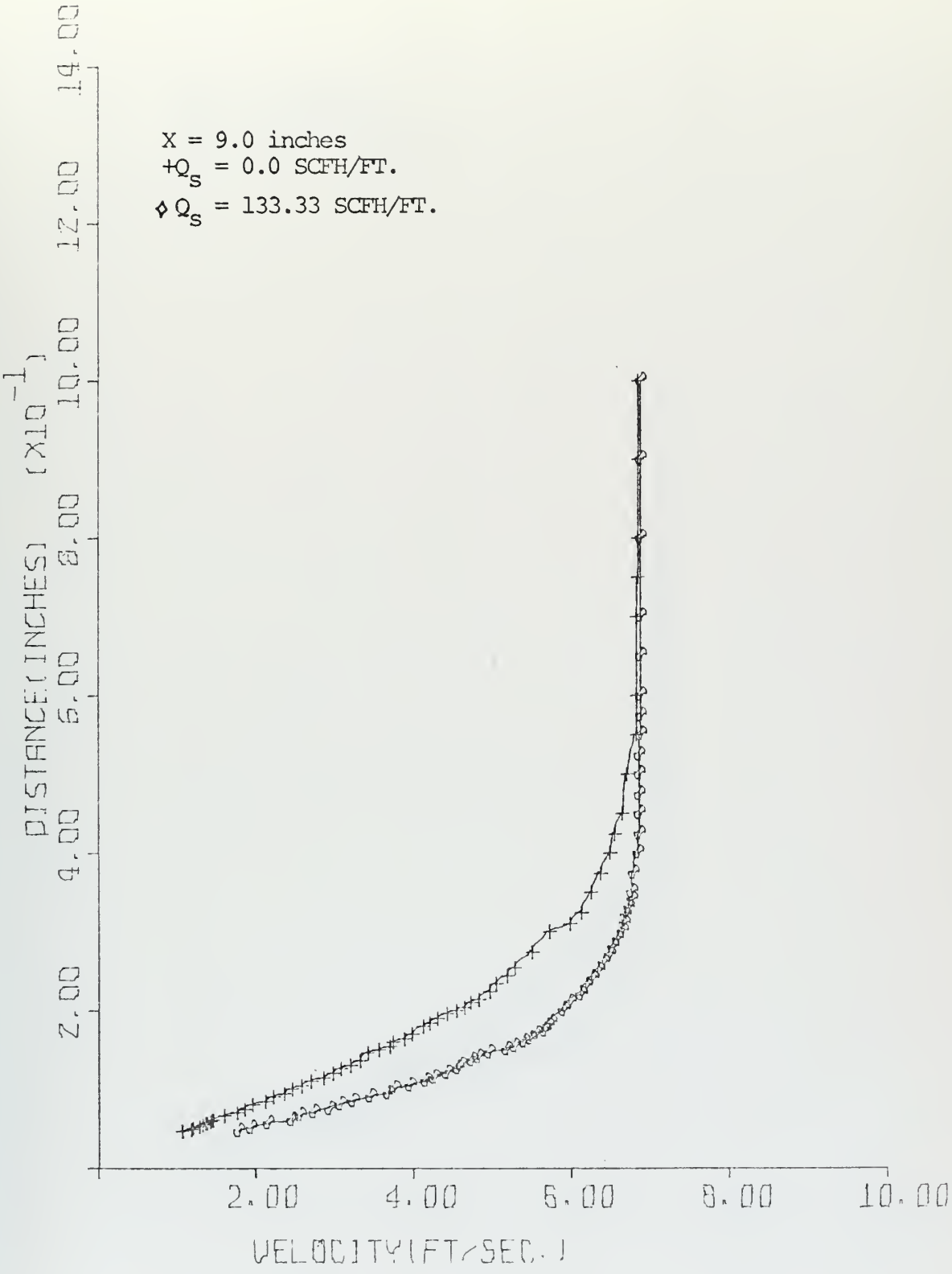

FIGURE 25
VELOCITY PROFILE

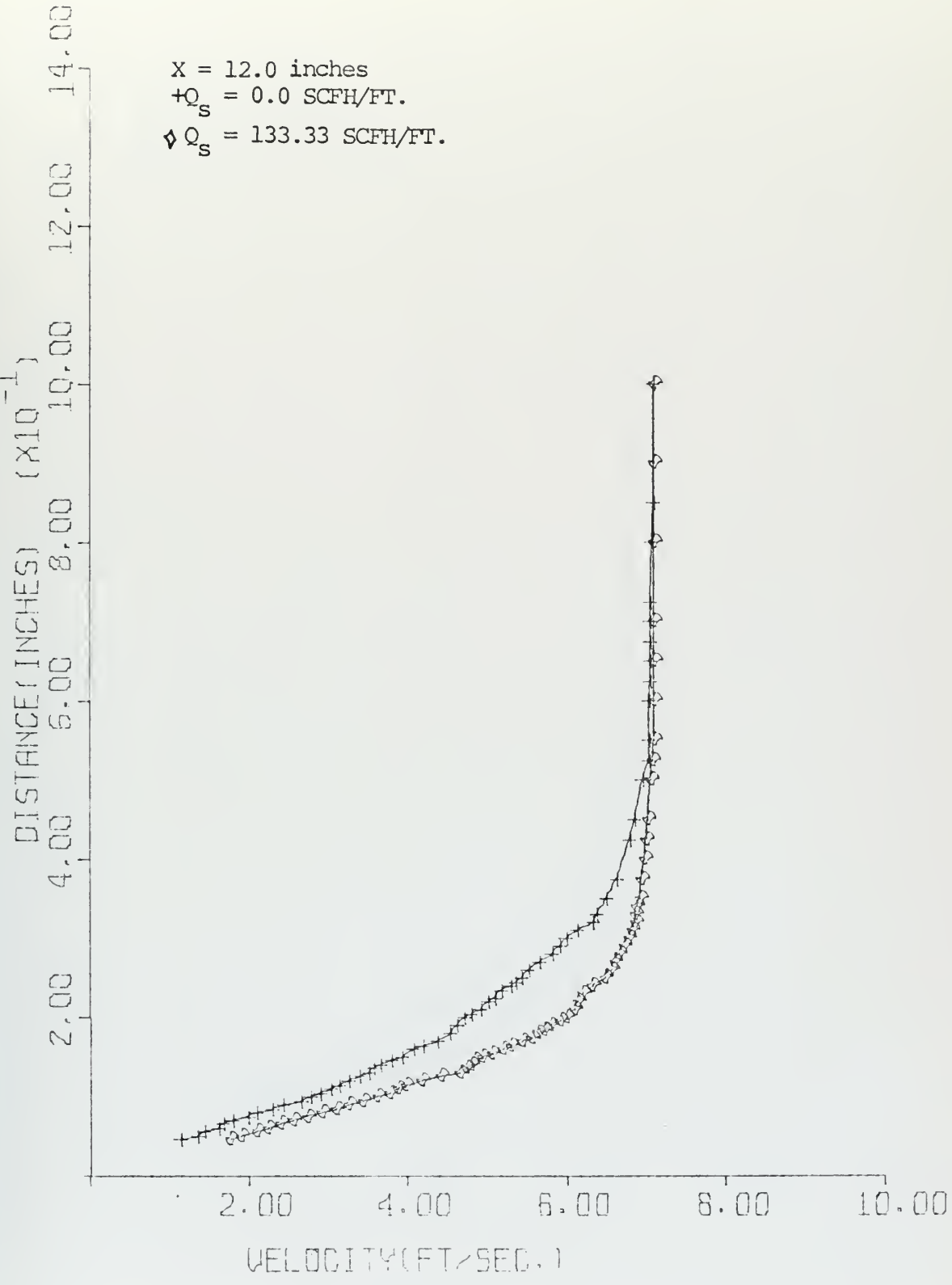

FIGURE 26
VELOCITY PROFILE

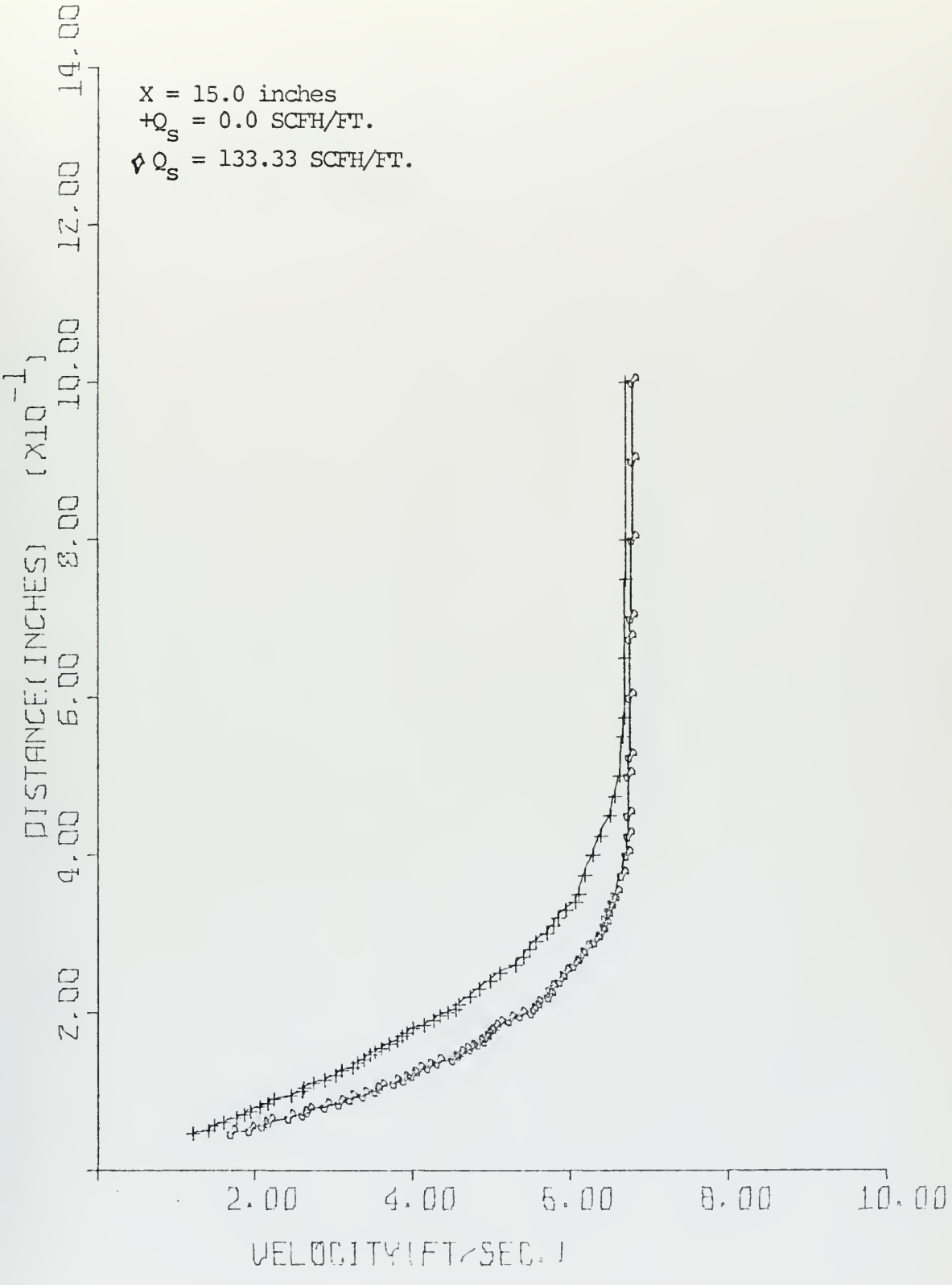

FIGURE 27
VELOCITY PROFILE

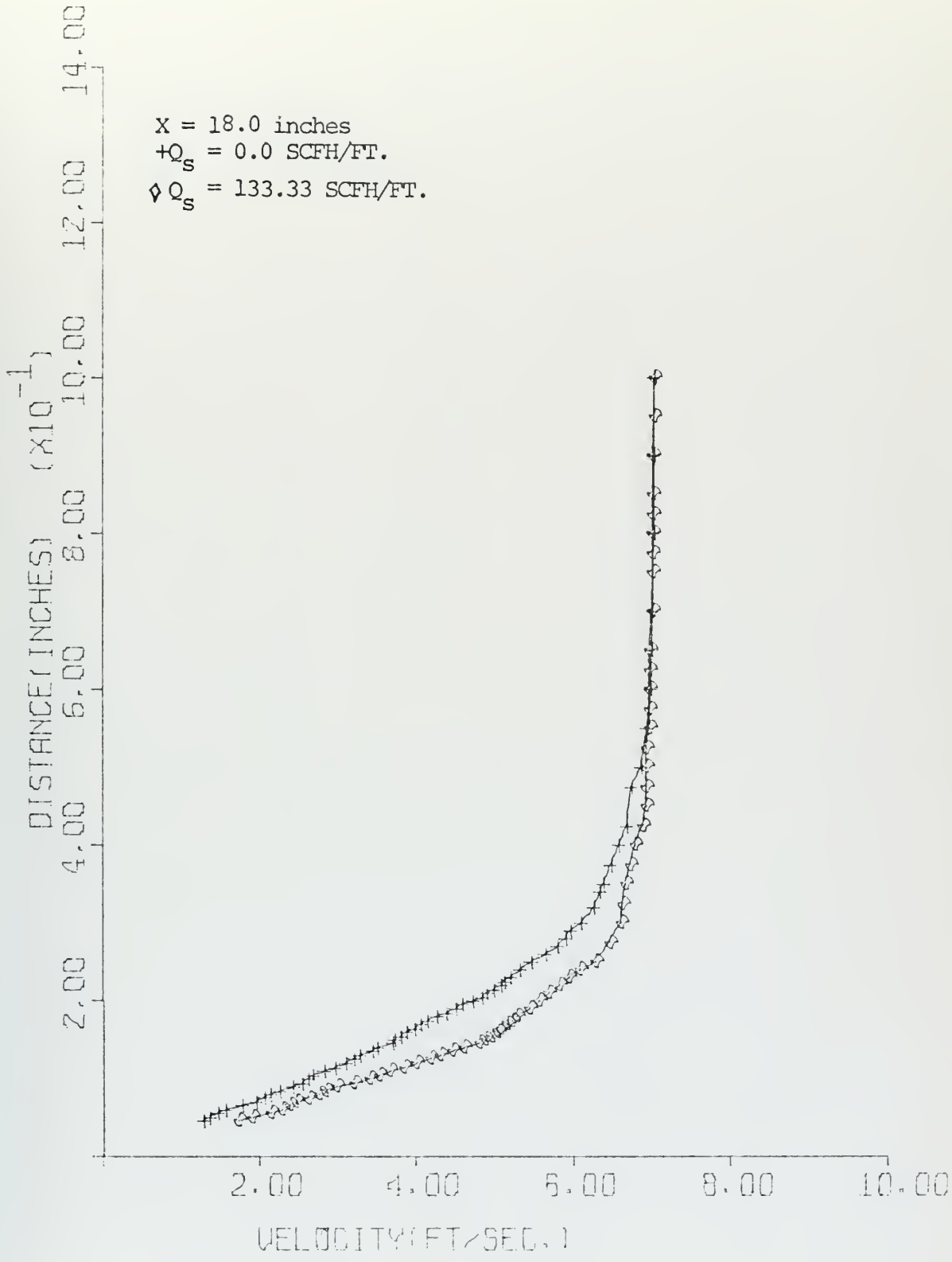

FIGURE 28
VELOCITY PROFILE

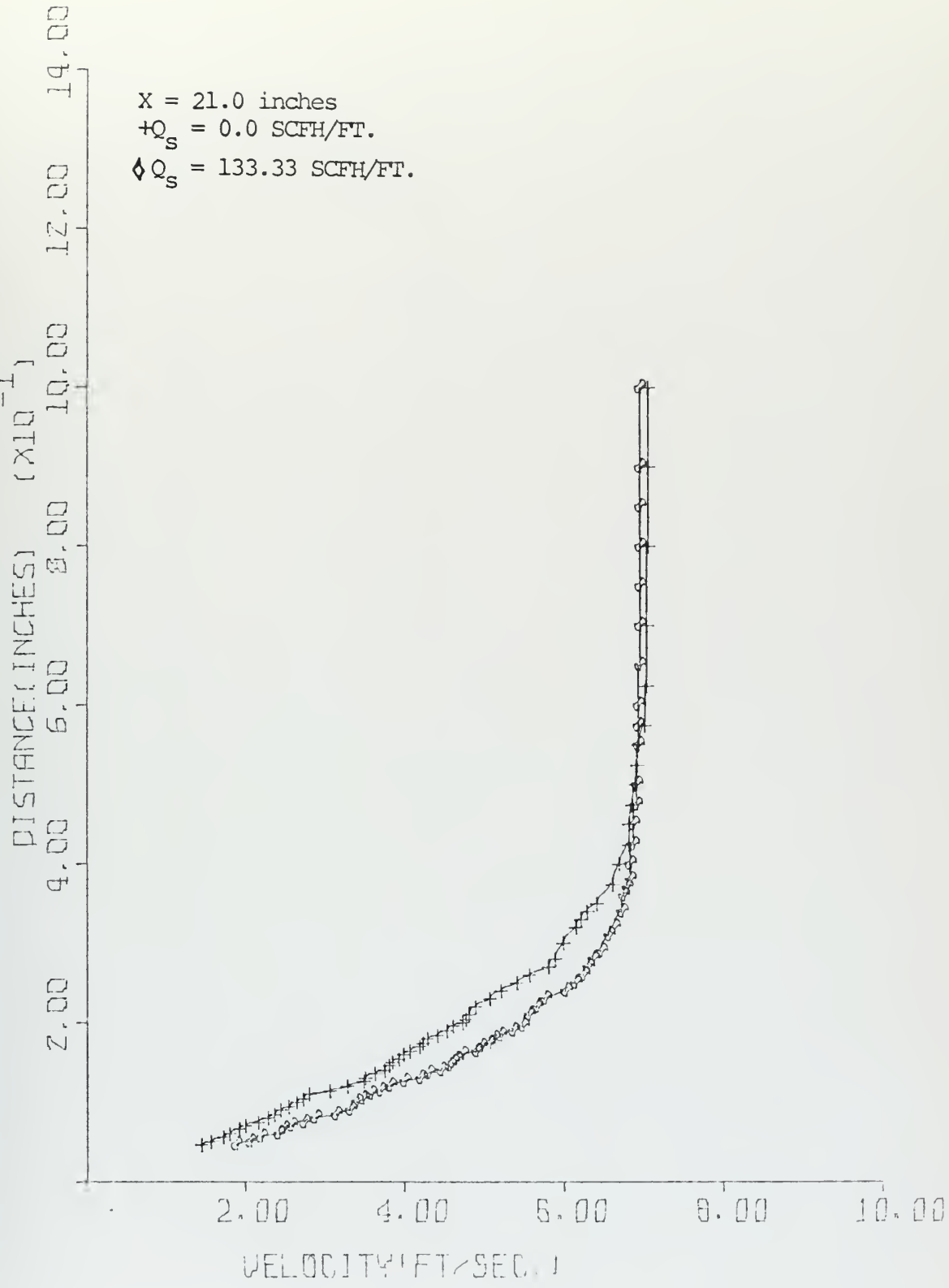

FIGURE 29
VELOCITY PROFILE

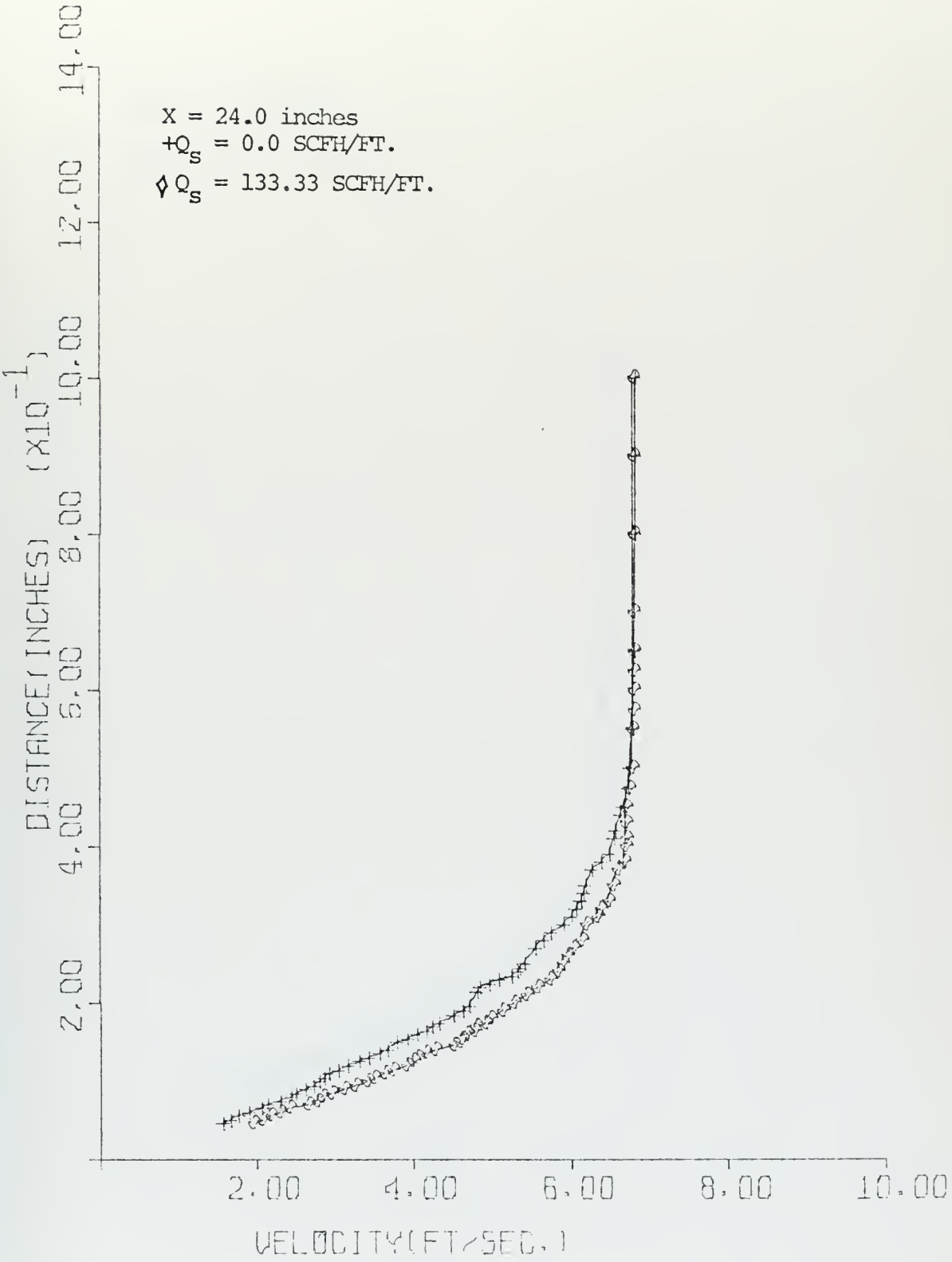

FIGURE 30
VELOCITY PROFILE

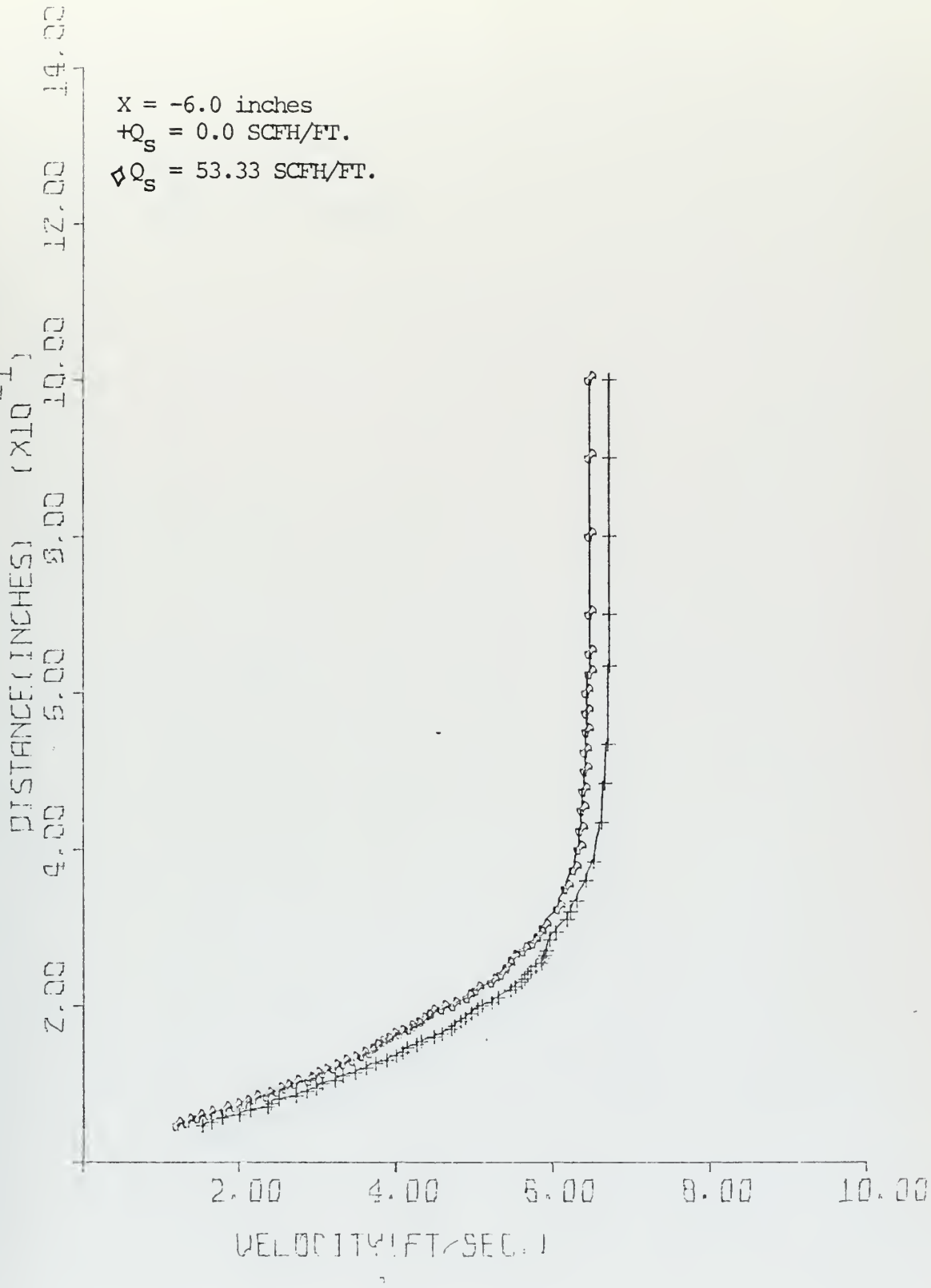

FIGURE 31
VELOCITY PROFILE

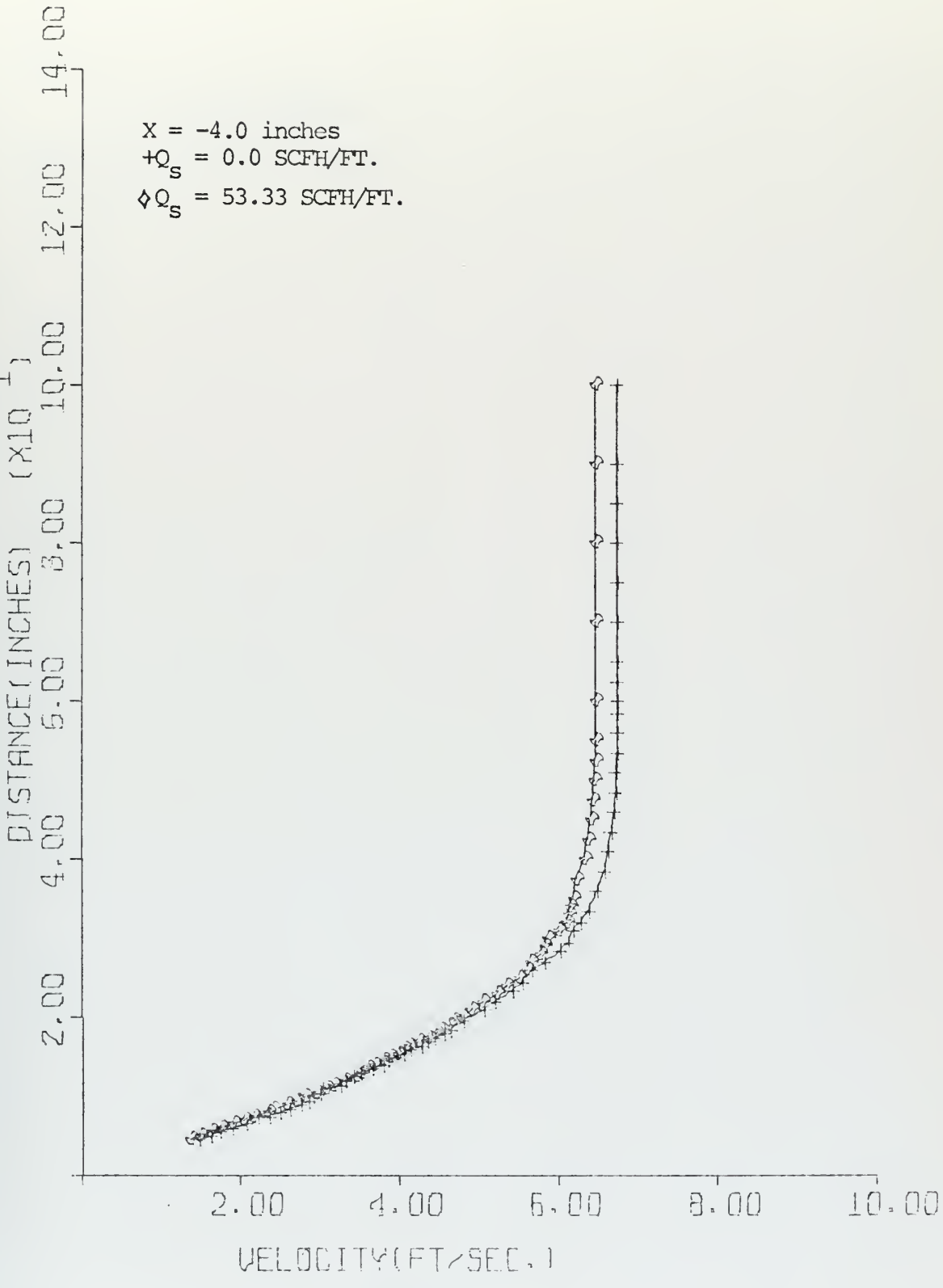

FIGURE 32
VELOCITY PROFILE

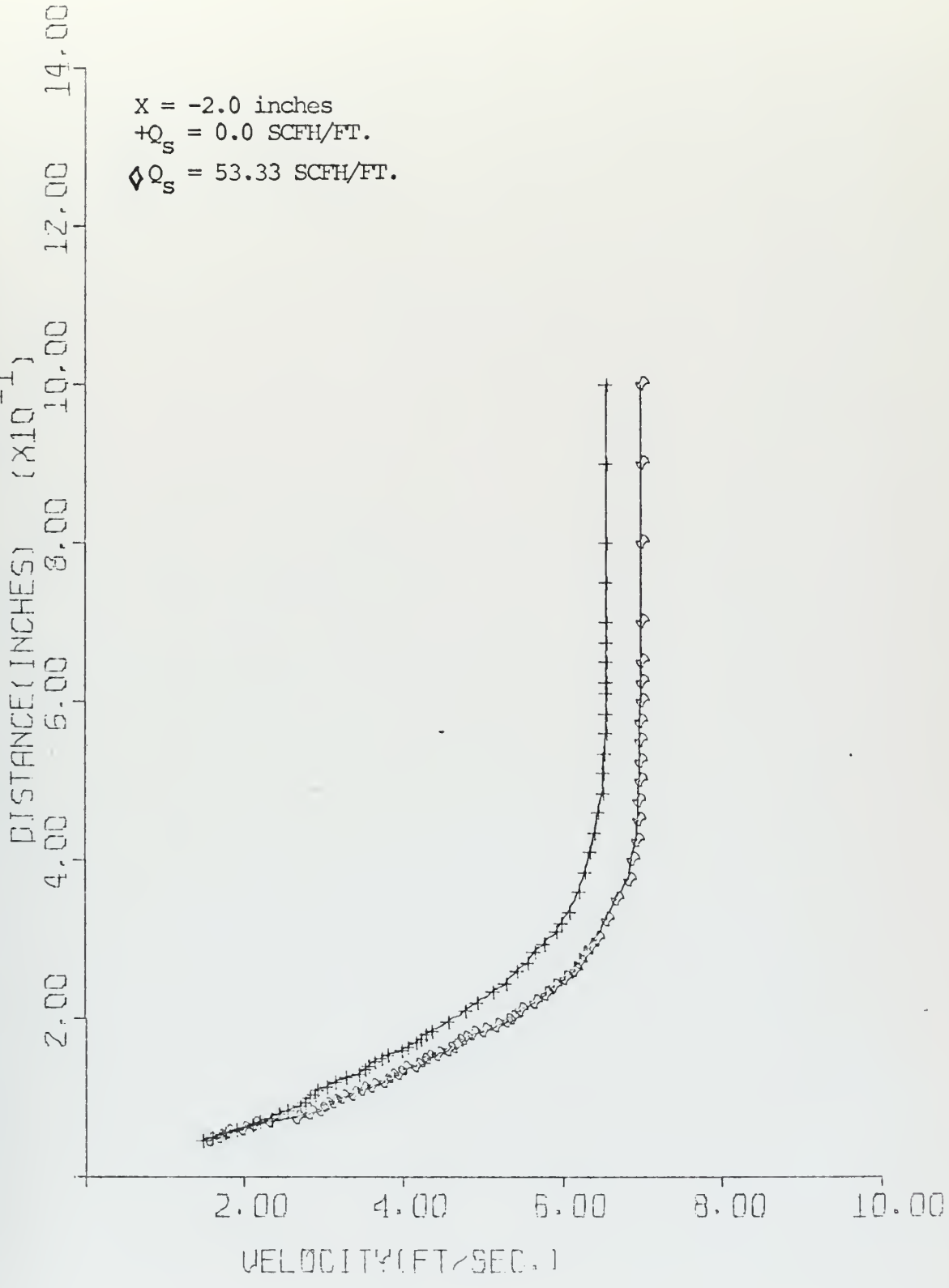

FIGURE 33
VELOCITY PROFILE

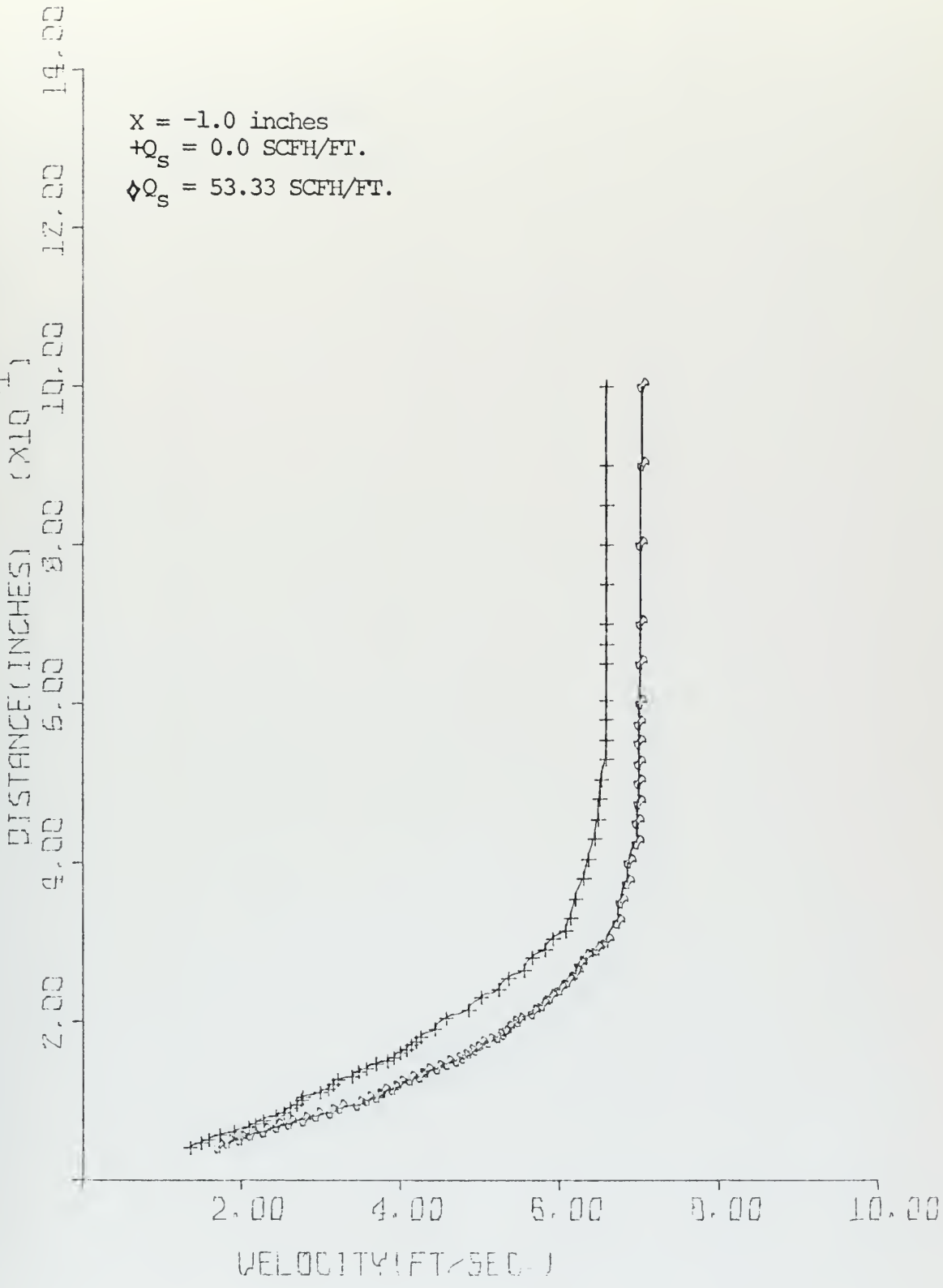

FIGURE 34
VELOCITY PROFILES

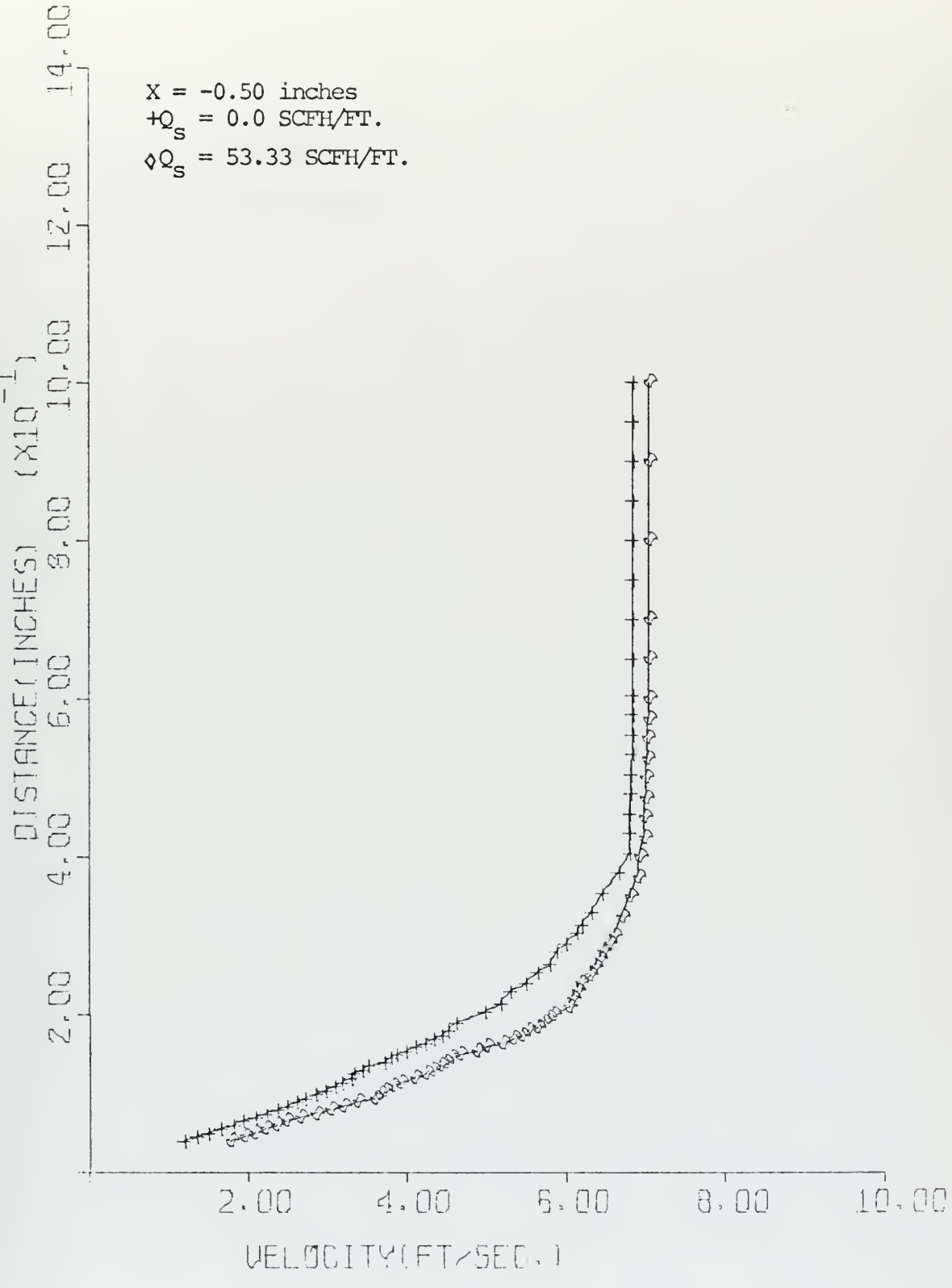

FIGURE 35
VELOCITY PROFILE

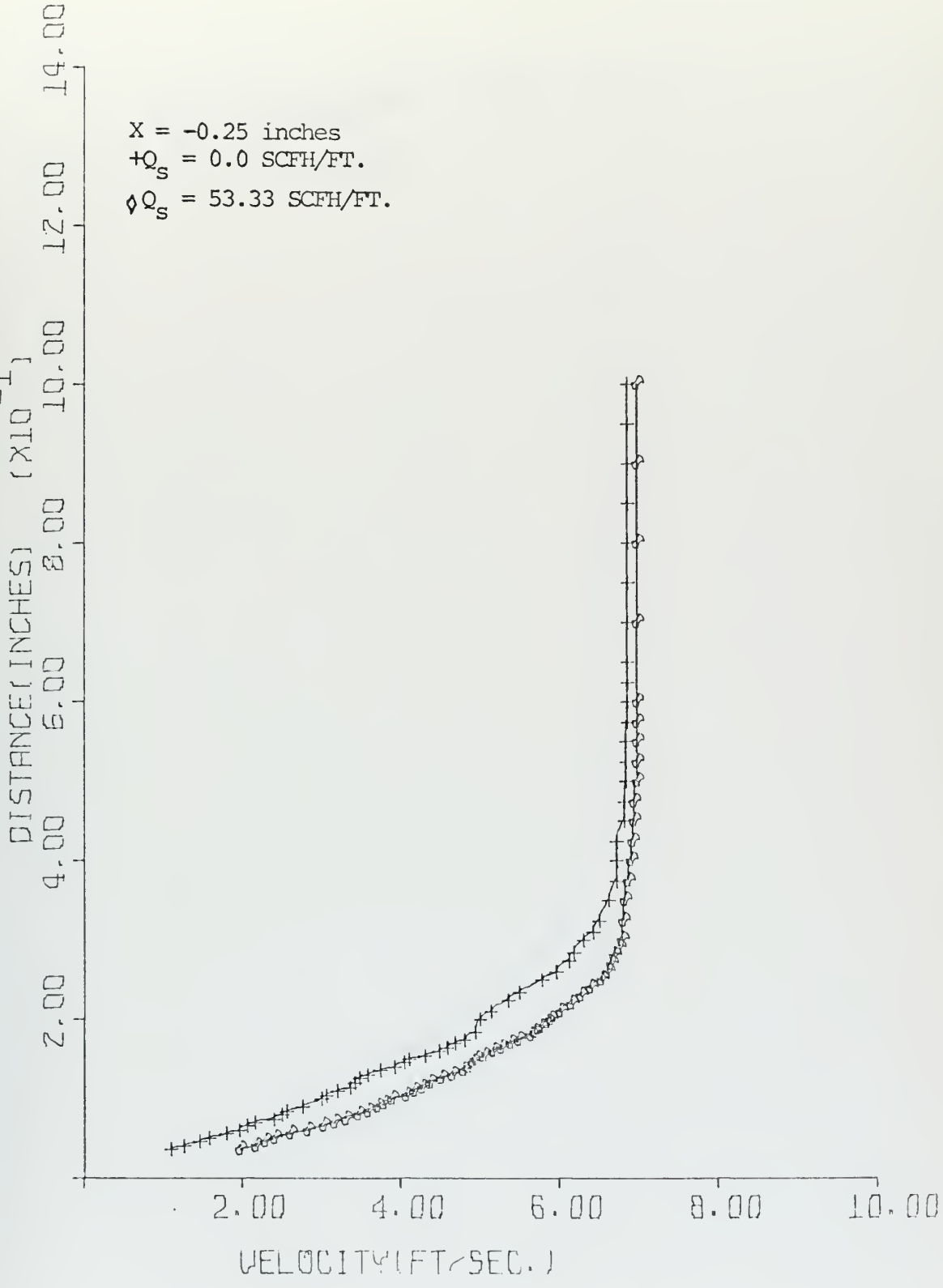

FIGURE 36
VELOCITY PROFILE

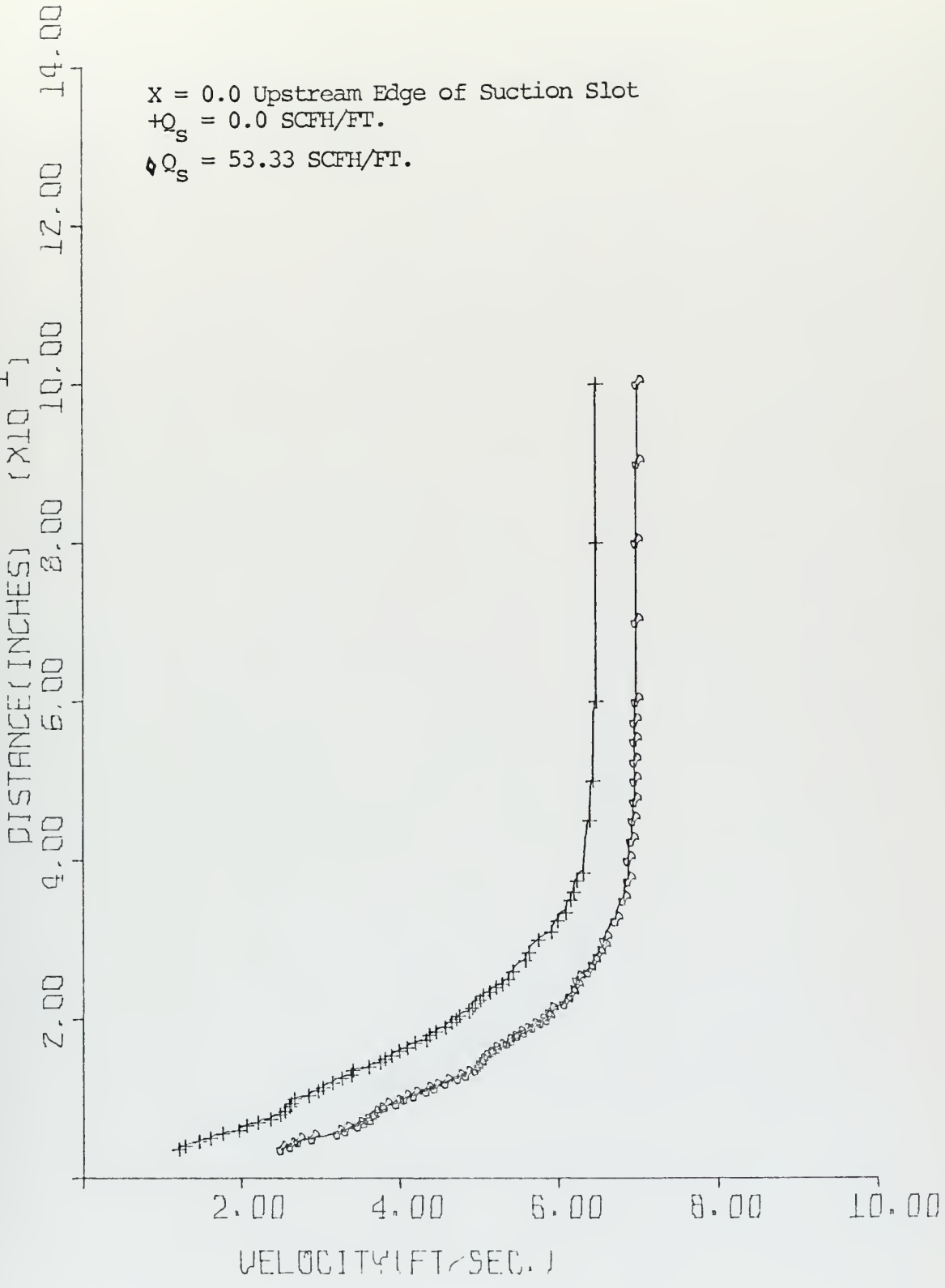

FIGURE 37
VELOCITY PROFILE

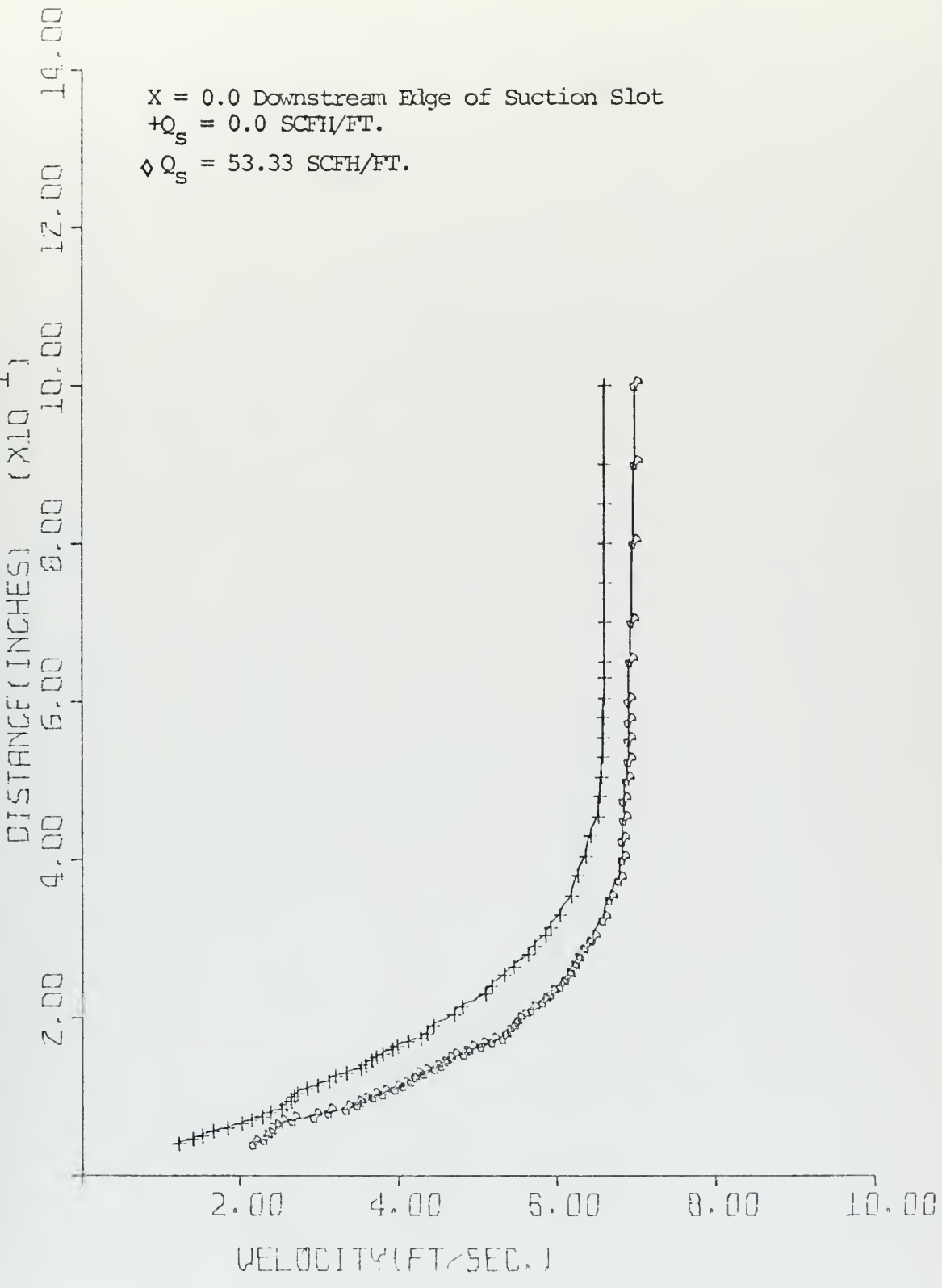

FIGURE 38
VELOCITY PROFILE

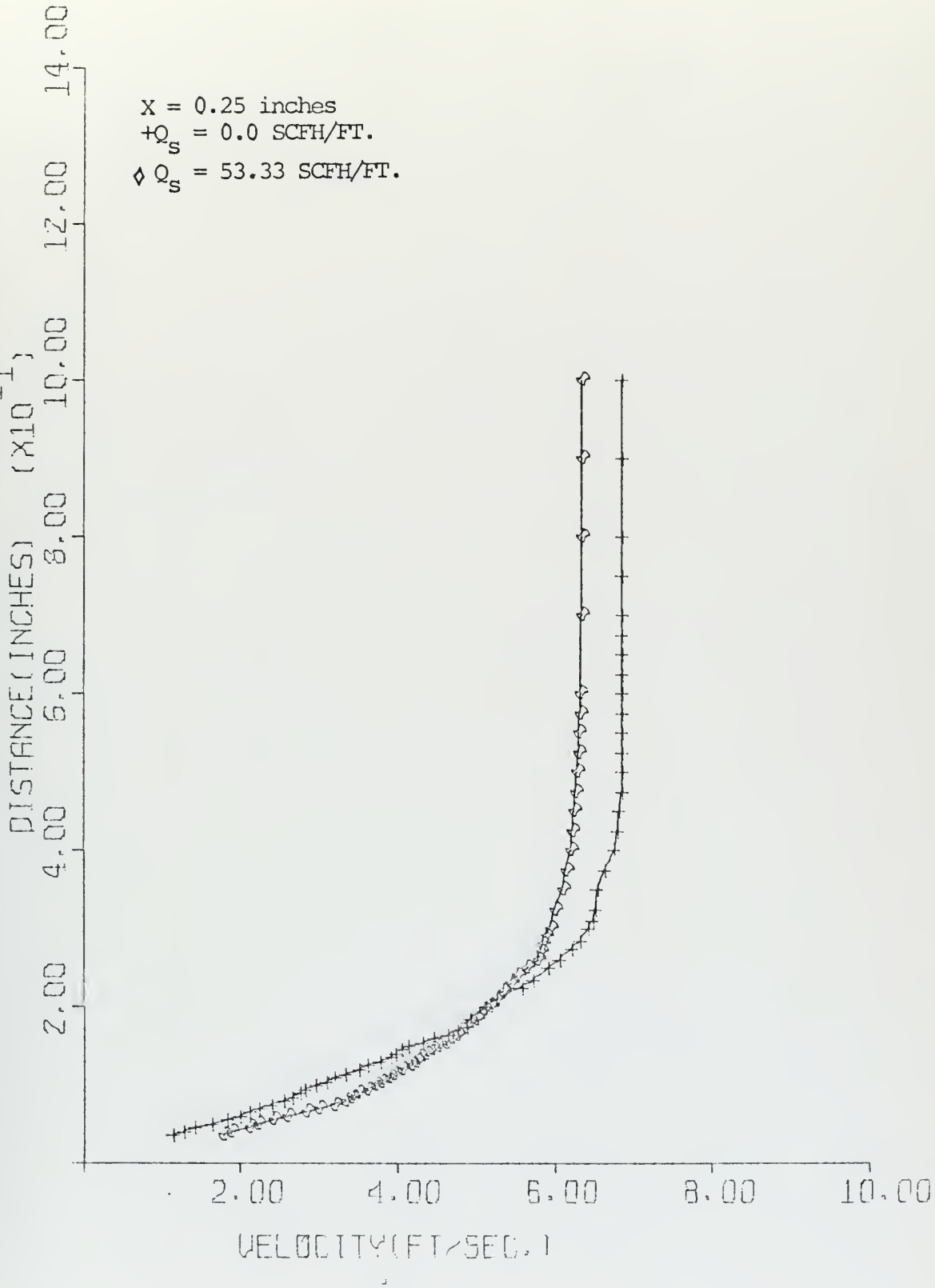

FIGURE 39
VELOCITY PROFILE

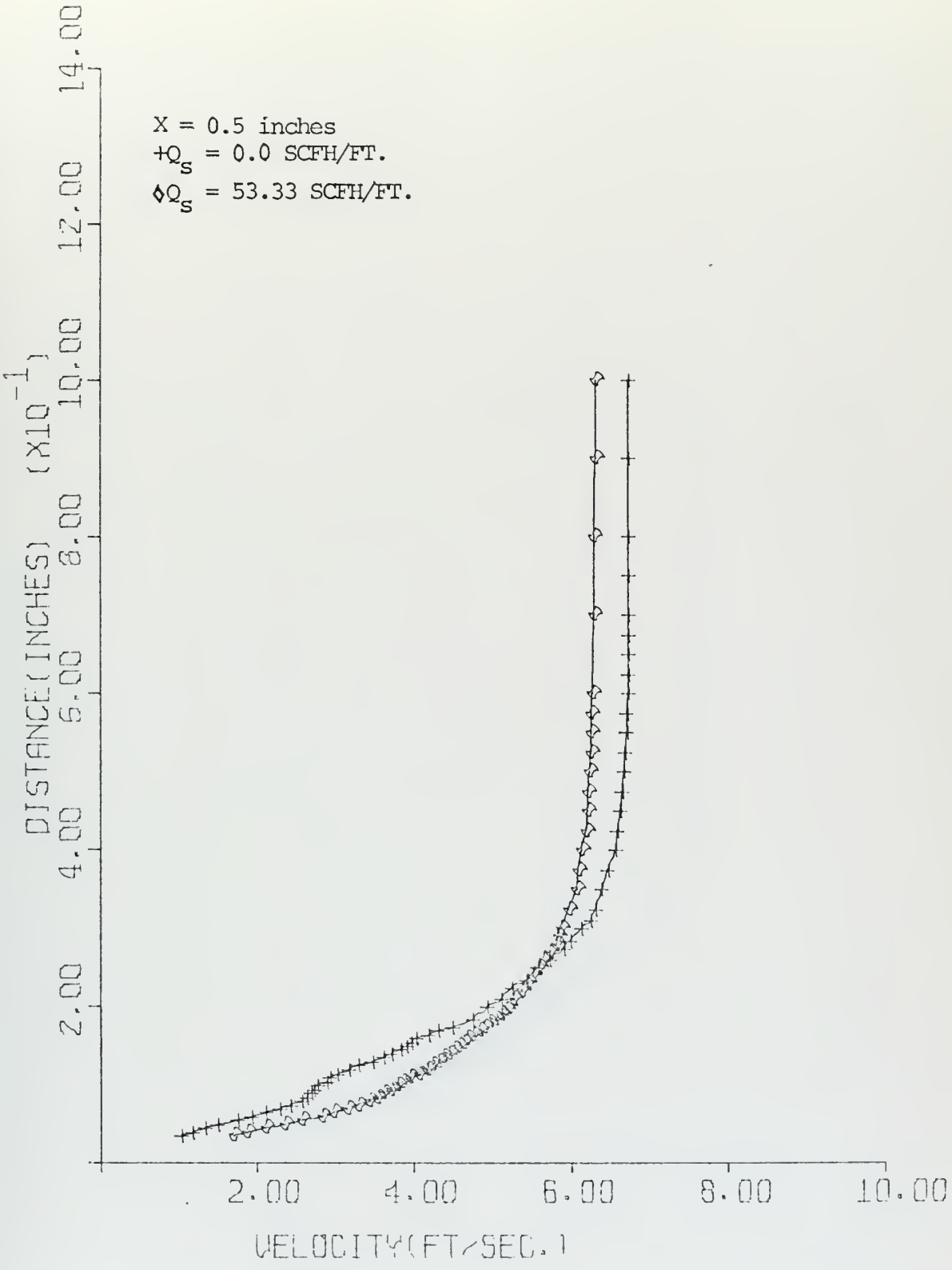

FIGURE 40
VELOCITY PROFILE

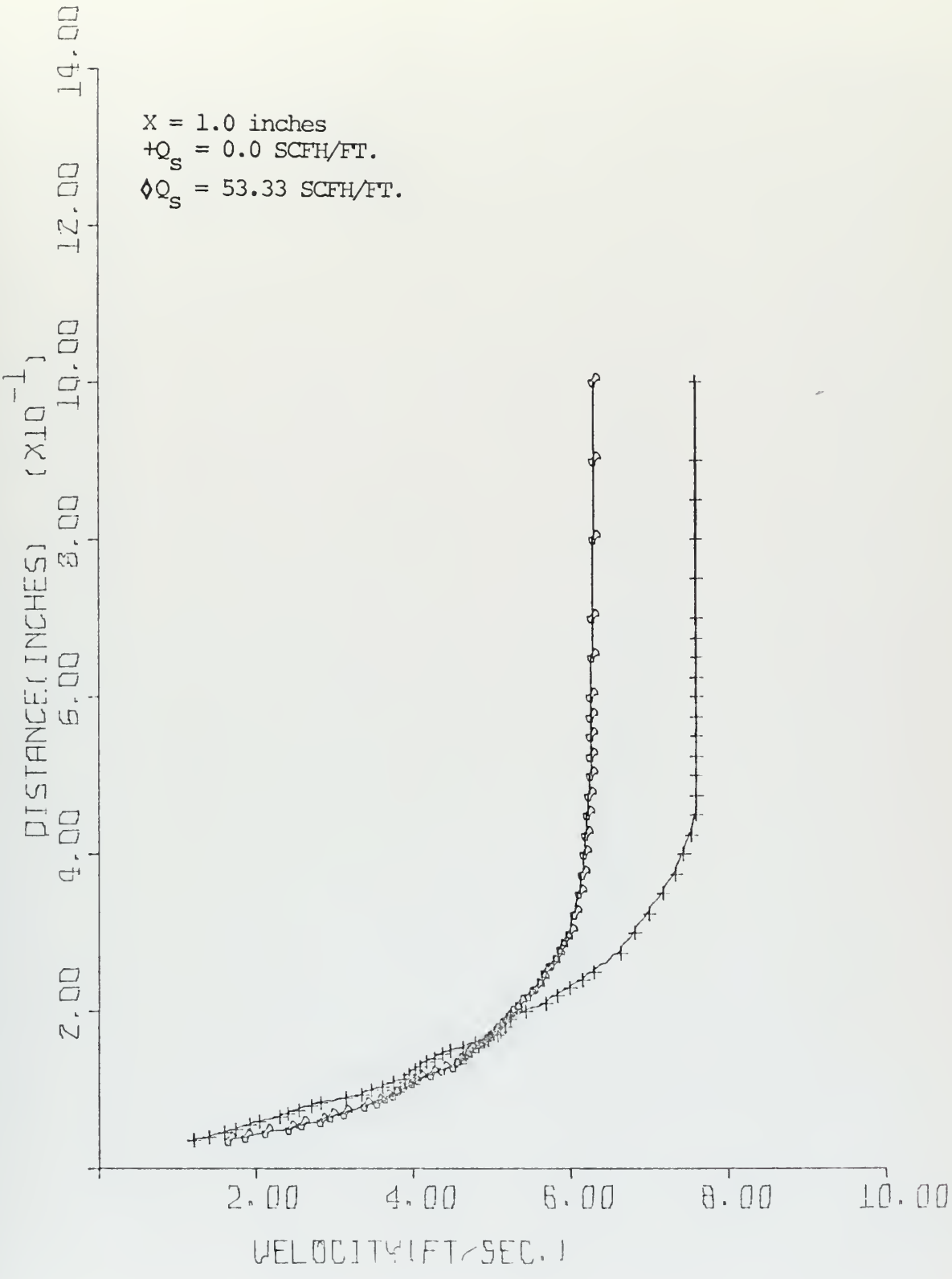

FIGURE 41
VELOCITY PROFILE

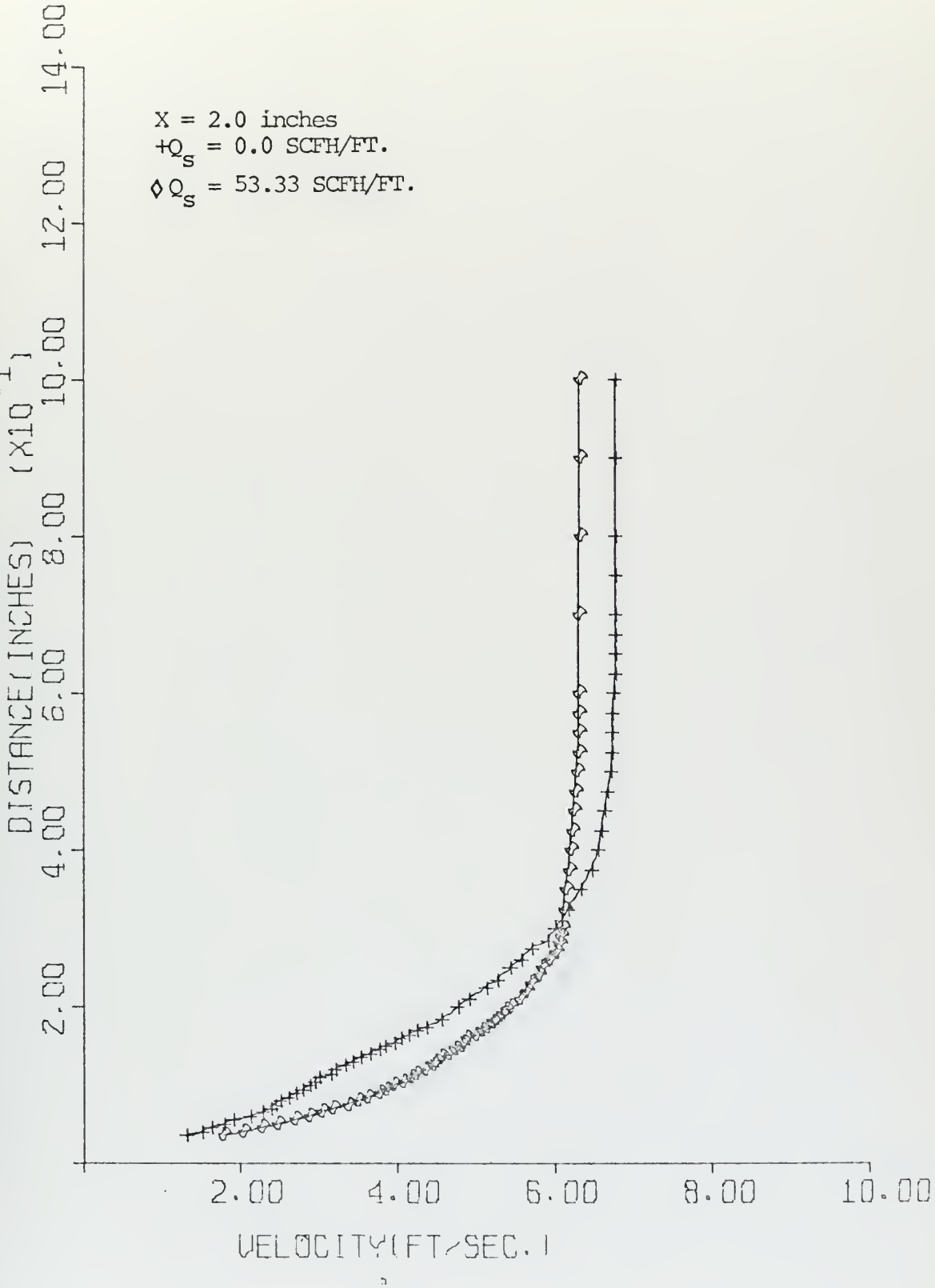

FIGURE 42
VELOCITY PROFILE

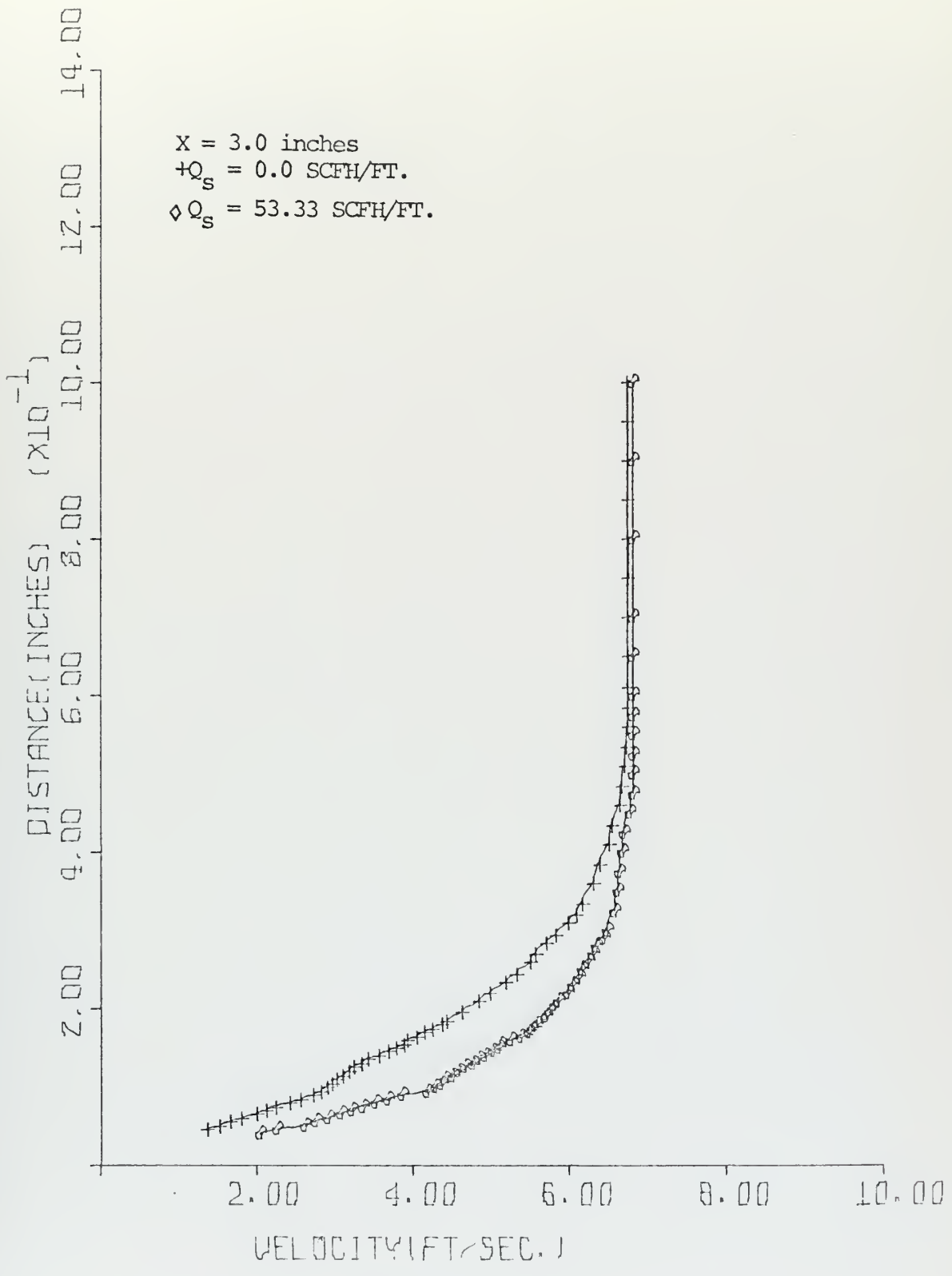

FIGURE 43
VELOCITY PROFILE

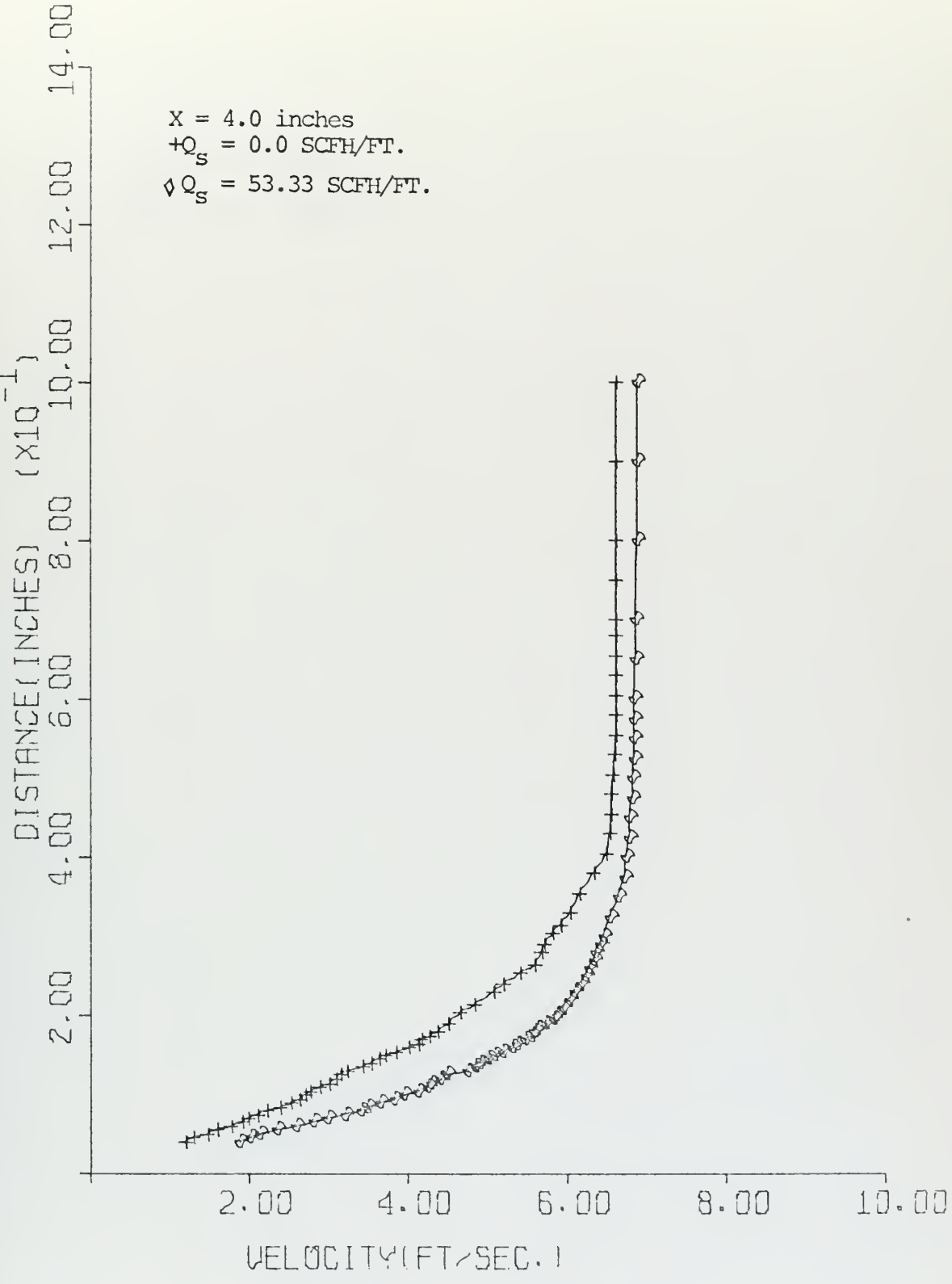

FIGURE 44
VELOCITY PROFILE

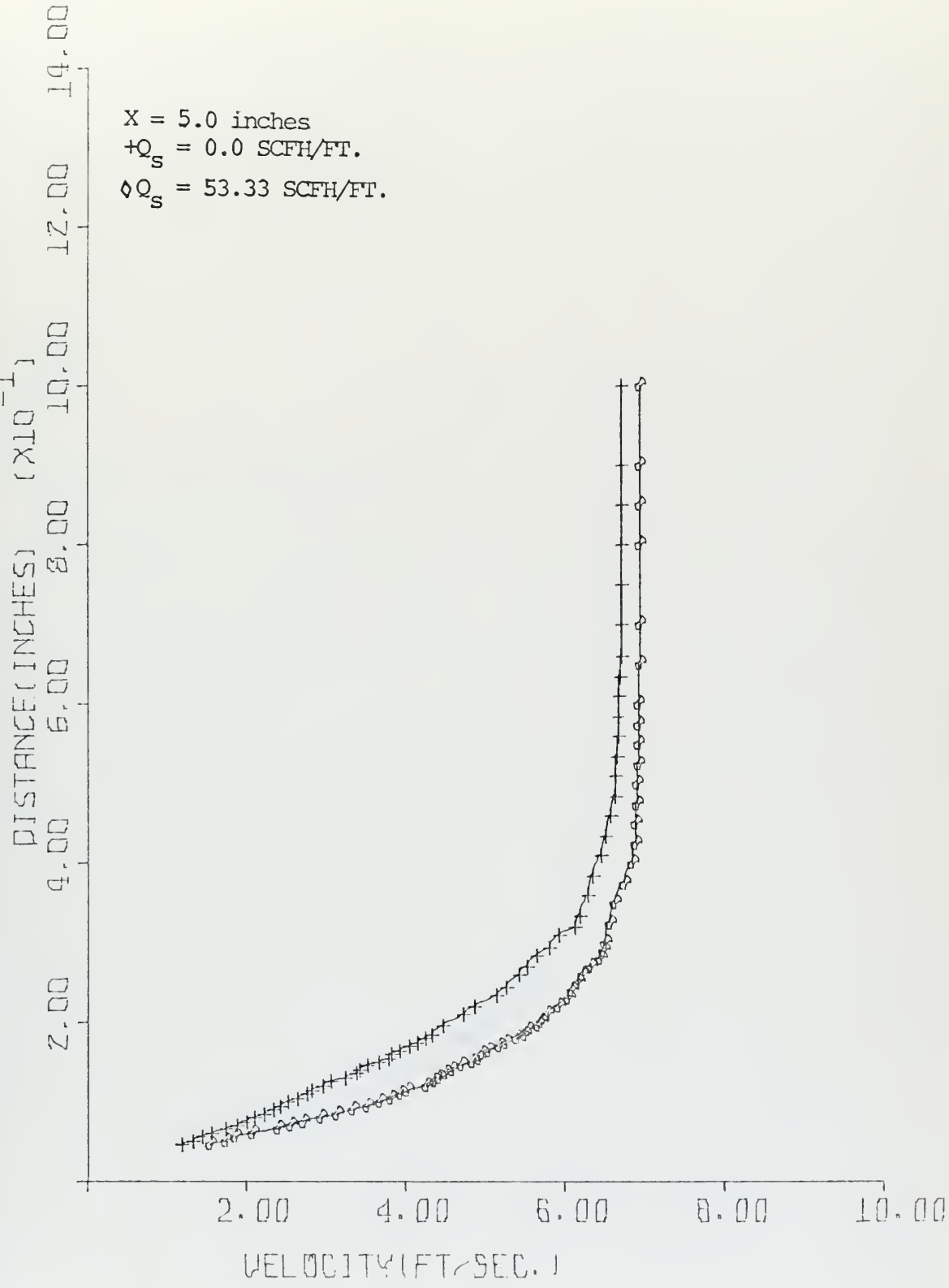

FIGURE 45
VELOCITY PROFILE

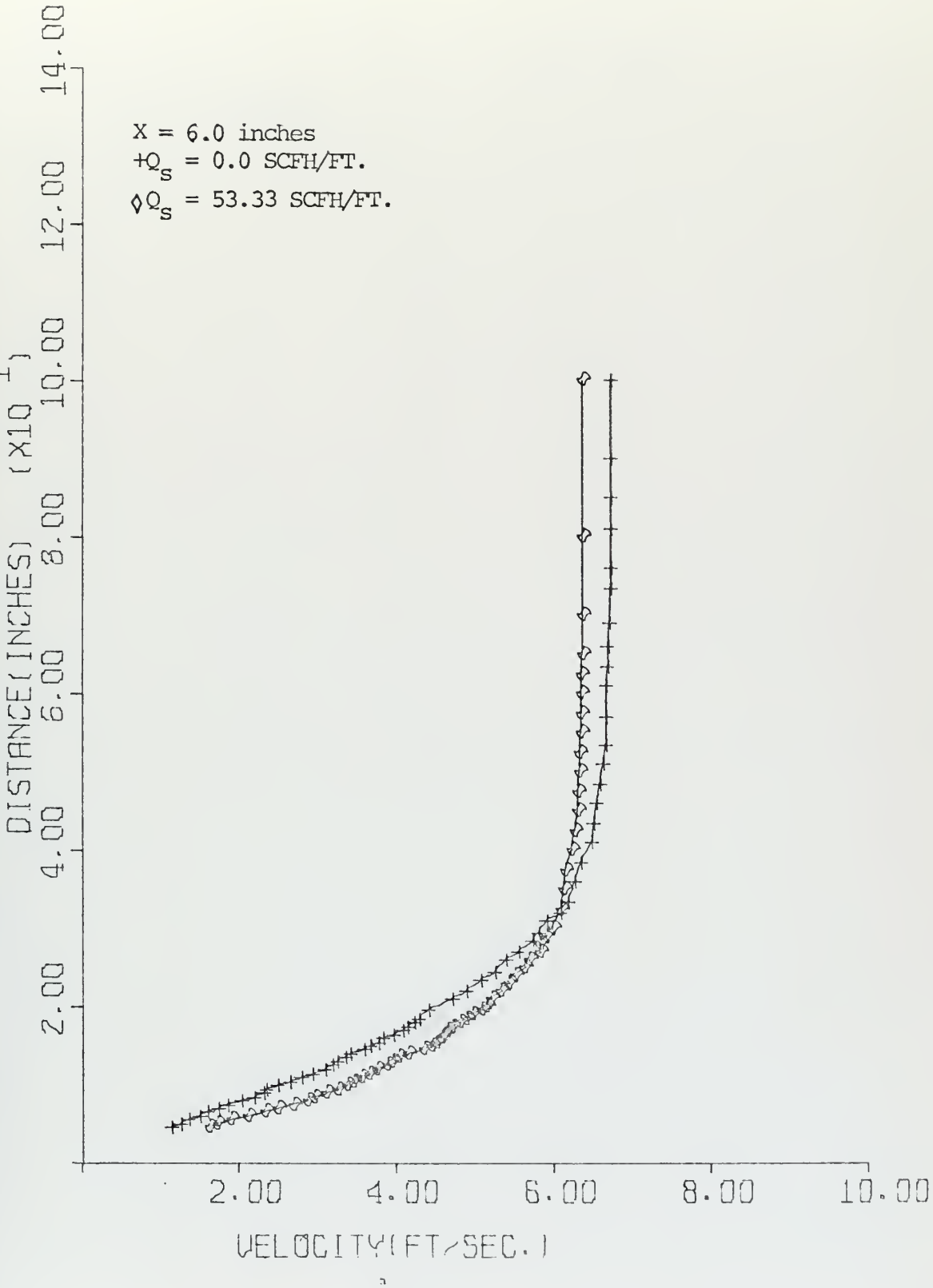

FIGURE 46
VELOCITY PROFILE

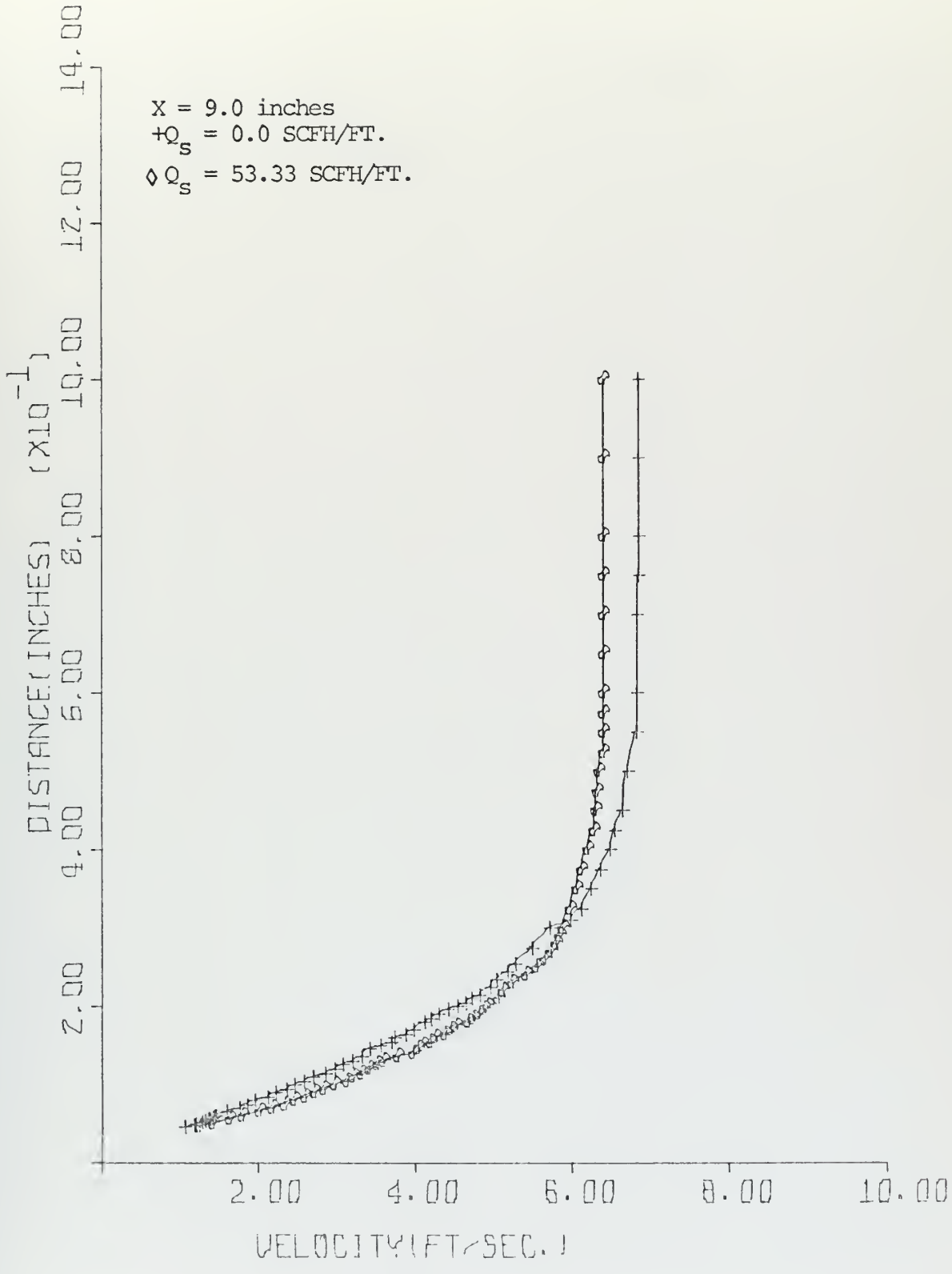

FIGURE 47
VELOCITY PROFILE

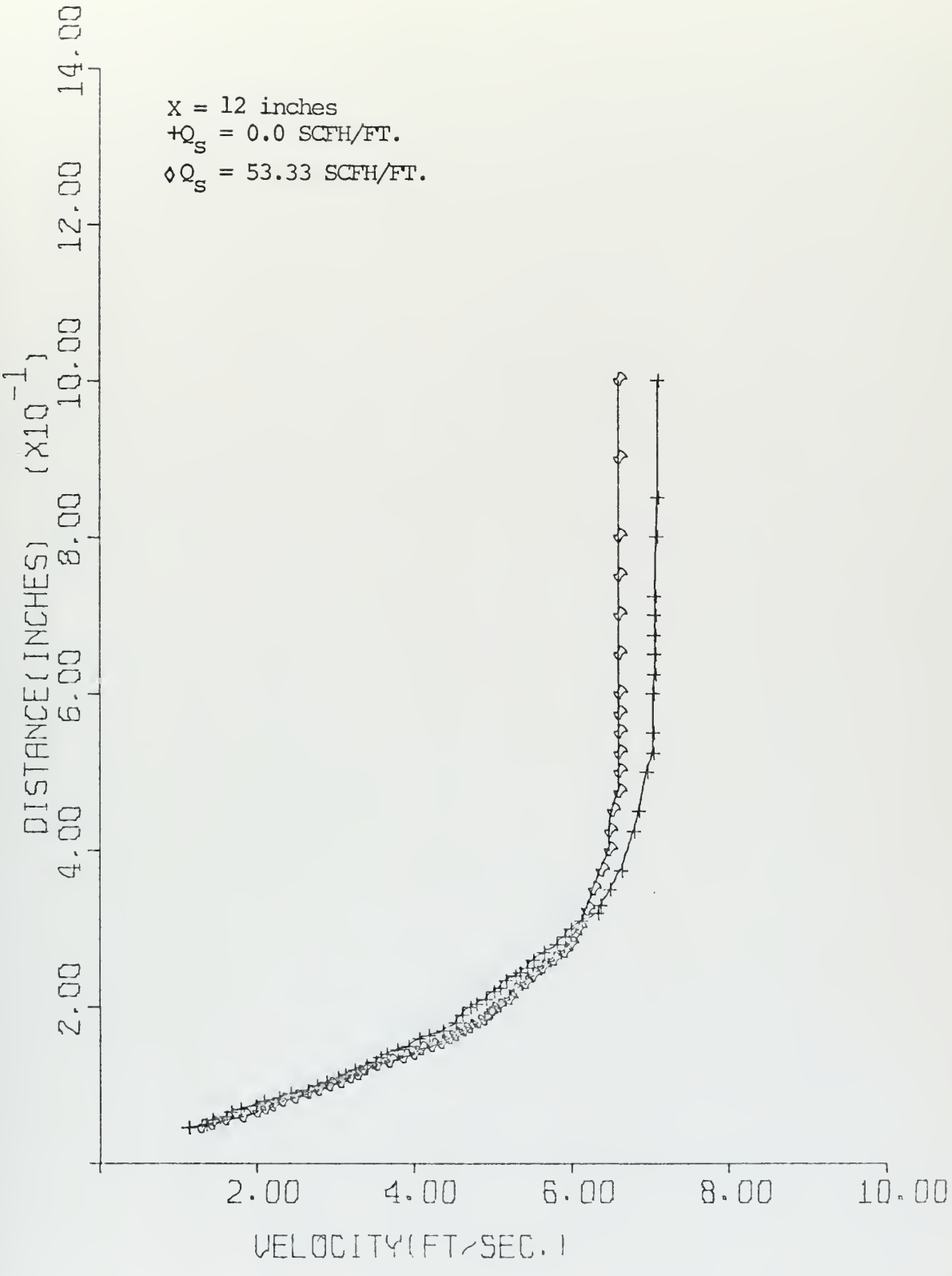

FIGURE 48
VELOCITY PROFILE

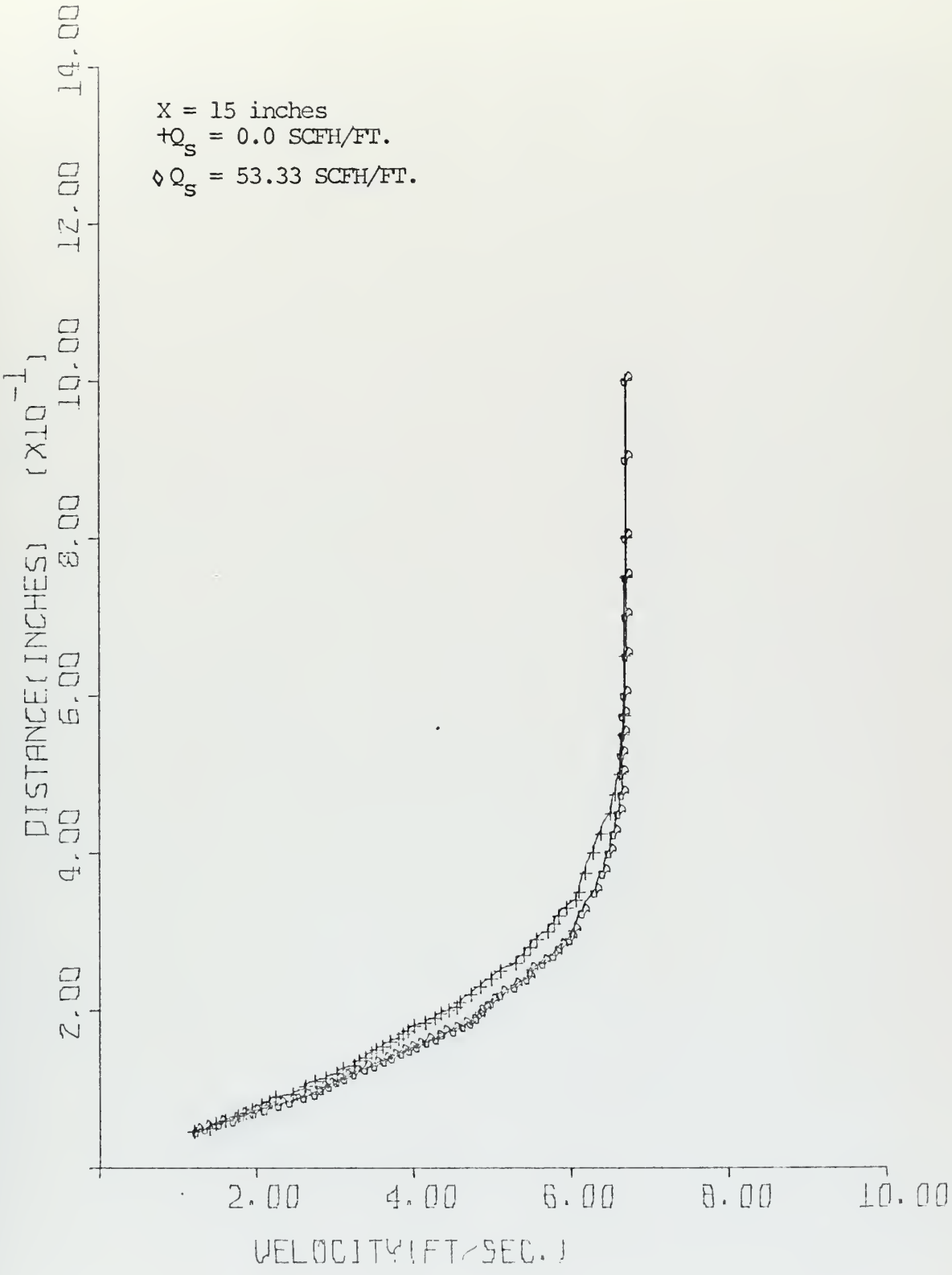

FIGURE 49
VELOCITY PROFILE

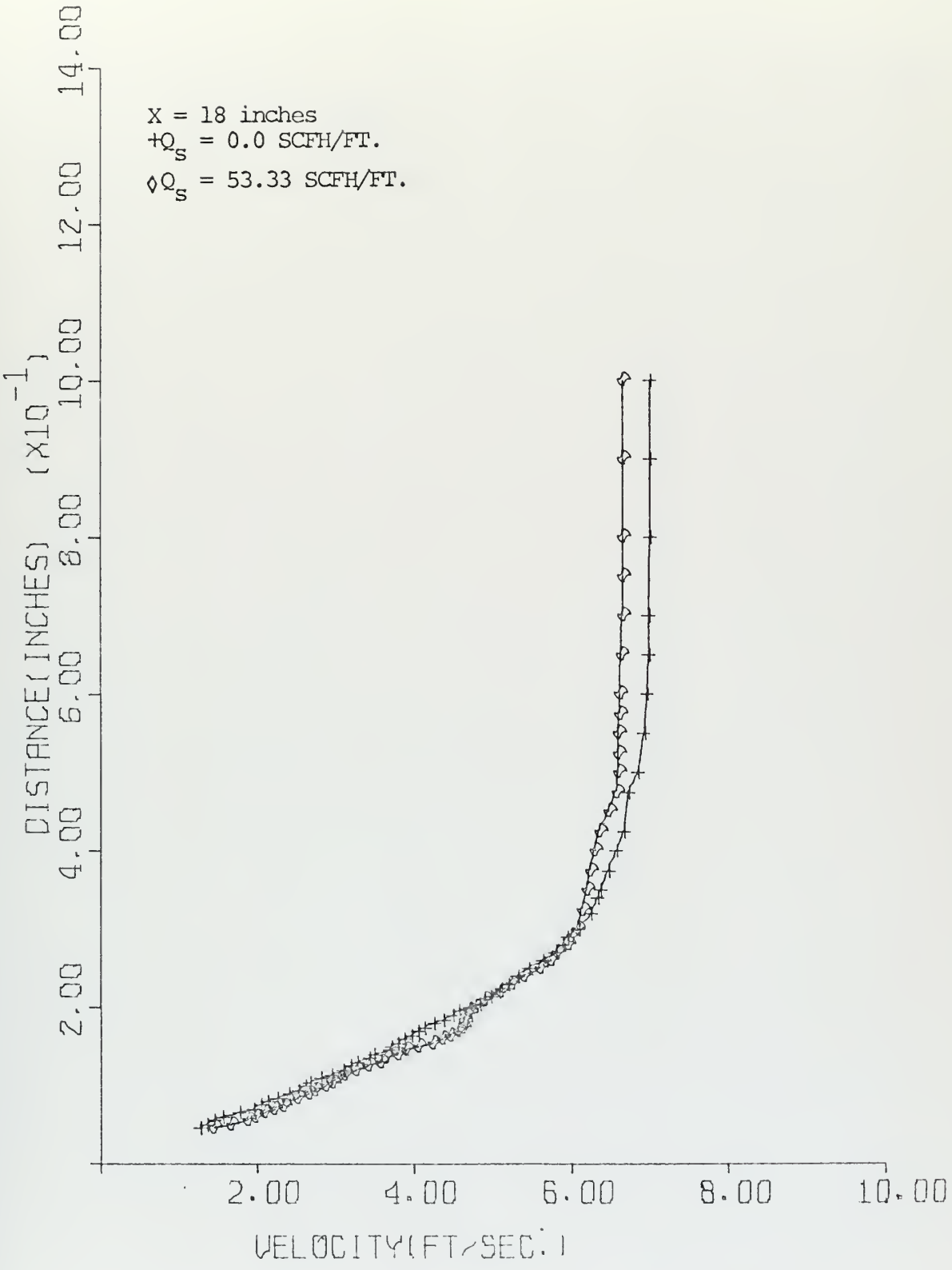

FIGURE 50
VELOCITY PROFILE

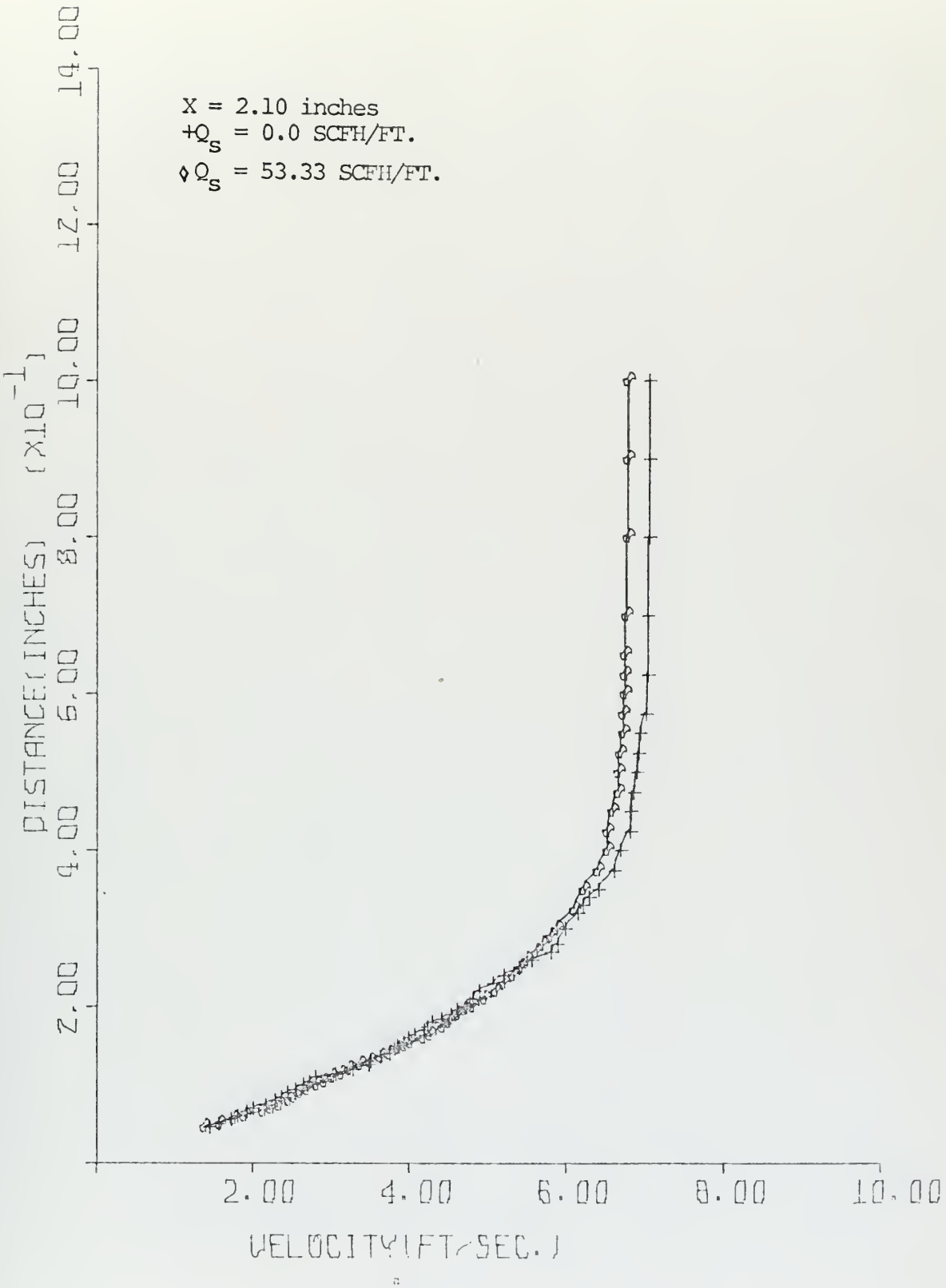

FIGURE 51
VELOCITY PROFILE

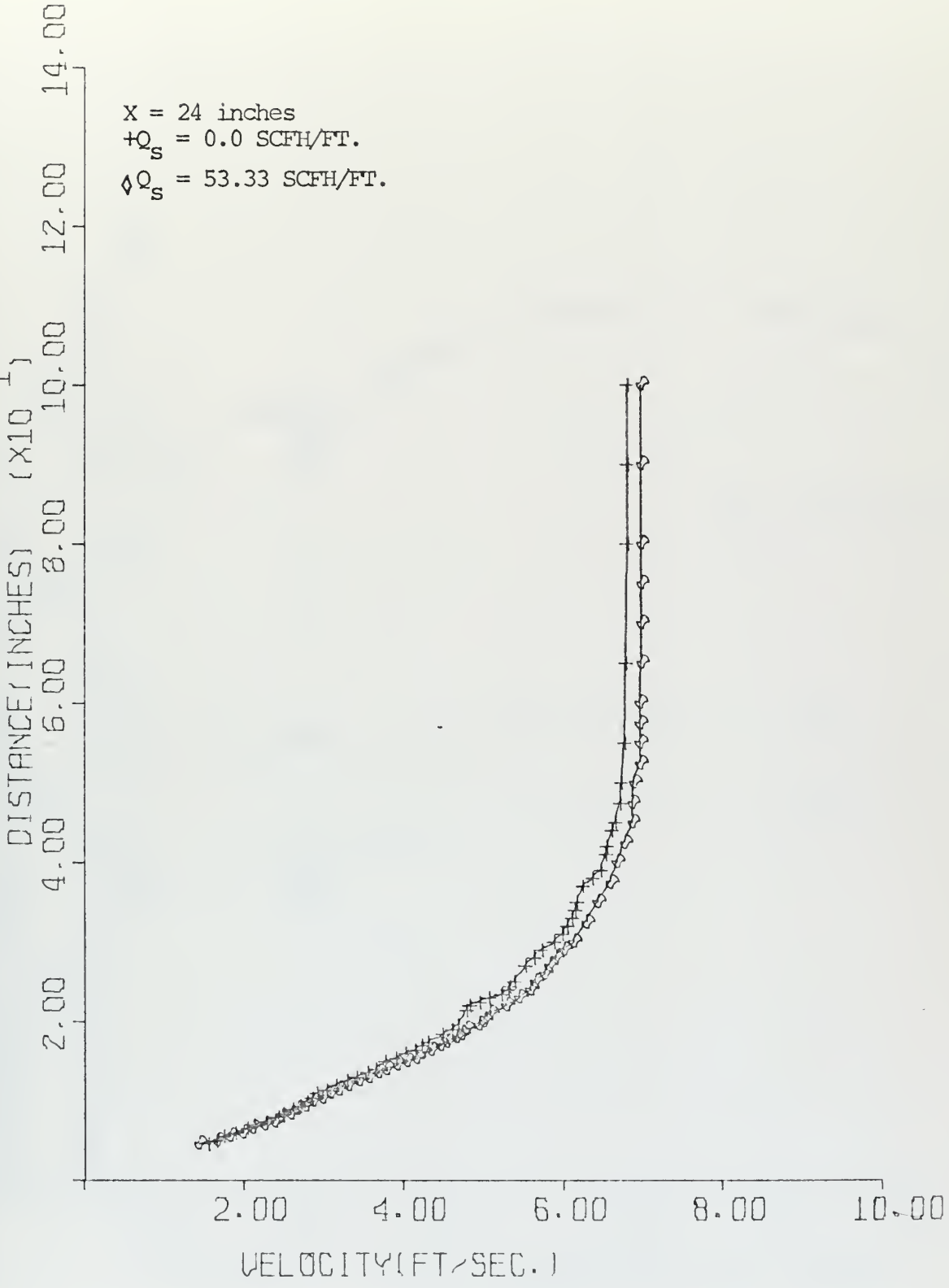

FIGURE 52
VELOCITY PROFILE

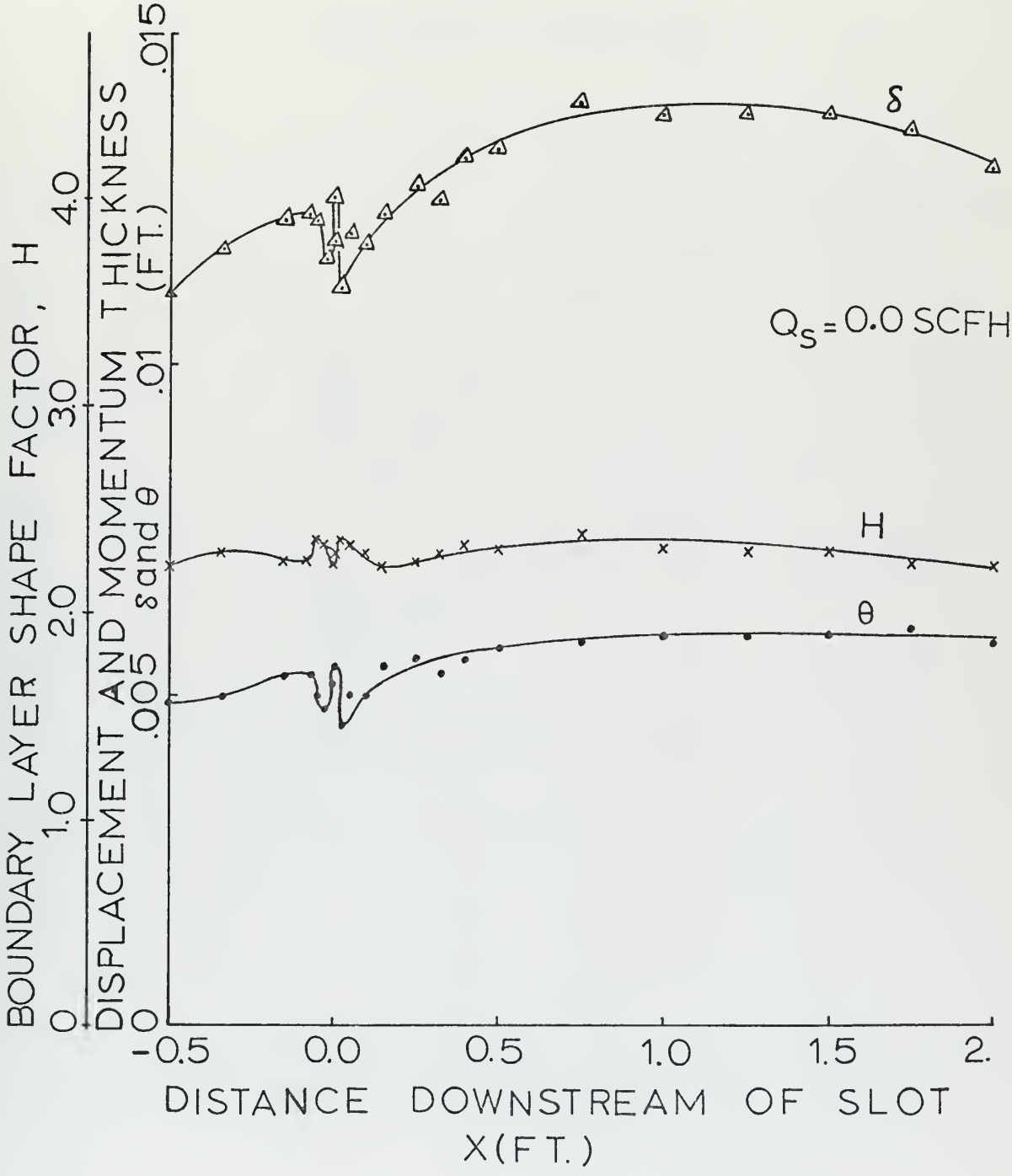

FIGURE 53
BOUNDARY LAYER SHAPE FACTOR, DISPLACEMENT THICKNESS AND MOMENTUM THICKNESS

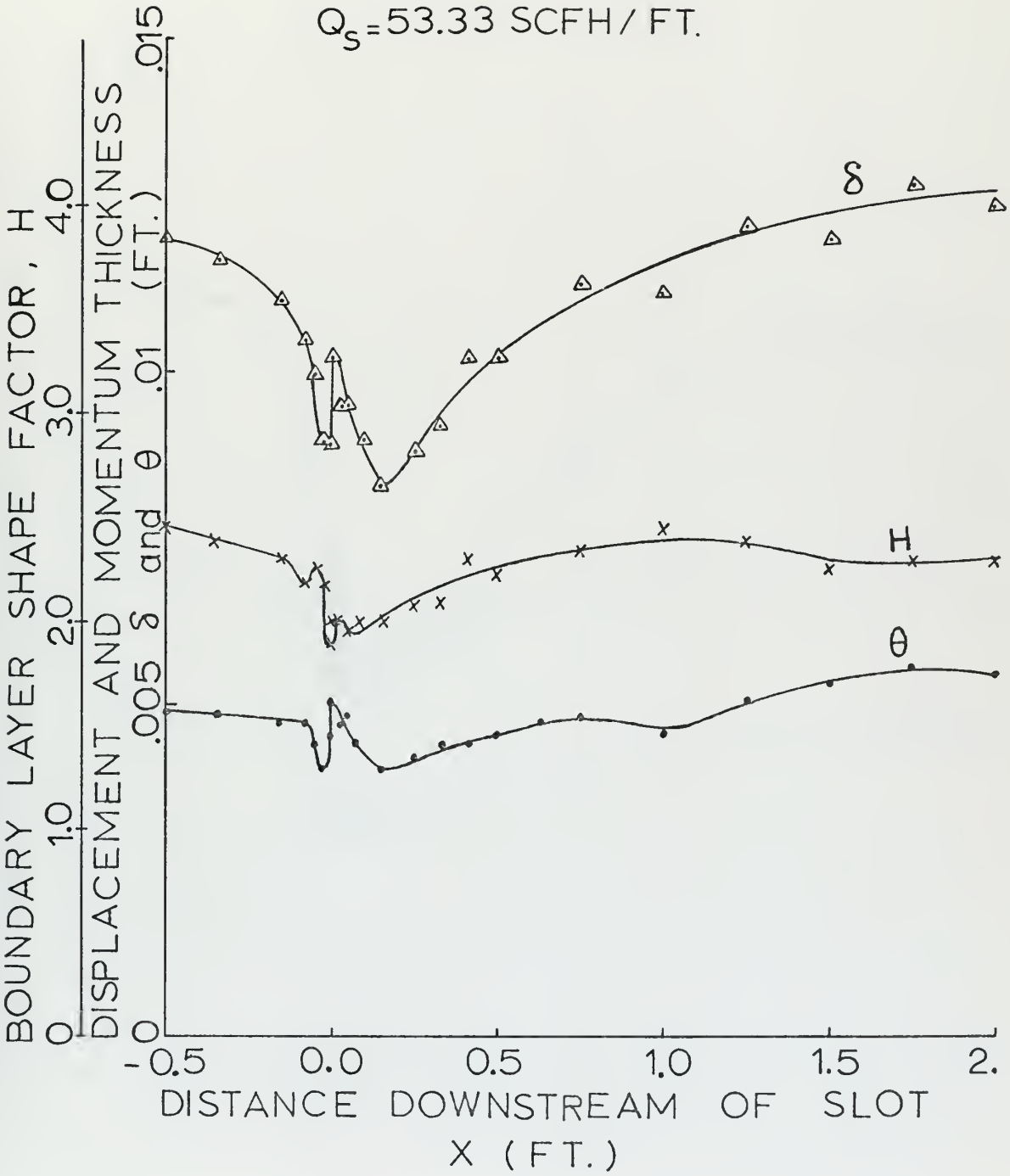

FIGURE 54

BOUNDARY LAYER SHAPE FACTOR, DISPLACEMENT THICKNESS AND MOMENTUM THICKNESS

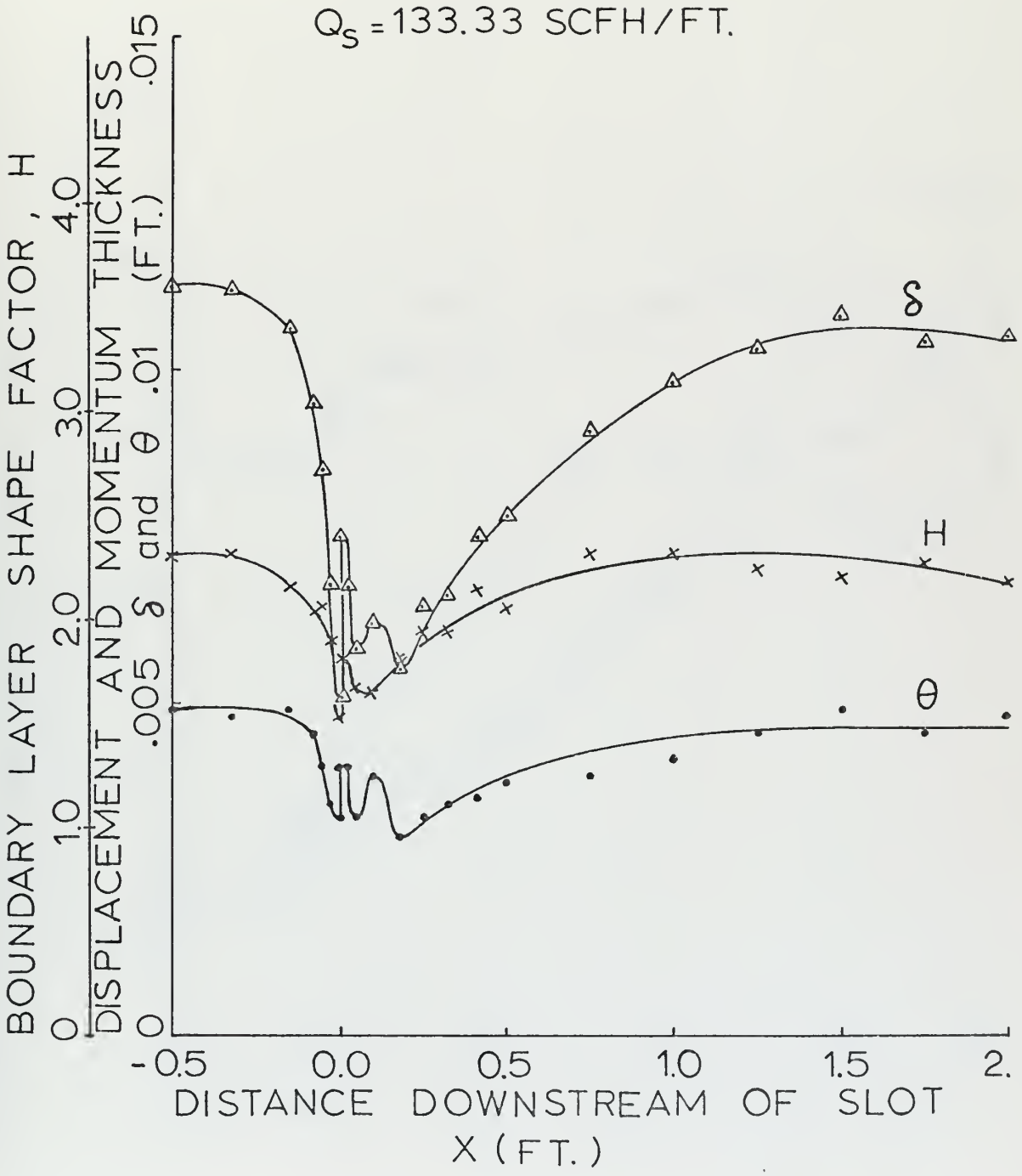

FIGURE 55

BOUNDARY LAYER SHAPE FACTOR, DISPLACEMENT THICKNESS AND MOMENTUM THICKNESS

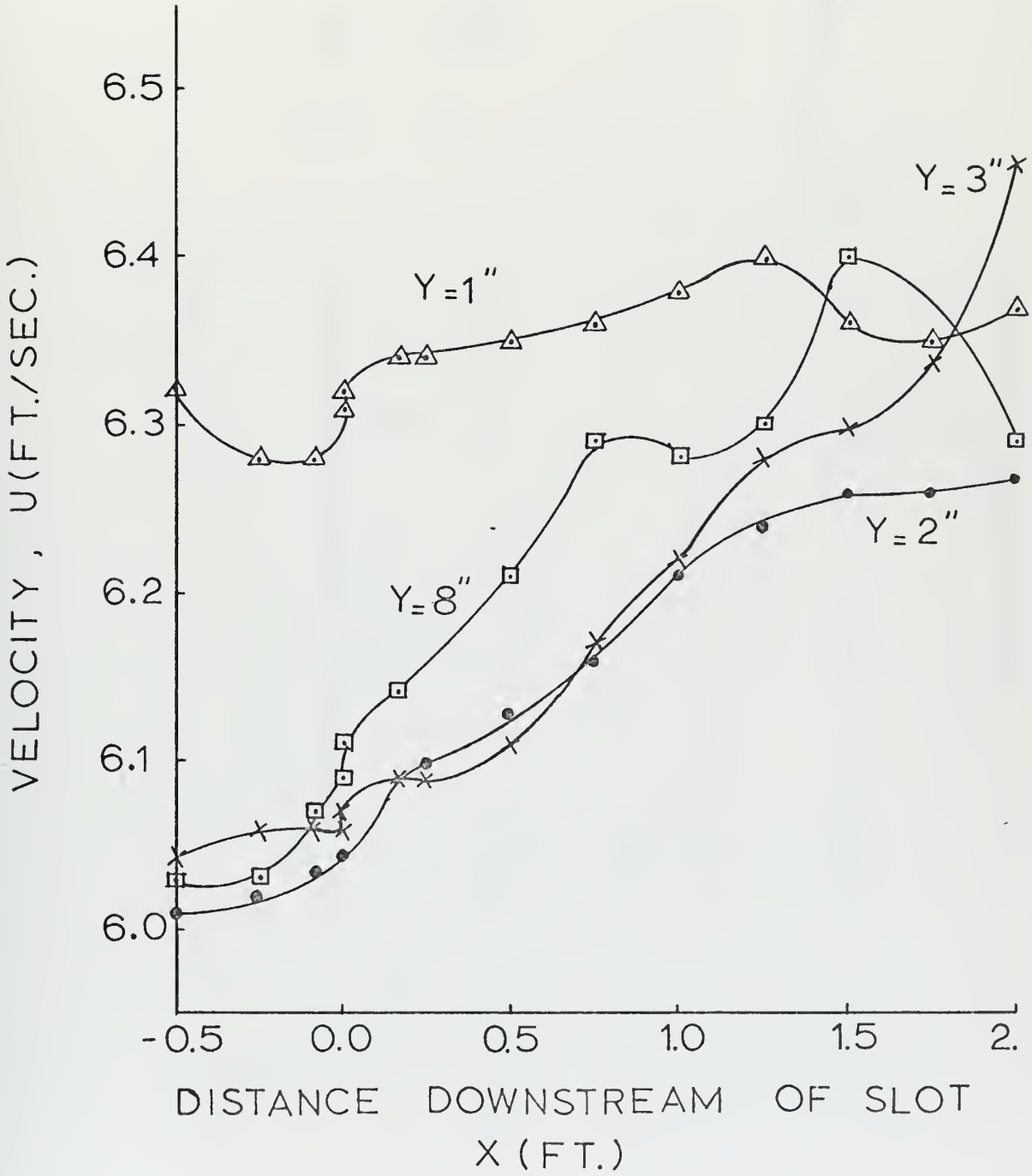

FIGURE 56
PRESSURE DISTRIBUTION IN THE TEST SECTION

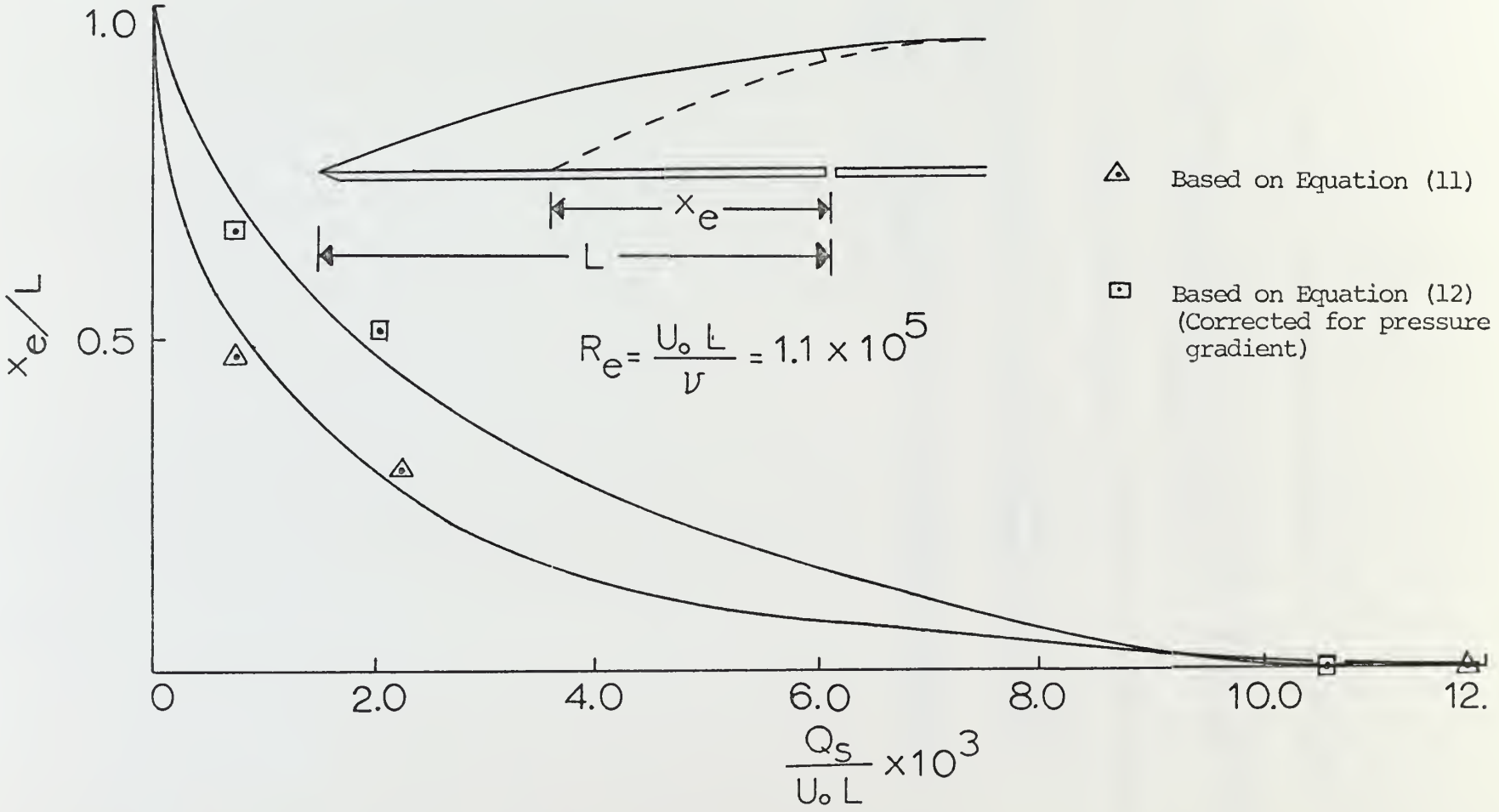

FIGURE 57
EFFECTIVE BOUNDARY LAYER LENGTH

REFERENCES

1. Lachmann, G. V., Boundary Layer and Flow Control, Vol. 1, Pergamon Press, 1961.

2. Holt, C. F., The Laminar Boundary Layer in the Vicinity of a Suction Slot, MS Thesis, Department of Aeronautical Engineering, The Pennsylvania State University, December 1965.

3. Schlichting, H., Boundary Layer Theory, McGraw Hill, Sixth Edition, 1968.

4. Schubauer, G. B., Spangenber, W. G., and Klebanoff, P. S., The Aerodynamic Characteristics of Damping Screens, NACA TN 2001, January 1950.

5. Thermo-Systems Inc., Hot Film and Hot Wire Anemometry, Theory and Application, Bulletin TB5.

INITIAL DISTRIBUTION LIST

		No. Copies
1.	Defense Documentation Center Cameron Station Alexandria, Virginia 22314	2
2.	Library, Code 0212 Naval Postgraduate School Monterey, California 93940	2
3.	Mechanical Engineering Department, Code 59 Naval Postgraduate School Monterey, California 93940	2
4.	Deniz Harb Okulu Komutanlig̈i Heybeliada, Istanbul, Turkey	1
5.	Istanbul Teknik Universitesi Makine Fakultesi Gumussuyu, Istanbul, Turkey	1
6.	Ortadog̈u Teknik Universitesi Makine Fakultesi Ankara, Turkey	1
7.	Professor C. J. Garrison, Code 59Gm Department of Mechanical Engineering Naval Postgraduate School Monterey, California 93940	2
8.	LTJG. Sabri Cig̈dem Istiklal Mah. Selim Sokak No. 15 Eskisehir, Turkey	2

Security Classification

DOCUMENT CONTROL DATA - R & D

(Security classification of title, body of abstract and indexing annotation must be entered when the overall report is classified)

1 ORIGINATING ACTIVITY (Corporate author)

Naval Postgraduate School
Monterey, California 93940

2a. REPORT SECURITY CLASSIFICATION

Unclassified

2b. GROUP

3 REPORT TITLE

Laminar Boundary Layer Development Downstream of a Suction Slot

4 DESCRIPTIVE NOTES (Type of report and inclusive dates)

Master's Thesis; December 1971

5 AUTHOR(S) (First name, middle initial, last name)

Sabri Cigdem

6. REPORT DATE	7a. TOTAL NO. OF PAGES	7b. NO. OF REFS
December 1971	117	5

8a. CONTRACT OR GRANT NO.	9a. ORIGINATOR'S REPORT NUMBER(S)
b. PROJECT NO.	
c.	9b. OTHER REPORT NO(S) (Any other numbers that may be assigned this report)
d.	

10 DISTRIBUTION STATEMENT

Approved for public release; distribution unlimited.

11. SUPPLEMENTARY NOTES	12. SPONSORING MILITARY ACTIVITY
	Naval Postgraduate School Monterey, California 93940

13. ABSTRACT

Laminar boundary layer development downstream of a suction slot was investigated in a low velocity wind tunnel. In order to observe the effect of suction on the boundary layer, detailed boundary layer profiles were measured at various stations upstream and downstream of a suction slot for different suction flow rates. The investigation was carried out for zero suction, 53.33 SCFH/FT. and 133.33 SCFH/FT. suction, by using 1/16 inch suction slot. The velocity profiles were plotted for 22 stations with different suction flow rates with respect to the no suction flow case. At the far upstream and downstream side of the slot, suction was ineffective and velocity profiles had the Blasius velocity profile shape. Suction had the maximum effectiveness a short distance in front of and downstream of the slot. As the distance from the slot increased both upstream and downstream, the velocity profiles tended to approach Blasius velocity profiles asymptotically.

DD FORM 1 NOV 65 1473 (PAGE 1)

S/N 0101-807-6811

Security Classification

A-31408

KEY WORDS	LINK A		LINK B		LINK C	
	ROLE	WT	ROLE	WT	ROLE	WT
Laminar Boundary Layer						
Suction Flow Rate						
Suction Slot						
Displacement Thickness						
Momentum Thickness						
Shape Factor						
Effective Boundary Layer Starting Length						
Velocity Profile						

Thesis 133498
C47884 Cigdem
c.1 Laminar boundary layer development downstream of a suction slot.